FLOW AND TRANSPORT IN WATER REPELLENT SANDY SOILS

Promotoren: Dr. Ir. R.A. Feddes
hoogleraar in de bodemnatuurkunde,
agrohydrologie en grondwaterbeheer

Dr. Ir. J. Bouma
hoogleraar in de bodeminventarisatie en landevaluatie,
speciaal gericht op de (sub)tropen

FLOW AND TRANSPORT IN WATER REPELLENT SANDY SOILS

Coen J. Ritsema

Proefschrift

ter verkrijging van de graad van doctor
op gezag van de rector magnificus
van de Landbouwuniversiteit Wageningen
Dr. C.M. Karssen,
in het openbaar te verdedigen
op dinsdag 1 september 1998
's middags te 16.00 uur in de Aula

This thesis is dedicated to my parents, Anne Reinier and Enriqueta.

CIP-DATA KONINKLIJKE BIBLIOTHEEK, DEN HAAG

Ritsema, C.J.

Flow and transport in water repellent sandy soils / C.J. Ritsema [S.l.:s.n.]
Thesis Landbouwuniversiteit Wageningen. - With ref. -
With summary in Dutch
ISBN 90-5485-915-6
Subject headings: water flow and solute transport; water repellent soils; hysteresis

STELLINGEN

1 In waterafstotende zandgronden onder grasland verloopt het transport van water en opgeloste stoffen via laterale stroming in de humeuze toplaag, preferente stroming in de waterafstotende laag, en divergerende stroming in de goed bevochtigbare ondergrond.
(*Dit proefschrift*)

2 Waterafstotende zandgronden worden gekenmerkt door een extreme mate van hysterese in de bodemwaterretentiekarakteristiek, waardoor natte en droge grond vlak naast elkaar kunnen voorkomen.
(*Dit proefschrift*)

3 In waterafstotende zandgronden kunnen de steeds terugkerende preferente stroombanen tot bodemheterogeniteit leiden.
(*Dit proefschrift*)

4 Om de lange termijndoelstellingen voor het mest-, bestrijdingsmiddelen-, grondwater- en saneringsbeleid veilig te stellen is aanvullend wetenschappelijk onderzoek naar het gedrag van stoffen in heterogene bodems nodig.
(*Ragas, A.M.J. en R.S.E.W. Leuven. 1996. Milieu 2:60-68; RMNO-publicatie 107. 1995. 'Omgaan met bodemheterogeniteit in het milieubeheer'; RMNO-publicatie 122. 1996. 'Het water- en bodemonderzoek over de eeuwwisseling heen'*)

5 Op bodemkaarten dient de mate van waterafstotendheid van gronden te worden aangegeven.
(*Dit proefschrift; Dekker, L.W. 1998*)

6 Aangezien hysterese in de bodemwaterretentiekarakteristiek grote gevolgen kan hebben op de wijze waarop water door de onverzadige zone stroomt dient deze te worden gemeten en opgenomen in de 'Staringreeks'.

7 Naast waterafstotend zand bestaat er zand dat kan zingen of dreunen.
(*Science, 6 maart, 1997*)

8 Planten kunnen het omliggend bodemmateriaal zodanig beïnvloeden dat de waterbeschikbaarheid wordt verhoogd.
(*Ritsema, C.J. and L.W. Dekker. 1996. Austr. J. Soil Res. 34:475-487*)

9 Om de natuurlijke spanning tussen onderzoekers en bestuurders van onderzoeksinstellingen niet te groot te laten worden verdient een organisatievorm van 'geneste zelfsturing' de voorkeur.

10 Iedere onderzoeksgroep dient vanuit de organisatie jaarlijks 10 tot 20% basisfinanciering te krijgen voor de letterlijk 'broodnodige' strategische expertiseontwikkeling.

11 Bezitters van oude auto's kunnen jaarlijks tot honderden guldens aan onnodige reparaties besparen door de verplichte APK keuring niet bij een garagebedrijf maar door de onafhankelijke Rijksdienst voor het Wegverkeer te laten uitvoeren.

12 Na de recente, geringe, verruiming van de openingstijden van winkels wordt door tegenstanders van dit beleid opeens gesuggereerd dat Nederland verworden is tot een niet meer te stuiten 24-uurs economie. Een cursus klokkijken lijkt voor deze categorie mensen uitermate op z'n plaats.

13 Gezien de uitslag van de recent gehouden gemeenteraadsverkiezingen zou de gemeente Utrecht er verstandig aan doen het zogenaamde 'Utrecht City Plan' te vergeten en de aanleg van de omstreden HOV-busbaan stop te zetten.

14 Om werknemers alert te houden zouden Nederlandse organisaties er goed aan doen om, in navolging van talloze Amerikaanse bedrijven, speciale slaapruimtes in te richten voor het doen van een 'power slaapje' na de lunch.
(*Intermediair, 7 mei, 1998, pag. 7; www.napping.com*)

15 'Je kunt me niet ontsnappen' zei de krokodil. 'Ik ben je noodlot en waar je ook gaat en wat je ook doet, je zult me altijd op je weg vinden. Er is maar één manier om aan mijn macht te ontkomen. ALS JE IN HET DROGE ZAND EEN KUILTJE KUNT GRAVEN DAT VOL WATER BLIJFT STAAN, ZAL DE BETOVERING WORDEN VERBROKEN. Lukt je dat niet, dan zal de dood je spoedig bezoeken. Dit is de enige kans die ik je geef. Ga nu.'
(*De gedoemde prins - sprookje uit het Soedanese Nijlgebied, in: L.A. Lang, 1907*)

Stellingen behorende bij het proefschrift 'Flow and transport in water repellent sandy soils' van Coen J. Ritsema, Wageningen, 1 september 1998.

ABSTRACT

Ritsema, C.J. 1998. Flow and transport in water repellent sandy soils. Doctoral thesis, Wageningen Agricultural University, the Netherlands. 215 pages.

Water repellency in soils is currently receiving increasing attention from scientists and policy makers, due to the adverse and sometimes devastating effects of soil water repellency on environmental quality and agricultural crop production. Soil water repellency often leads to severe erosion and runoff, rapid leaching of surface-applied agrichemicals, and loss of water and nutrient availability for crops.

In general, soils become water repellent through the coating of soil particles or structural elements with water repellent organic substances originating from decaying plant material. Soil water repellency manifests itself when the water content of the soil drops below a critical level. Water flow and solute transport patterns are complex under such conditions. The present study deals with flow and transport processes in an untilled, grass-covered water repellent sandy soil consisting of three layers.

Extensive tracer experiments indicate that distribution flow dominates in the humous top layer, preferential flow in the water repellent sand layer, and diverging flow in the underlying wettable zone. Preferential flow paths or fingers occur almost throughout the year. Fingers develop rapidly during severe rain storms, causing significant portions of the infiltrating water to be preferentially transported to the deep subsoil. Fingers form at sites with relatively low degrees of water repellency, and finger diameters range from 10 to 25 cm.

Model simulations show that fingered flow results from hysteresis in the water retention function, and the nature of the formation depends on the shape of the main wetting and drainage branches of that function. Once fingers are established, hysteresis causes them to recur along the same pathways during subsequent rain events. In the long term, recurrence of fingers may lead to changes in physical and/or chemical properties of the soil within the fingered flow pathways. It is only under initially dry conditions, with soil water contents below the critical level, that fingers will be formed during infiltration. Under wetter conditions, with soil water contents above the critical level, wetting fronts will remain stable and no fingers will develop.

Future research should focus on improving our understanding of the origins, occurrence, hydrological responses and agricultural functioning of water repellent soils.

Front cover: Cross-section of preferential flow paths (dark areas) embedded in dry soil (light areas) at a depth of 15 cm in a water repellent sandy soil.

PREFACE

The best ideas are often born when travelling abroad. It was 2 years ago, at a 3 week research trip in New Zealand and Australia, during which severely water repellent regions were visited, that Louis W. Dekker and myself decided to start work on a Doctoral thesis. On that occassion, we already dreamed of combining our Doctoral ceremonies with the organization of an international workshop on soil water repellency, and, surprisingly enough, it looks as if we have succeeded.

Numerous colleagues from the DLO Staring Centre and from other organizations in and outside the Netherlands have contributed to this work in one way or another.

First of all, a special word of thanks goes to Louis W. Dekker for introducing me to the 'world' of soil water repellency. Louis, I will never forget our first field trip to Ouddorp, and your never ending enthusiasm for digging in water repellent soils around the world. Your interest in the topic was catching, and your 'critical eye' prevented many textual mistakes during the preparation of our co-authored manuscripts. I hope that we will be able to continue working on the topic for the years to come.

I would like to thank Aad van Wijk and my former colleague Hans Bronswijk for their stimulating and critical discussions, which helped us to keep 'on track' in the early stages of this 'project'.

Pim Hamminga provided valuable assistance in the collection of samples and the execution of numerous laboratory measurements. The assistance of Gerard Veerman in measuring soil physical properties is highly appreciated.

Klaas Oostindie played a key role in drawing many of the graphs incorporated in this thesis. His endless patience in perfecting the figures is highly appreciated.

Special thanks go to Anton Heijs for the many pleasant hours behind the SGI computer trying to achieve three-dimensional visualizations of water content distributions. Wilfred Janssen and Rik Leenders offered useful assistance, and kindly allowed us to use the SGI-ONYX of the SARA Visualization Center, Amsterdam, the Netherlands for final color prints and slides. Anton, I hope you will find some way to get your own thesis finished!

I am indebted to Erik van den Elsen for the many hours he spent constructing the stand-alone TDR-device and installing it at Ouddorp, and to Jannes Stolte for developing the automated laboratory method for measuring water uptake rates of initially dry water repellent soil samples. Unfortunately, data derived from this set-up could not be incorporated in this thesis!

A special word of thanks goes to Henk van Ledden for drawing (sometimes twice!) many of the graphs incorporated in this thesis; a process which always seemed to take place under a bad constellation and continuous pressure of time. My gratitude also goes to Martin Jansen for preparing the beautiful cover of this thesis.

The cooperation with Jan Hendrickx was motivating and pleasant, and I really enjoyed the visits to New Mexico to search for water repellent soils in the Sevilletta region, and farther away across the border of Mexico.

I am deeply indebted to Tammo Steenhuis, who from the very beginning proved to be the most ardent supporter of this study. Tammo, the first visit to your place was unforgettable. I was amazed about everything: your immense scientific production, your devoted support and patience in guiding students and staff, and last but not least, your personality, which makes it a real pleasure to be at your place either for work, for delicious pizzas, or for playing soccer with your family team.

A very special word of thanks goes to John Nieber, who guided me through the simulation part of this study. I am very grateful for the many highly motivating and pleasant discussions we had during the last years, and the unique collaboration we have established. I hope we will find some time again to drink a beer and to play another game of 'table football'! I would also like to thank Hung V. Nguyen and Debasmita Misra for their unfailing help with simulations and graphics.

It is with pleasure that I remember the fruitful discussions and cooperation with many other researchers all over the world, of whom the following played an important role during several phases of the research: Paul Blackwell, Larry Boersma, Warren Bond, Brent Clothier, Jan Feyen, Hannes Flühler, Robert Glass, Nick Jarvis, Dirk Mallants, Jean-Yves Parlange, Pieter Raats, Frank Stagnitti, Zhi Wang, Ole Wendroth.

I would like to express my gratitude to my supervisors, Reinder Feddes and Johan Bouma, for their professional guidance and strong encouragement. The final compilation of this thesis at first seemed a simple matter: use the same font throughout, select some articles, and place the references at the end of the booklet, that was the idea... During the preparation of the thesis, however, articles were adapted to become chapters, simple graphs redrawn as color figures, etc, etc. Despite the unforeseen workload, some time was left to keep track of the organization of the international workshop on soil water repellency. I hope both events will be fruitful.

Last but not least, I am deeply indebted to Marleen, Joyce and Richard, and many friends for their continuous interest and support, especially during the evenings on which I intended to work, and ended up having a beer instead.

ACKNOWLEDGMENTS

Preparation of this thesis was made possible through financial support from

- Research Programme 223, 'Physical Soil Quality', of the Dutch Ministry of Agriculture, Nature Management and Fisheries;
- The Environment and Climate Research Programme of the European Union (DG XII, Contract: EV5V-CT94-0467);
- The Netherlands Integrated Soil Research Programme (Project C3-13);
- The USA Army High Performance Computing Research Centre, under the auspices of the Department of the Army, Army Research Laboratory cooperative agreement number DAAH04-95-2-0003 (Contract: DAAH04-95-C-0008);
- NATO Collaborative Research Grants 920108 and 960704;
- The DLO Winand Staring Centre (seo-project 726).

Dissemination of the research results at international congresses and symposia was made possible by travel grants supplied on a regular basis by the Netherlands Integrated Soil Research Programme. SHELL graciously provided financial support to present part of this thesis at the 16th World Congress of Soil Science, Aug. 1998, Montpellier, France.

The author is greatly indebted to the European Union (Grant ENV4-CT97-6129), The Royal Netherlands Academy of Arts and Sciences (RC 241.612.2697), The Netherlands Integrated Soil Research Programme (Project 350370, subsidy 185), and the Australian Department of Industry, Science and Tourism (Grant 97/686) for sponsoring the International Workshop on Soil Water Repellency, which will be held after the Doctoral ceremony in Wageningen on September 2 to 4, 1998.

CONTENTS

CHAPTER 1

INTRODUCTION

1 INTRODUCTION

1.1 BACKGROUND AND PROBLEM DEFINITION

Water repellent soils have been a topic of study for soil scientists, hydrologists and soil physicists around the world since the beginning of this century.

Origins of soil water repellency

Schreiner and Shorey (1910) were among the first to mention the existence of water repellent soils. In describing the effect of organic compounds on the water holding capacity of soils, they wrote: '*To illustrate this, there was found in California a soil which could not be properly wetted, either by man, by rain, irrigation, or movement of water from the subsoil, with the result that the land could not be used profitably for agriculture. On investigation it was found that this peculiarity of the soil was due to the organic material, which when extracted had the properties of a varnish - repelling water to an extreme degree.*'

From the end of the 1940s until the end of the 1960s, research on water repellent soils focused on identifying *vegetation types* responsible for inducing water repellency (Jamison, 1945, 1946; Krammes and DeBano, 1965; Gilmour, 1968; Savage et al., 1969a; Bond 1969; Adams et al., 1969), and on developing techniques to quantify the degree of water repellency (Letey et al., 1962; Emerson and Bond, 1963; Letey, 1969; Hammond and Yuan, 1969; Watson and Letey, 1970). Furthermore, causes of water repellency were investigated (Wander, 1949; Van 't Woudt, 1959; Bond, 1964, 1969). In 1968, a symposium on water repellent soils was held at the University of California, Riverside, USA, whose proceedings (DeBano and Letey, 1969) summarizes most of the work that had been done.

Of special interest has been the effect of *wildfire* on the development of soil water repellency. Fire was already considered of major importance in inducing water repellency at the beginning of the 1960s (Krammes, 1960; DeBano and Krammes, 1966). Since then, numerous studies have been undertaken to investigate the effects of fire on soil water repellency (Adams et al., 1970; Savage et al., 1972; Savage, 1974; DeBano et al., 1976; DeBano, 1979; Giovannini et al., 1987; Scott and Van Wyk, 1990, 1992; Imeson et al., 1992).

Amelioration of water repellent soils

From the beginning of the 1960s, modification of water repellent soil to improve its wettability for crop production became a topic of interest.

In addition to the use of *wetting agents*, which had been studied extensively during the 1960s and 1970s (a.o. Pelishek et al., 1962; DeBano et al., 1967; Osborn et al., 1967; Osborn, 1969; Mustafa and Letey, 1971; Letey et al., 1975; Miyamoto, 1985; Wallis et al., 1990), research focused on *cultivation aspects* attempting to dilute the repellent soil fraction with wettable soil (Holzhey, 1969) or to cause abrasion of repellent soil particles (Ma'shum and Farmer, 1985). Furthermore, clay amendments were tested for their ability to decrease soil water repellency (Roberts, 1966; McGhie and Posner, 1980, 1981; Ma'shum et al., 1989). Special irrigation schemes were invented, in combination with alternative sowing techniques, to avoid formation of water repellency as the soil dries (DeBano, 1971; Danneberger and White, 1988; Wallis et al., 1989; Way, 1990; Blackwell, 1993).

Effect on water flow and transport behavior

Due to increasing concern over the threat to surface and groundwater quality posed by the use of agrichemicals and organic fertilizers, studies on water repellent soils during the last decades have mainly focused on its typical flow and transport behavior.

To begin with, the effects of soil water repellency on *runoff* generation were studied quite intensively. Osborn et al. (1964) and Krammes and DeBano (1965) had already indicated that water repellent soil surfaces might seriously affect water infiltration and, as a result, might promote runoff in hilly regions. Since then, several studies around the world have dealt with this topic (Krammes and Osborn, 1969; McGhie, 1980; Burch et al., 1989; Witter et al., 1991; Crockford et al., 1991; Jungerius and ten Harkel, 1994).

Secondly, it had already been shown by Jamison (1945, 1946) that large variations in water content exist in water repellent soils, indicating that infiltrating water followed *specific pathways* instead of moving in a planar wetting front. Van Dam et al. (1990) and Hendrickx et al. (1993) showed that water and solutes may travel rapidly through water repellent soils, bypassing large parts of the unsaturated zone. The unsaturated or vadose zone of the soil, particularly the biologically and chemically reactive topsoil, acts as an important buffer for various chemical compounds. When water flow

bypasses large parts of the unsaturated zone, the risk of pollution of any receiving water bodies, such as groundwater or surface water, might seriously increase. Theoretical considerations by Saffman and Taylor (1958), Hill and Parlange (1972), Raats (1973), Philip (1975a,b), Parlange and Hill (1976), Diment et al. (1982), Diment and Watson (1983), Hillel and Baker (1988) and Baker and Hillel (1990) already indicated possible conditions under which perturbations at an infiltrating wetting front might grow into '*fingers*' or '*preferential flow paths*' instead of flattening out by lateral diffusion. On the basis of theoretical considerations, Raats (1973) was the first to indicate that soil water repellency might lead to the formation of preferential flow paths. Field evidence of preferential flow of bromide through a water repellent sandy soil, resulting in early arrival times, and high bromide concentrations in the groundwater, was presented by Hendrickx et al. (1993).

Attempts to model flow and transport in water repellent soils have been undertaken by Van Dam et al. (1990) and De Rooij (1995). In both cases, however, analytical approaches were used which neglected specific processes like hysteresis in the water retention function, which is of significance in water repellent media.

Despite the numerous theoretical considerations, the few field observations of preferential flow in water repellent soils, and the rare modeling attempts, no clear view exists at present about the general flow and transport mechanisms through water repellent soils. Unraveling and understanding water flow and transport processes in water repellent field soils is essential if we are to arrive at a suitable simulation approach. Leaching risks of surface-applied agrichemicals in water repellent soils can only be quantified with an acceptable degree of accuracy if knowledge of the underlying physics and an appropriate simulation model are available.

Occurrence of water repellent soils

As water repellency of soils is probably the rule rather than the exception in most field soils (Wallis et al., 1991; Wallis and Horne, 1992; Dekker, 1998), efforts to study the effects of water repellency on flow and transport processes would seem to be highly relevant, not only from a soil physics point of view, but from those of soil management and soil protection as well. This is supported by the fact that water repellent soils are being identified in an increasing number of agricultural and natural environments in different climatic conditions around the world. At present, areas where water repellent

soils are known to occur include the USA (DeBano, 1981), Canada (Dormaar and Lutwick, 1975), Australia (Roberts and Carbon, 1971, 1972), New Zealand (Wallis and Horne, 1992), Japan (Nakaya, 1982), India (Das and Das, 1972), South Africa (Scott and Van Wyk, 1990, 1992), Mali (Rietveld, 1978), Egypt (Bishay and Bakhati, 1976), Colombia (Jaramillo and Herrón, 1991), Italy (Giovannini and Lucchesi, 1984), Spain (Imeson et al, 1992), Portugal (Doerr, 1996), Poland (Grelewicz and Plichta, 1985), and the Netherlands (Dekker and Jungerius, 1990).

From the above current state of knowledge, it may be concluded that

- Water repellent soils occur in agricultural and natural areas all over the world.
- Water repellency may lead to the development of unstable wetting fronts and preferential flow paths.
- Preferential flow has a wide-ranging significance for the rapid transport of surface-applied solutes, such as agrichemicals, to groundwater and surface water, and thus, for management strategies to minimize environmental degradation.
- Attempts to model preferential flow in the vadose zone of water repellent soils have been rare, due to insufficient knowledge about the principles of the associated water flow and transport processes.
- At present, we lack the systematic, detailed field data which are necessary to develop and validate such models.

To increase our basic knowledge of the occurrence of water repellent soils and the effects of water repellency on flow and transport processes, three Doctoral studies were initiated a few years ago. The first study, by Louis W. Dekker (1998), aimed at investigating the occurrence of water repellency in different soil types in the Netherlands in relation to soil water content variability. The second (present) study, by Coen J. Ritsema, aimed at unraveling process mechanisms in a water repellent sandy soil in relation to the modeling of water flow and solute transport processes. The third, ongoing, study by Hung V. Nguyen elaborates on the work of both previous studies and mainly deals with the application of models to simulate the observed flow and transport processes in the water repellent sandy soil investigated in the present study.

1.2 OBJECTIVES OF THE STUDY

The present study investigated water flow and solute transport processes in the unsaturated zone of water repellent sandy soils, and focused specifically on

- Determining the general flow and transport mechanisms in water repellent sandy soils by executing detailed tracer experiments on small and large plots.
- Obtaining high-resolution soil water content, water repellency and tracer concentration distributions by detailed sampling of soil trenches and soil blocks.
- Monitoring finger formation and finger recurrence during successive rain events in a natural field soil.
- Deterministic modeling of the process of finger formation and finger recurrence.

1.3 OUTLINE OF THE THESIS

This thesis discusses detailed field, laboratory and modeling studies on the topic of water flow and solute transport in water repellent soils. These studies were performed at an experimental site in Ouddorp, in the southwestern part of the Netherlands, which consists of an extremely water repellent sandy soil to a depth of approximately 50 cm.

Chapter 2 discusses the results of a detailed bromide tracer experiment, and a general flow and transport concept is derived.

In Chapter 3, attention is focused on distribution flow, i.e., lateral flow and transport through the humous top layer towards the vertical fingers in the underlying subsoil.

Chapter 4 deals with the identification of preferential flow paths, presenting two-dimensional soil water content distributions in ten trenches.

In Chapter 5, this type of work is extended to three-dimensional soil water content and water repellency distributions, obtained from ten soil blocks sampled during a one year cycle.

Chapter 6 presents dynamic changes in soil water content distributions during multiple rain events obtained by using a detailed TDR measurement set-up. The corresponding three-dimensional distributions of soil water content, water repellency, bromide concentration and soil pH determined after the conclusion of the TDR measurement campaign are described in Chapter 7.

In Chapter 8, a two-dimensional finite element water flow and transport model, including hysteresis, is introduced and applied to simulate the process of finger formation and finger recurrence.

Chapter 9 highlights the effect of antecedent soil water content on the evolution of infiltrating wetting fronts, on basis of numerical results.

Finally, summary, conclusions and recommendations for further research are given in Chapters 10 and 11.

CHAPTER 2

PREFERENTIAL FLOW MECHANISM

Adapted version of 'Preferential flow mechanism in a water repellent sandy soil' by C.J. Ritsema, L.W. Dekker, J.M.H. Hendrickx and W. Hamminga, published in Water Resources Research 29:2183-2193, 1993.

2 PREFERENTIAL FLOW MECHANISM

Abstract

Dry water repellent soils are difficult to wet, forcing water and solutes to flow via preferential paths through the unsaturated soil. A tracer experiment was used to investigate the mechanism of preferential flow and transport in a water repellent sandy soil. Water and solutes were distributed by lateral flow within the relatively wet, thin humous top layer towards preferential flow paths below this zone. This flow in the upper layer, which is of major importance in the spatial distribution of water and solutes in field soils, is generally neglected, and is introduced here as 'distribution flow'. The preferential flow paths were separated by dry soil regions, which were highly persistent due to their extremely water repellent character and low hydraulic conductivity. In the wettable zone, below a depth of around 45 to 50 cm, water and solutes diverged towards areas situated below dry soil regions. Despite this process, the spatial variation in solute concentration in this zone remained relatively high.

2.1 INTRODUCTION

At present, it is generally accepted that water may flow through the soil via preferential paths, bypassing large volumes of the soil matrix (e.g. Gee et al., 1991). This reduces the availability of water and nutrients for plants, and causes accelerated transport of surface-applied pollutants.

Preferential flow paths may originate from cracks and macropores (Bouma and Dekker, 1978; Beven and Germann, 1982; Bronswijk, 1991), from soil heterogeneity (Kung, 1990a,b) or from unstable wetting fronts (Raats, 1973; Philip, 1975a,b; Parlange and Hill, 1976; Glass et al., 1989a,b; Selker et al., 1989; Hendrickx and Dekker, 1991). Factors leading to the development of unstable wetting fronts include soil layering (Hillel and Baker, 1988; Glass et al., 1989b; Baker and Hillel, 1990), air entrapment (Glass et al., 1990) and water repellency (Van Dam et al., 1990; Dekker and Jungerius, 1990; Hendrickx et al., 1993).

In water repellent soils, preferential flow paths usually arise with the first rains just after a prolonged dry period. These preferential paths can persist for long periods

(Glass et al., 1989c) and, probably, disappear either after a drastic rise in the groundwater level, saturating the entire soil, or during an extensive drought.

Although the occurrence of preferential flow paths in water repellent soils has been verified by lysimeter experiments (Hendrickx and Dekker, 1991) and field studies (Van Dam et al., 1990; Hendrickx et al., 1993), the mechanisms of preferential flow and transport in water repellent sandy soils are not yet fully understood.

The objective of the study discussed in this Chapter was to describe, explain, and illustrate the mechanism of preferential flow in a water repellent sandy soil. For this purpose, a detailed tracer experiment was carried out. Conceptualization of the flow mechanism is a necessary step in developing a well-founded numerical simulation model (Glass et al., 1988; Bear and Bachmat, 1990).

2.2 MATERIALS AND METHODS

2.2.1 Water repellency tests

The degree of water repellency of a soil can be measured with the Water Drop Penetration Time (WDPT) and alcohol percentage tests (Letey et al., 1975; DeBano 1969 and 1981; King, 1981; Hendrickx et al., 1993; Dekker and Ritsema, 1994).

In the ***WDPT test***, three water drops are placed on the surface of a soil sample and the time required for infiltration is recorded. In the present study, the test was used to distinguish a maximum of ten classes of water repellency, based on the time needed for the water drops to penetrate into the soil: wettable soil (infiltration within 5 s), slightly water repellent soil (5 to 60 s), strongly water repellent soil (60 to 600 s), severely water repellent soil (600 s to 1 h), and extremely water repellent soil, with classes of 1 to 2 h, 2 to 3 h, 3 to 4 h, 4 to 5 h, 5 to 6 h, and more than 6 h. The WDPT test can be applied to either field-moist or oven-dried soil samples. Using field-moist samples reveals information about the actual water repellency of a soil sample. Field-moist samples were classified as *actually wettable* if water drops penetrated within 5 s, and as *actually water repellent* if more time was needed. Based on such measurements, *critical soil water contents* could be derived *below which a soil is water repellent* and *above which it is wettable.*

Applying the WDPT test to oven-dried soil samples yields information about the

degree of *potential water repellency*. Before applying the test, oven-dried samples were allowed to equilibrate in the laboratory for three days at a temperature of 20°C and at 50% air humidity. The effect of oven-drying on the possible development of water repellency was tested in advance by measuring water repellency degrees of samples after drying at 25, 45 and finally 65°C. For the samples used in the present study, originating from Ouddorp in the Netherlands, no indications were found that the degree of water repellency changed by drying the samples at 65°C compared to drying at 25°C or 45°C. In this study, therefore all samples were dried at 65°C for the assessment of the degree of potential water repellency. The upper part of the Ouddorp soil is extremely water repellent, while potential water repellency decreases deeper in the profile (Fig. 2.1).

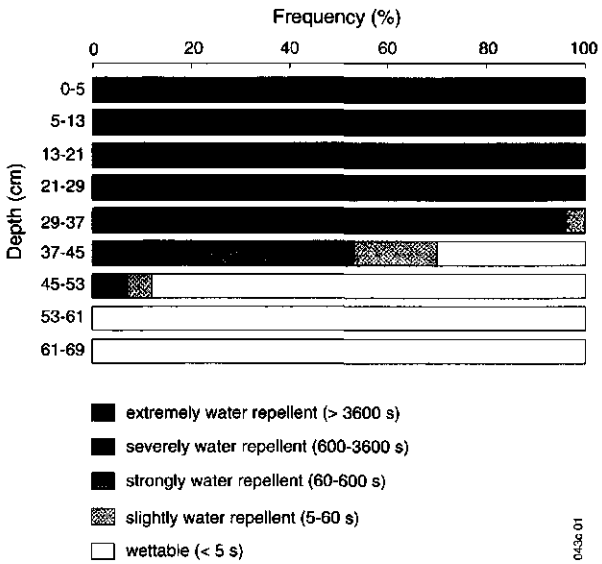

Fig. 2.1 *Relative frequencies of varying degrees of potential water repellency for nine layers of the Ouddorp experimental field.*

The ***alcohol percentage test*** was applied by preparing a series of aqueous ethanol solutions ranging in concentration between 0% and 27.5% (Dekker and Ritsema, 1994; Dekker, 1998). In this test, drops of the various solutions are placed on the surface of

field-moist or oven-dried (65°C) soil samples, and *the degree of actual or potential water repellency is then defined as the alcohol percentage of the weakest solution that still penetrates the soil within 5 s or less* (Dekker, 1998).

2.2.2 Soil and weather conditions

The field experiment was carried out on a grass-covered water repellent sandy soil, classified as a Mesic Typic Psammaquent (De Bakker, 1979), near Ouddorp in the southwestern part of the Netherlands. The soil consists of an approximately 10 cm thick humous surface layer, on top of non-calcareous fine dune sand to a depth of 75 cm, overlying calcareous fine sea sand. The organic matter content of the humous layer is approximately 20 w%, while below a depth of 10 cm it is less than 0.5 w%. The clay content of the soil profile is less than 3%.

Precipitation was collected at the experimental field and measured once a week. Daily precipitation rates were derived from daily measurements by a nearby meteorological station. Daily potential evaporation rates were also collected by this station. Groundwater levels were measured in observation tubes distributed at random over the experimental field (Fig. 2.2).

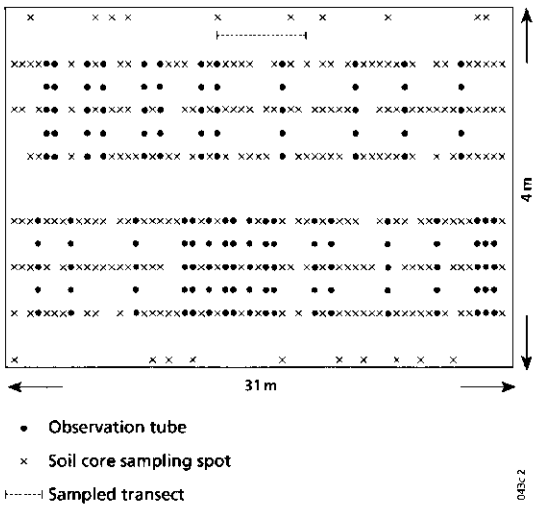

Fig. 2.2 *Lay-out of the experimental field.*

Precipitation rate, potential evaporation rate and groundwater levels during the period of field measurements are shown in Fig. 2.3. During the first 150 days, precipitation was relatively high and potential evaporation low, in contrast with the final part of the experiment, when precipitation decreased and potential evaporation increased. The groundwater level rose very quickly upon precipitation, dropping again during the final part of the experiment (Fig. 2.3). A total precipitation of 555 mm was measured in 206 days.

2.2.3 Field experiment

On November 6, 1988, a KBr tracer was applied to the surface of the experimental field (Fig. 2.2). The solution was sprayed manually onto the field with 6 nozzle sprinklers (Teejet 11002) spaced 0.33 m apart. The spraying pressure was 0.2 MPa and the spraying height 0.25 m. Speed of walking during spraying was 0.23 $m.s^{-1}$. During spraying, tracer samples were collected at 80 locations around the experimental field to measure the amount and distribution of the solution. The mean bromide application equalled 8.47 $g.m^{-2}$ (standard deviation 0.51 $g.m^{-2}$), which resembles a uniform tracer application.

The unsaturated zone was sampled just before spraying around the border of the experimental field, and within the field at 11, 17, 45, 60, 67, 81, 88, 103, 130, 152 and 206 days after the tracer application. Each sampling campaign consisted of a random selection of 20 spots in the experimental field. At each spot, the soil was sampled using a cylindrical soil core sampler with a length of 1 m and an internal diameter of 0.1 m (Hendrickx et al., 1991). After the cover had been removed from the cylindrical core sampler, the soil inside was contiguously sampled using 10 to 12 small (205 cm^3) steel cylinders. In 12 sampling campaigns (12 times 20 soil cores = 240 soil cores), nearly 3000 samples were taken and used to measure soil water contents (oven-drying method), degree of potential water repellency (WDPT test), and bromide concentrations (HPLC technique).

The samples were first oven-dried for at least two days at 65°C to determine the water content and the water drop penetration time. Subsequently, a fixed amount of distilled water was added to the samples, they were shaken for a couple of hours, and the water itself was used to determine bromide concentrations.

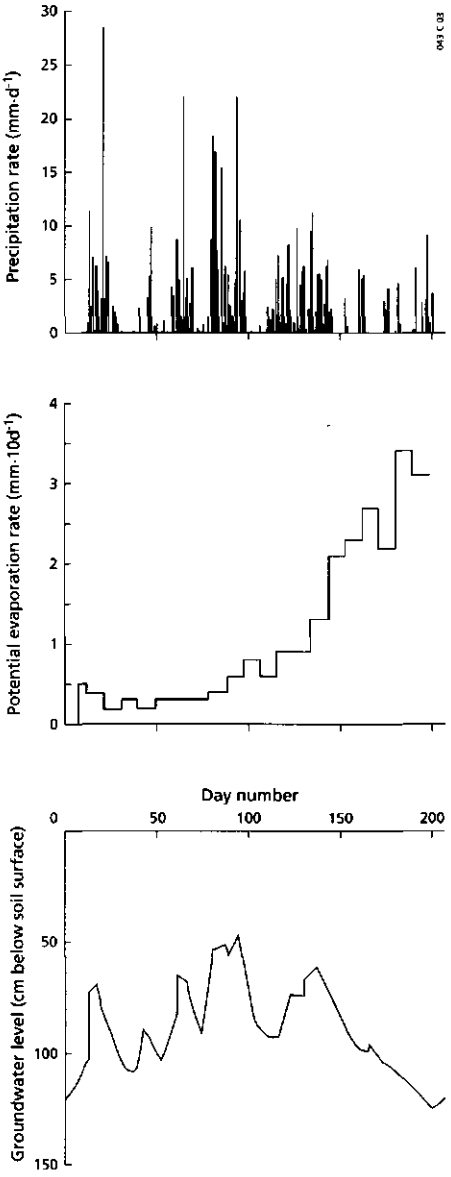

Fig. 2.3 *Precipitation rate, potential evaporation rate and groundwater levels measured during the experiment.*

The saturated zone was sampled regularly by extracting water from the groundwater tubes (Fig. 2.2), which had either filters at depths of 55-75, 75-95, 95-115, 115-135 or 145-165 cm.

The spatial distribution and the dimensions of preferential flow paths and dry soil parts could be visualized using volumetrically determined soil water contents of samples taken at five depths in a 5.5 m long transect (see Fig. 2.2). For each depth, 100 contiguous soil samples were taken.

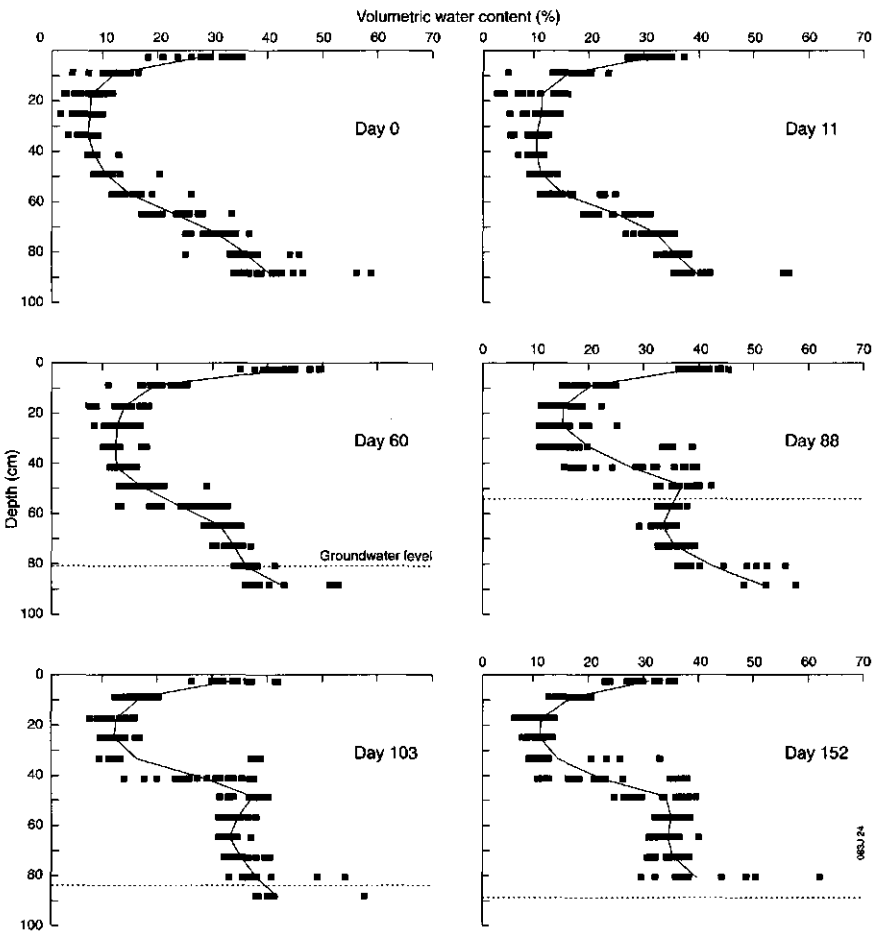

Fig. 2.4 *Measured volumetric water contents and the calculated mean versus depth for days 0, 11, 60, 88, 103 and 152.*

2.3 RESULTS AND DISCUSSION

2.3.1 Soil water content and tracer concentrations

The initial volumetric water contents per layer are shown in Fig. 2.4, together with the calculated average profile. Below the wet humous surface layer there was approximately 40 cm of relatively dry soil, and then a progressively wetter zone. The groundwater level on the day of sampling was 120 cm below the soil surface.

Soil water contents measured on days 11, 60, 88, 103 and 152 are also shown in Fig. 2.4. Despite the total rainfall of 486 mm in 152 days, the zone just below the humous layer remained relatively dry (Fig. 2.4). Volumetric water contents in the lower part of the profile clearly increased in the course of the experiment, especially around day 80, due to a sharp rise in the groundwater level (Fig. 2.3).

Fig. 2.5 shows for days 11, 17, 60, 88, 103 and 152, measured bromide concentrations versus depth together with the average tracer concentration profile. The bromide concentrations varied greatly even at equal depths, especially just after the beginning of the experiment. The mechanisms that led to these patterns are explained below.

2.3.2 Flow patterns

'Distribution flow' toward preferential paths

Contiguous sampling of the soil profile offers the possibility of calculating the total quantity of tracer in each vertical soil core. The tracer quantities within each of the 20 cores sampled on a specific day can be compared and related to the initial quantity of the tracer sprayed on the soil surface per unit of surface area at the beginning of the experiment (see Fig. 2.6).

Fig. 2.7 shows the total quantity of bromide found in each soil core on day 11. Ten of the 20 soil cores contained more bromide than had been applied to the soil per unit of surface area. This indicates that the uniform bromide application (8.47 $g.m^{-2}$, SD 0.51 $g.m^{-2}$) to the soil surface had been converted into a non-uniform distribution in the unsaturated zone within 11 days. Bromide quantities as high as 170% and as low as 40% of the original application were found in individual cores. However, the total

bromide recovery within the 20 soil cores on day 11 equalled 99.6%. Bromide recovery rates in the soil layer to a depth of 69 cm are summarized in Table 2.1 for all sampling days. After day 11, bromide started to leach from this layer into the region below 69 cm depth.

Thus within 11 days, the uniformly applied tracer solution had become unevenly distributed in the soil, due to spatial variations in soil water content within the experimental field. At the moment of tracer application, the humous surface layer was

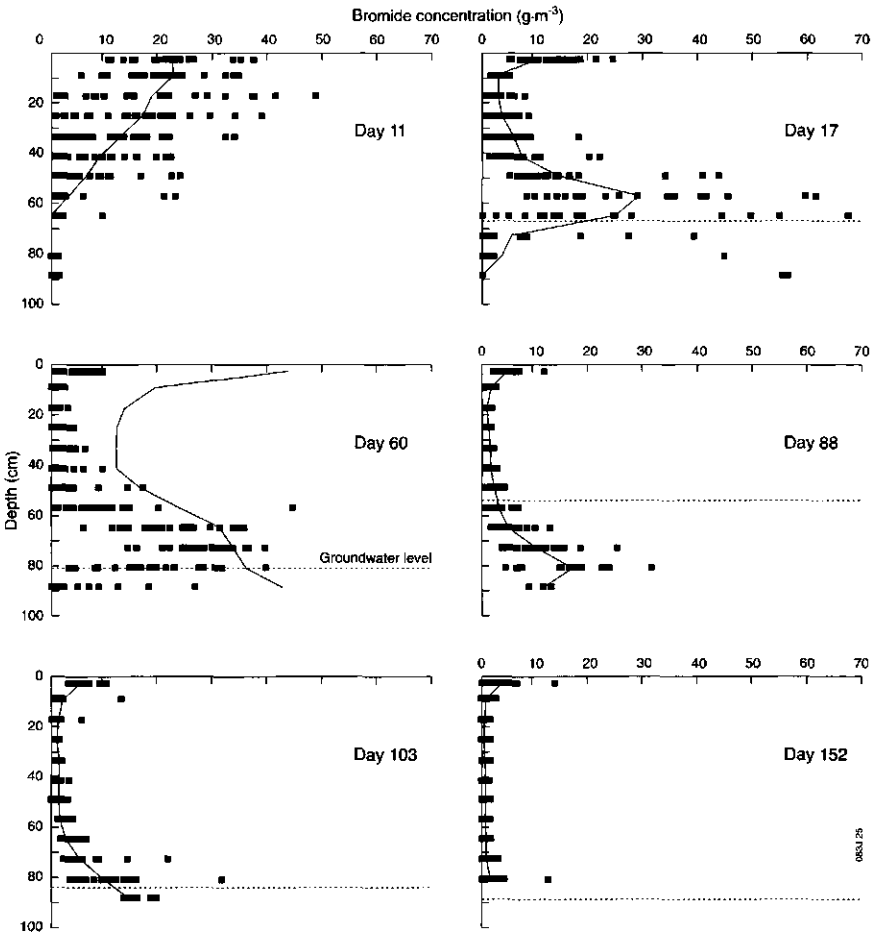

Fig. 2.5 *Measured bromide concentrations and calculated mean versus depth for days 11, 17, 60, 88, 103 and 152.*

Table 2.1 *Bromide recovery rates (% of total application) in the soil profile to a depth of 69 cm for all sampling days.*

	Day										
	11	17	45	60	67	81	88	103	130	152	206
Bromide											
% of total	99.6	93.2	59.2	40.2	22.3	15.9	17.9	15.5	7.4	5.3	4.3

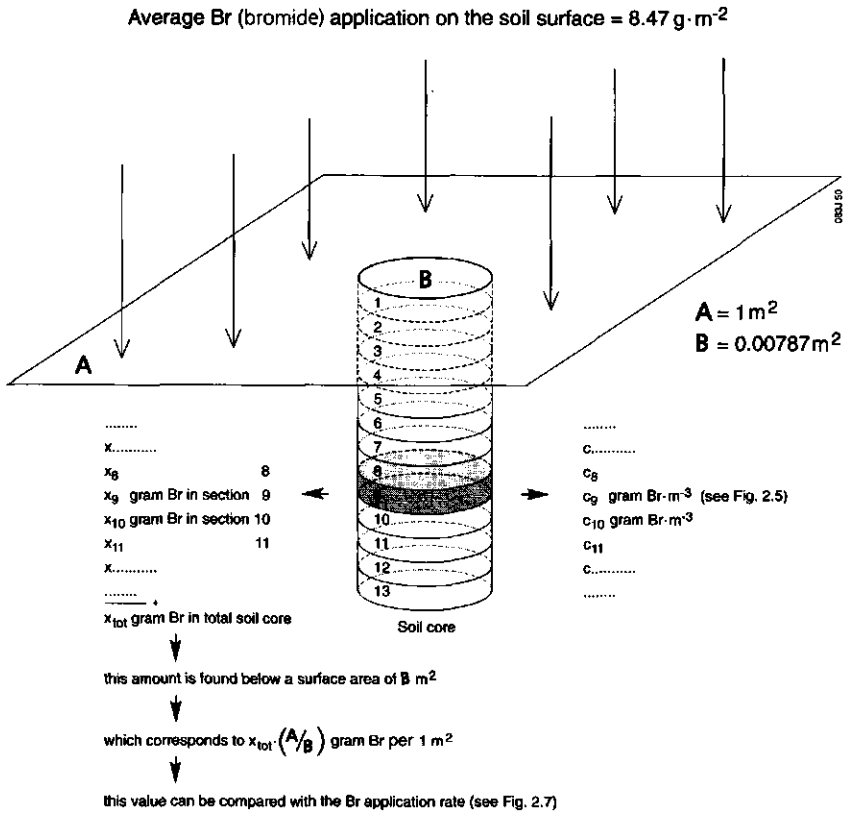

Fig. 2.6 *Calculation procedure to convert bromide amounts per soil core section into bromide concentrations ($g.m^{-3}$) and recovered bromide amounts per m^2.*

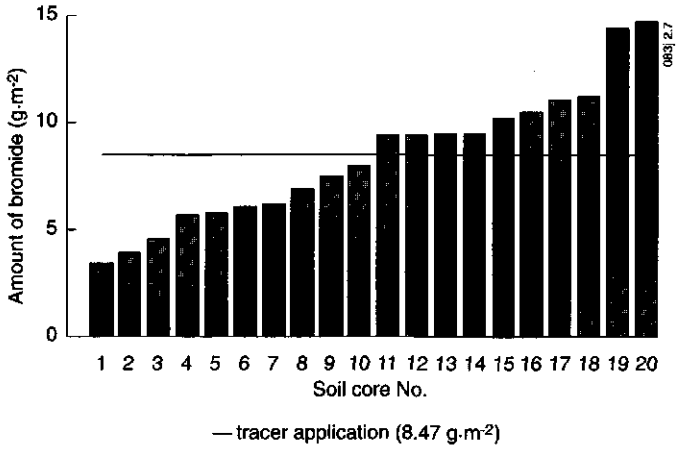

Fig. 2.7 *Measured quantity of bromide per unit of surface area for all soil cores sampled on day 11.*

relatively wet compared with deeper layers (see Fig. 2.4). Below the 10 cm top layer, the soil showed dry regions alternating with vertical preferential flow paths. An illustration of this pattern is given in Fig. 2.8, in which the dark areas represent the wet and the light areas the dry soil zones.

Rainwater infiltrating into the relatively wet humous surface layer and reaching a dry zone like that shown in Fig. 2.8 will deviate from its vertical path and flow laterally through the topsoil towards a preferential path.

The lateral flow in the surface layer distributes water and solutes towards individual preferential flow paths and is referred to as '*distribution flow*' in this study. Fig. 2.9 illustrates the effects and confirms the existence of distribution flow. It shows the total bromide quantity per soil core on day 11 versus the water content of the soil layer at depths between 5 and 21 cm.

A clear relationship exists between the water content of this layer and the total quantity of bromide found within each sampled core. The wetter the soil, the higher the observed bromide amounts, indicating that dry, water repellent zones prevent the

Fig. 2.8 *Wet top layer with vertically directed preferential flow paths below it.*

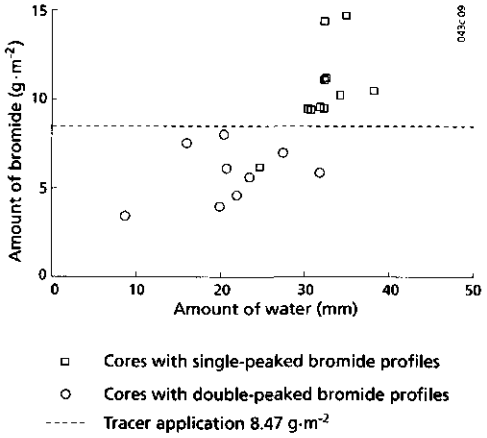

Fig. 2.9 *Relation between the total amount of bromide in the soil cores taken on day 11 and the amount of water in the layer between 5 and 21 cm depth.*

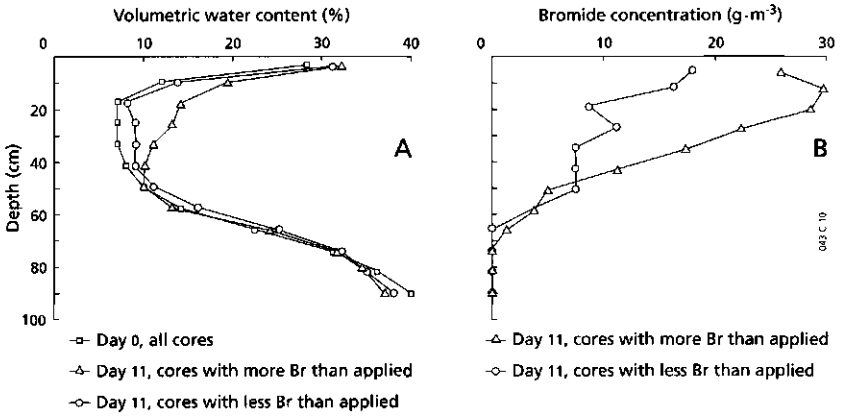

Fig. 2.10 A. *Mean volumetric water contents for day 0, and for day 11 for cores with more and less bromide than the average bromide application.*
B. *Mean bromide concentrations on day 11 for cores with more and less bromide than the average application.*

downward flow of water and solutes, whereas wet areas act as preferential paths for a concentrated transport to deeper regions. This pattern is also illustrated by Fig. 2.10. The cores containing more bromide than had been applied not only had more water in the top 45 cm of the soil profile (Fig. 2.10A), but they also had higher mean bromide concentrations compared to the other cores (Fig. 2.10B).

After 11 days, a totally heterogeneous distribution of bromide was established within the soil. This typical pattern largely determined the further flow of water and solutes within the experimental field during the remaining part of the experiment. The soil conditions at the beginning of the experiment, i.e. the presence of the wet humous layer and the alternation between dry soil regions and vertical preferential flow paths below it, were found to be of major importance to the way in which water and solutes moved through the experimental field.

Preferential flow paths and dry soil regions

An indication of the spatial distribution and dimensions of the preferential flow paths

and dry soil regions on October 11, 1988, is shown in Fig. 2.11. In the upper part of the profile, horizontal dimensions of the (wet) preferential flow paths varied between 10 and 20 cm, and exceptionally reached sizes of 25 cm. Deeper in the profile, the

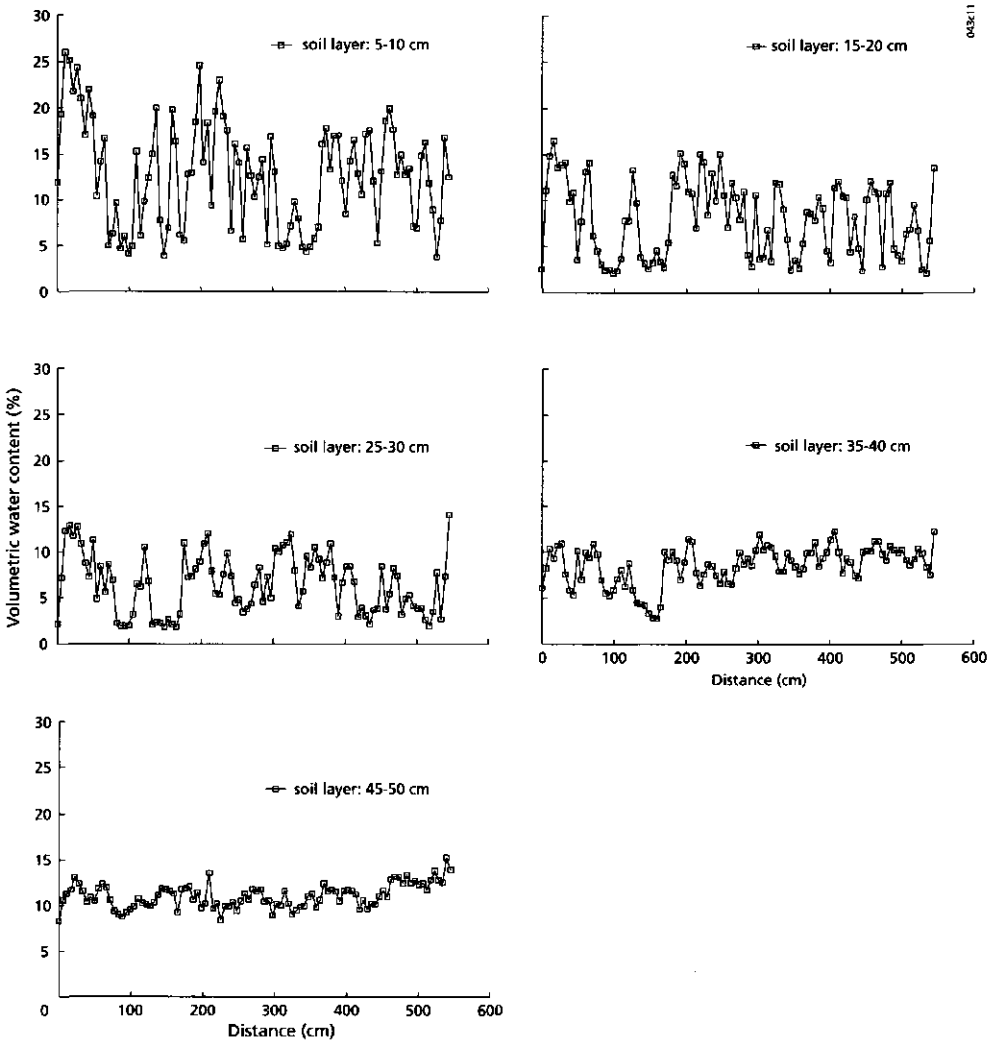

Fig. 2.11 *Measured volumetric water contents at five depths in a 5.5 m long transect on October 11, 1988.*

differences between dry and wet zones diminished, leading to more uniform volumetric water contents.

Fig. 2.12 shows a soil core sampled during the experiment, containing an almost complete preferential path (dark area), embedded in dry soil (light area). The spatial distribution and dimensions of the preferential paths and dry soil parts determine whether each sampled soil core will contain material from preferential flow paths or dry soil zones alone, or from both. The soil core depicted in Fig. 2.12 clearly shows that a mixed sampling of wet (dark) and dry (light) soil had occurred in this case.

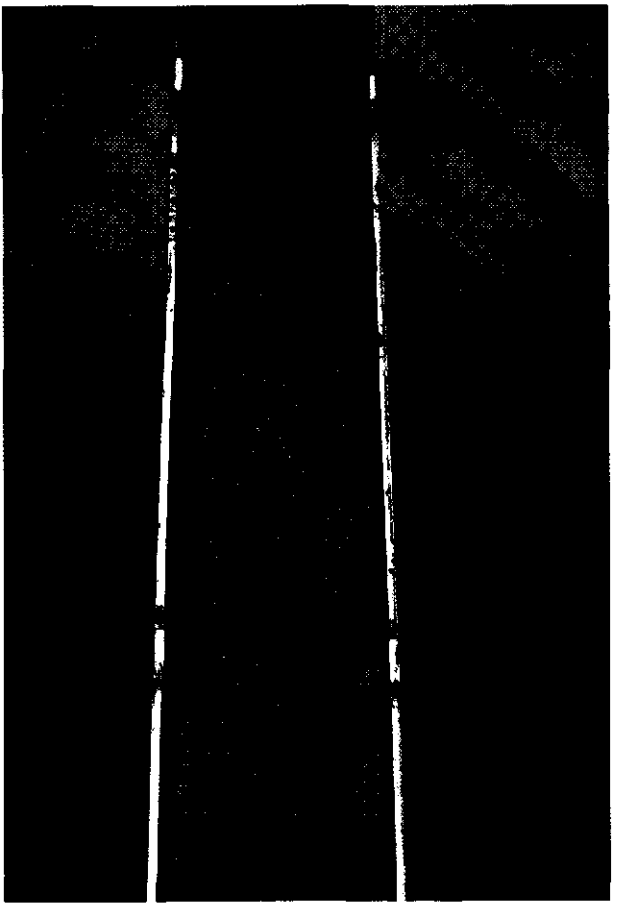

Fig. 2.12 *Sampled soil core with an almost complete preferential path (dark area) embedded in dry soil (light area).*

Diverging flow below the water repellent zone

Fig. 2.1 shows that the degree of potential water repellency of the Ouddorp sandy soil decreases with depth. Below around 50 cm depth, the soil is classified wettable. The flow mechanism in this zone differs distinctly from that in the upper parts of the soil profile. Whereas in the humous layer, water and solutes are horizontally transported by distribution flow to the vertical preferential flow paths, the opposite occurs deeper in the profile: water and solutes spread out, i.e., diverge from the bottom end of the preferential flow paths, reducing spatial differences in volumetric water contents and solute concentrations. In Fig. 2.13 this layer is represented by the wet (dark) zone starting below the bottom end of the preferential flow paths and the intermediate dry soil regions.

That flow actually diverged during the first 11 days of the experiment is illustrated by Fig. 2.14, which shows a double-peaked bromide profile for one of the soil cores sampled on day 11. Bromide recovered in this core was less than the average

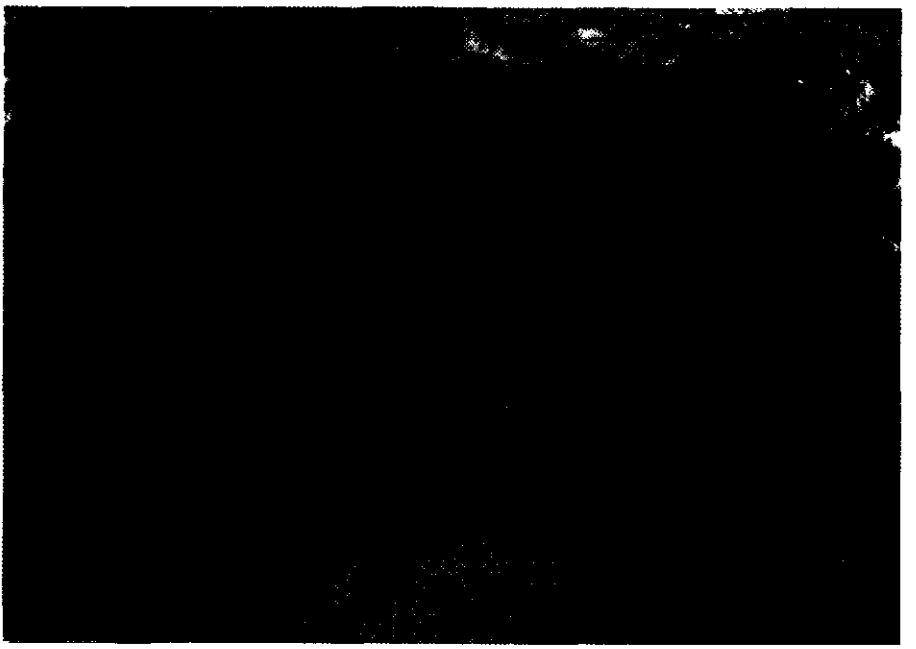

Fig. 2.13 *Relatively wet (dark) zone below the heterogeneously wetted water repellent soil layer.*

application per unit of surface area. Nine of the 10 soil cores sampled on day 11 which contained less bromide than the original application exhibited such double-peaked tracer profiles (Fig. 2.9). The deeper bromide peaks were caused by the diverging flow of water and bromide from the bottom end of preferential flow paths towards surrounding areas below dry soil parts. This process resulted in a more widespread occurrence of bromide in the wettable zone than was observed in the water repellent layer. This was confirmed by the fact that the first detection of bromide in the saturated zone occurred on exactly the same day (15 days after the tracer application) all over the experimental field (samples collected from the randomly placed groundwater tubes, see Fig. 2.2). Despite this fact, spatial variability in bromide concentration remained relatively high in the wettable zone (see Fig. 2.5), and in the groundwater. Bromide concentrations in the groundwater at different locations on day 15 ranged from 1 to 160 $mg.l^{-1}$. On day 11, bromide could not be detected in any of the samples collected from the groundwater tubes. The large variability in bromide concentrations in the wettable zone and in the groundwater was mainly caused by the heterogeneous input from out of the water repellent layer with the preferential flow paths.

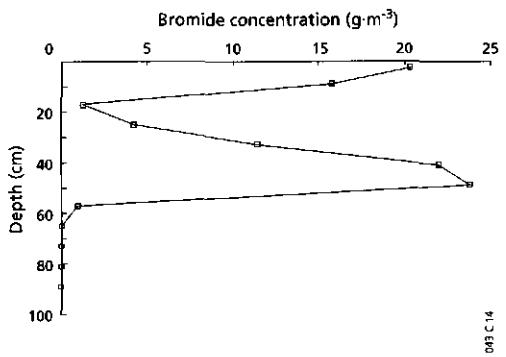

Fig. 2.14 *A double-peaked bromide profile of one of the soil cores collected on day 11.*

2.3.3 Conceptualization

A two-dimensional visualization of the flow pattern within this water repellent sandy soil is shown schematically in Fig. 2.15. The various dimensions are only indicative

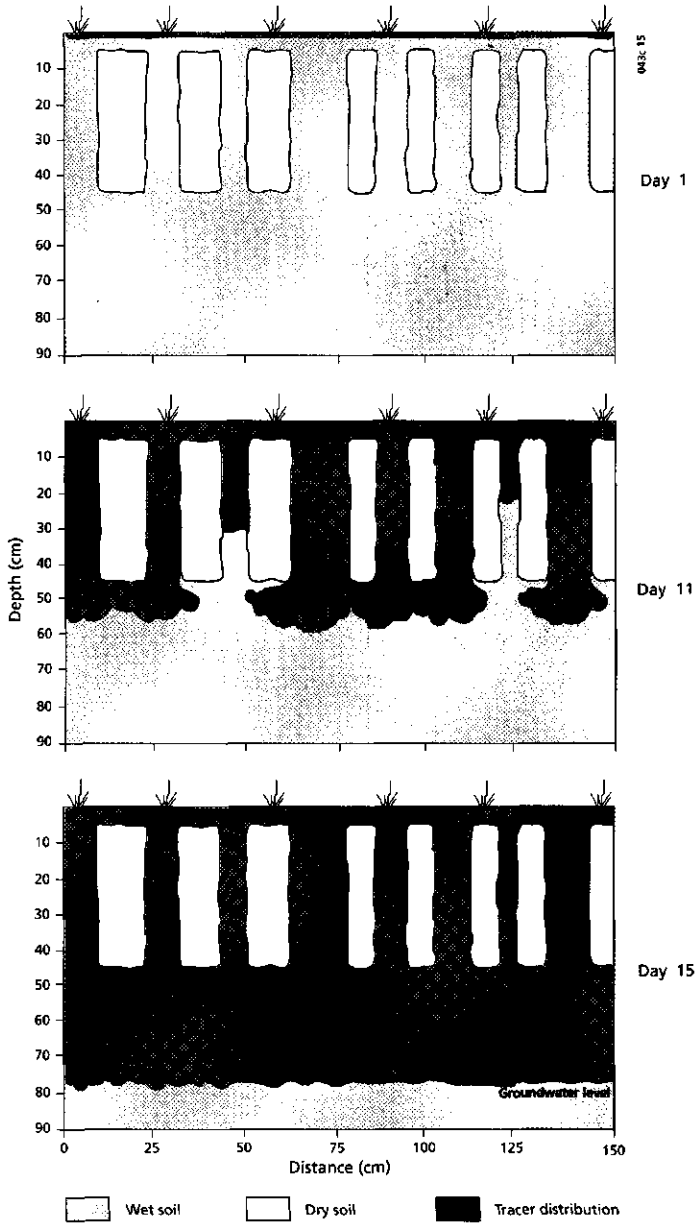

Fig. 2.15 *Two-dimensional visualization of the flow pattern within the water repellent sandy soil in Ouddorp.*

and are estimations from field observations. Nevertheless, Fig. 2.15 is useful, as it clearly illustrates and exemplifies the heterogeneity and complexity of the flow of water and solutes in this type of water repellent sandy soil. This conceptual model, arisen from and based on a detailed analysis of numerous measurements and field observations, is an essential step in developing a numerical simulation model to describe flow and transport in water repellent sandy field soils.

So far, most studies dealing with preferential flow have focused mainly on the vertical flow paths themselves. The existence of preferential flow paths is, however, inherently connected with the occurrence of distribution flow in the zone above the layer with preferential flow paths. In the immediate vicinity of the preferential flow paths, the distribution flow converges towards the vertical paths, 'feeding' them with water and solutes. *A completely new finding from this study is the occurrence of diverging flow in wettable zones below water repellent soil layers.* This may counteract the rapid transport through the water repellent soil layers as water and solutes are laterally redistributed in the wettable zone. This process may well occur in all water repellent field soils, as water repellency decreases with depth in most soils due to the decreasing quantities of roots and humic substances, which are an important cause of water repellency. Expectations of environmental effects of preferential flow in water repellent soils based on laboratory experiments (i.e. without diverging flow) may thus be overestimated for field conditions.

Finally, it may be observed that *preferential flow in water repellent sandy field soils involves the complete, integrated process of distribution flow in the humous surface layer, the vertical flow through the preferential flow paths, and the diverging flow in the wettable zone below the water repellent soil layers.*

2.4 CONCLUSIONS

Within 11 days after a uniform surface application of bromide, distribution flow in the relatively wet humous layer resulted in a spatially heterogeneous bromide distribution within the experimental field. Just below the relatively wet surface layer, preferential flow paths were present with diameters generally ranging between 10 and 20 cm. Between the flow paths, dry soil regions were found with widths ranging from 5 to 30 cm. Due to their extremely water repellent character, the dry soil parts were difficult

to wet from above, forcing infiltrating water and solutes to move laterally toward preferential flow paths, and then through the preferential flow paths to deeper regions. Deeper in the profile, in the wettable zone below a depth of around 45 to 50 cm, water and solutes diverged from the preferential flow paths toward surrounding areas below dry soil zones, as could be concluded from the double-peaked bromide profiles. Below this zone, bromide was transported to deeper regions with a tracer front which was more or less parallel to the soil surface. Despite this process, spatial variations in bromide concentrations remained high in both the wettable zone and the underlying groundwater system.

CHAPTER 3

DISTRIBUTION FLOW

Adapted version of 'Distribution flow: a general process in the top layer of water repellent soils' by C.J. Ritsema and L.W. Dekker, published in Water Resources Research 31:1187-1200, 1995.

3 DISTRIBUTION FLOW

Abstract

Water and solute input rates on the soil surface may vary considerably from place to place. Distribution flow, i.e. the process of water and solute flow in a lateral direction over and through the surface layer of the soil profile, is an important process in distributing the rainfall towards places where vertical transport occurs. The study reported on in this Chapter was carried out to quantify the process of distribution flow and its underlying process mechanism. A KBr tracer was applied to a water repellent sandy soil to follow the actual flow paths of water and solutes in the upper part of the profile. In the experimental field, distribution flow actually displaced the applied bromide laterally through a very thin surface layer, referred to here as the '*distribution layer*'. Distribution flow was directed towards those locations within the 0-2.5 cm layer where the soil was the least potentially water repellent. At these relatively wet areas, bromide was detected at greater depths and concentrations of bromide were among the highest.

3.1 INTRODUCTION

Simulation models are widely used for predicting water and solute transport through the unsaturated soil (Gee et al., 1991; Van Genuchten, 1991). As models are a simplified schematization of reality, model output often shows discrepancies when compared with actual field measurements (Philip, 1991; Jury and Flühler, 1992). This is unfortunate, as models are supposed to be reliable tools for predicting water and solute transport under a variety of soil and climatic conditions. In reality, water and solute transport through unsaturated soil is often a much more complex process than assumed and formulated in simulation models. One of the main simplifications in models is the use of spatially uniform water and solute input rates on the soil surface. In reality these rates vary considerably from place to place (Beven, 1989, 1991a), sometimes even within short distances (Dunne et al., 1991; Agus and Cassel, 1992). Such highly variable input rates may locally accelerate the downward transport of water and solutes, leading to losses of surface-applied nutrients and/or to higher

contamination risks of groundwater reservoirs.

Several factors contribute to the occurrence of spatially variable input rates. It is well-known that vegetation is able to intercept rainwater (Návar and Bryan, 1990) and to direct this water towards the root zone by stemflow (Gwyne and Glover, 1961; Saffigna et al., 1976; Crabtree and Trudgill, 1985; Parkin and Codling, 1990). According to Beven (1991b), stemflow may account for as much as 15 percent of the incident rainfall, depending on vegetation type and vegetation cover density (Glover and Gwynne, 1962; Reynolds, 1970; Dunne et al., 1991). The stemflow is concentrated on a narrow region around the base of the plant and, in the case of infiltration, a wetter soil can be expected at these spots than in surrounding areas (Specht, 1957; Glover and Gwynne, 1962; Hills and Reynolds, 1969; Van Wesenbeeck and Kachanoski, 1988a,b).

If rainwater reaches the soil surface, either directly or via throughfall or stemflow, lateral flow over and within the soil profile may further displace water and solutes. Within the soil profile, textural discontinuities, characterized by pronounced permeability breaks, may induce lateral flow components parallel to the layer interfaces (Ahuja and Ross, 1982; Selim, 1987; Parlange et al., 1989; Steenhuis et al., 1991). Recently, it has been shown by McCord and Stephens (1987) and McCord et al. (1991) that such textural discontinuities are not a prerequisite for the inducement of lateral flow, because soil water differences themselves may already result in a system which behaves anisotropically with respect to water flow. In addition to these aspects, a certain degree of slope is generally needed to induce lateral flow over or through soils (Sinaï et al., 1981; Zaslavsky and Sinaï, 1981a,b,c).

The most pronounced textural and structural changes (Nielsen et al., 1973; Cameron, 1978), and the most distinct soil water content differences (Hills and Reynolds, 1969; Loague, 1992) are often found in the upper part of the soil. Furthermore, the soil surface and layer interfaces themselves are to some extent irregularly configurated, at least at microscale (Bruneau and Gascuel-Odeux, 1990). At mesoscale or macroscale, particularly in uneven terrains, analogous topographic features or irregularities of a greater magnitude can be superimposed over those present at the microscale. These micro-, meso- and macrotopographic irregularities of soil surfaces and layer interfaces directly induce and promote the occurrence of lateral flow. The fact that in the top layer of soils, lateral flow may actually dominate vertical infiltration has already been demonstrated in previous studies for a variety of soils (Mosley, 1982; Bathke and

Cassel, 1991; Wilson et al., 1991; Bathke et al., 1992) and modeling studies (Hurley and Pantelis, 1985; Wallach and Zaslavsky, 1991; Jackson, 1992). However, the direct effects of this lateral flow process under natural field conditions have so far not been quantitatively evaluated.

Recently, Ritsema et al. (1993) indicated that lateral flow within the surface layer of a water repellent sandy soil was the process responsible for displacing a uniformly applied bromide tracer (Chapter 2). In those places within the experimental field where, due to lateral flow, water and bromide were concentrated, distinct vertically directed preferential flow paths were found with diameters between 10 and 20 cm. The term 'distribution flow' was introduced to account for the overall process of lateral flow over and through the surface layer of the soil profile towards places where vertical infiltration actually occurs. Subsequently, those places which receive considerably more water and solutes than the areal average are the places where accelerated downward transport can be expected. This may have serious environmental consequences such as local pollution of groundwater reservoirs. Reynolds (1970), Cameron et al. (1979), Beven (1989, 1991a), and Jury and Roth (1990) have already stipulated the existence of lateral flow in the top layer of soils and its possible consequences in terms of accelerating downward water and solute transport in specific places. However, no serious attempts have so far been made to quantify to what extent distribution flow is able to displace water and solutes at field-scale. The objectives of the present study were to describe and illustrate the process of distribution flow, and to quantify its effects on the displacement of water and solutes in a water repellent sandy soil.

3.2 MATERIALS AND METHODS

3.2.1 Tracer experiment

In a 4 m by 30 m experimental field at Ouddorp, a KBr solution was applied manually with six nozzle sprinklers (Teejet 11002) on November 6, 1988 (see Chapter 2). The mean bromide application equalled 8.47 $g.m^{-2}$, with a standard deviation of 0.51 $g.m^{-2}$.

The unsaturated zone was sampled twelve times (see Chapter 2) using the cylindrical soil core sampler (Hendrickx et al., 1991). The present Chapter focuses on the sampling campaigns on days 11, 17 and 45. On each sampling day, 20 soil cores were

randomly collected in the experimental field. Each sample was used to determine soil water content and bromide concentration (see Chapter 2). Groundwater levels and precipitation were also measured (see Fig. 2.3).

3.2.2 Soil sampling for the analysis of correlative patterns

At the Ouddorp experimental field, a total of 1400 samples were collected on November 2, 1992. An 1.2 m by 0.6 m area had been selected for this purpose. The microtopography of this area was determined by using a simple device to measure the distance of the soil surface to a fixed leveled reference plate installed at a certain height above the soil surface. Elevation values were obtained for 200 individual points regularly spaced in an equidistant grid of 20 by 10 points. The distance between the points was 5.5 cm. At each grid point, soil samples (diameter 5 cm, height 5 cm) were also taken. A total of seven layers were sampled in this way, at depths of 0-5, 7-12, 14.5-19.5, 22-27, 29.5-34.5, 39-44 and 47-52 cm. Samples taken in the 0-5 cm layer were split into two parts to obtain information about both the 0-2.5 cm and the 2.5-5.0 cm layers.

All samples were used to determine soil water content, dry bulk density and the degree of potential water repellency. Soil surface microtopography was visualized using a spatial interpolation program which was able to generate contour plots. This was also done to visualize spatial distributions of soil water content, dry bulk density and water repellency for individual horizontal and vertical planes. The present study concentrated on the 0-2.5 cm layer and on a selected vertical cross-section intersecting this surface layer.

3.3 RESULTS

3.3.1 Tracer experiment

Table 3.1 summarizes the average values, standard deviations and coefficients of variation for soil water contents, dry bulk densities and bromide concentrations at the Ouddorp experimental field.

Table 3.1 *Volumetric soil water content, dry bulk density, and bromide concentrations per depth interval at the Ouddorp site on days 11, 17 and 45. Mean values, standard deviations (SD), and coefficients of variation (CV) are listed.*

Depth	Soil water content			Dry bulk density			Bromide conc.		Number
	Mean	SD	CV	Mean	SD	CV	Mean	SD	
(cm)	(%)	(%)	(%)	($g.cm^{-3}$)	($g.cm^{-3}$)	(%)	($g.m^{-3}$)	($g.m^{-3}$)	*n*
				Day 11					
0- 5	31.4	2.8	8.8	0.69	0.12	17.1	22.2	6.8	20
5-13	16.3	3.8	23.4	1.39	0.06	4.5	22.9	12.3	20
13-21	11.0	3.8	34.8	1.53	0.04	2.5	18.8	13.2	20
21-29	11.1	2.3	21.2	1.56	0.03	1.8	16.9	10.3	20
29-37	10.0	1.8	17.8	1.56	0.03	1.9	12.7	9.0	20
37-45	9.8	1.1	10.8	1.54	0.02	1.4	9.4	7.3	20
45-53	10.6	1.2	11.7	1.54	0.03	1.9	6.4	6.9	20
53-61	14.7	3.9	26.3	1.56	0.04	2.4	3.3	6.5	20
61-69	24.4	4.1	16.7	1.61	0.03	1.8	0.7	2.1	20
69-77	31.8	2.3	7.4	1.63	0.03	2.1	<0.1	-	20
77-85	35.1	1.5	4.3	1.63	0.03	1.8	<0.1	-	20
85-93	39.3	5.9	14.9	1.55	0.18	11.3	<0.1	-	20
				Day 17					
0- 5	36.4	3.8	10.5	0.82	0.12	14.1	15.5	6.4	20
5-13	19.3	4.0	20.5	1.42	0.05	3.3	2.9	0.9	20
13-21	13.5	2.8	21.0	1.52	0.03	1.9	2.7	1.7	20
21-29	12.9	1.9	14.6	1.55	0.03	1.7	3.8	2.1	20
29-37	13.2	2.2	16.7	1.54	0.02	1.5	5.5	3.6	20
37-45	14.8	3.0	20.1	1.53	0.03	1.6	7.5	5.2	20
45-53	18.5	4.3	22.6	1.54	0.02	1.0	14.7	11.0	20
53-61	26.7	3.1	11.5	1.59	0.03	1.7	29.4	15.3	20
61-69	31.8	1.5	4.7	1.62	0.02	1.0	24.4	22.6	20
69-77	34.5	2.1	6.2	1.62	0.03	1.7	5.4	10.4	20
77-85	38.2	7.1	18.7	1.56	0.20	13.0	3.6	11.5	14
85-93	38.2	-	-	1.63	-	-	<0.1	-	1
				Day 45					
0- 5	33.5	3.2	9.5	0.76	0.13	17.0	9.6	3.8	20
5-13	16.1	3.2	19.7	1.43	0.06	4.1	3.4	1.2	20
13-21	10.2	3.5	34.0	1.52	0.03	2.0	2.7	0.9	20
21-29	9.7	2.6	27.3	1.54	0.03	1.7	2.6	0.9	20
29-37	10.0	1.6	15.7	1.54	0.03	1.6	2.5	1.2	20
37-45	10.1	2.4	24.2	1.54	0.04	2.8	3.1	1.8	20
45-53	13.6	4.1	30.3	1.53	0.03	2.2	4.9	2.9	20
53-61	20.4	5.6	27.3	1.56	0.03	2.1	12.7	10.0	20
61-69	30.4	2.1	7.0	1.61	0.03	1.9	24.8	10.1	20
69-77	33.9	1.7	5.1	1.62	0.03	1.8	24.2	10.4	20
77-85	36.9	2.5	6.7	1.61	0.09	5.3	12.4	8.0	20
85-93	43.0	8.0	18.5	1.41	0.23	16.7	3.1	3.8	12

Mean volumetric soil water contents within the experimental field varied between 9.8% and 39.3% on day 11, between 12.9% and 38.2% on day 17, and between 9.7% and 43% on day 45. In general, high water contents were found within the humous top layer (i.e. 0-5 cm) and in the deeper parts of the profile. It was particularly the intermediate depth, between approximately 15 and 50 cm, which remained relatively dry throughout the experiment. Standard deviations ranged between 1% and 8% (Table 3.1). The high standard deviation observed in the bottom layer on each sampling day was caused by the presence of peaty material in two of the soil cores sampled on days 11 and 17, and in five of the soil cores collected on day 45. Soil cores containing such peaty material had extremely high soil water contents and low dry bulk densities, leading to high standard deviations (SD) and coefficients of variation (CV) for these layers (Table 3.1). Mean dry bulk density varied between 0.69 and 0.82 $g.cm^{-3}$ for the humous top layer, and values of around 1.5 to 1.6 $g.cm^{-3}$ were commonly found in the deeper parts of the profile. Highest standard deviations and coefficients of variation were found for the 0-5 cm layer and for the bottom layers of the sampled profiles which contained peaty material.

Between the day of bromide application and day 11, 37.2 mm of precipitation were recorded, causing the bromide to advance rather deeply into the profile (Table 3.1). The highest mean bromide concentration was found in the 5-13 cm layer, and the highest standard deviation just below this zone. Between days 11 and 17, another 50.7 mm of rain were registered, resulting in an even deeper movement of water and bromide. Highest bromide concentrations on day 17 were found in the 53-61 cm layer, and the highest standard deviation somewhat deeper (Table 3.1). Between days 17 and 45, 34.0 mm of precipitation were measured. On day 45, the highest mean bromide concentration was found in the 61-69 cm layer and the highest standard deviation just below this layer.

The total amount of bromide recovered to a depth of 93 cm in the 20 soil cores equalled 99.6 % for day 11, 102.5% for day 17, and 95.5% for day 45. Fig. 3.1 shows the total recovered bromide per soil core per unit surface area, together with the mean bromide application quantity (based on 80 measurements) and its lower and upper 95% confidence limits.

Around 95% of the soil cores sampled were expected to contain total bromide quantities within the given range of application shown in Fig. 3.1A. On day 11, eight

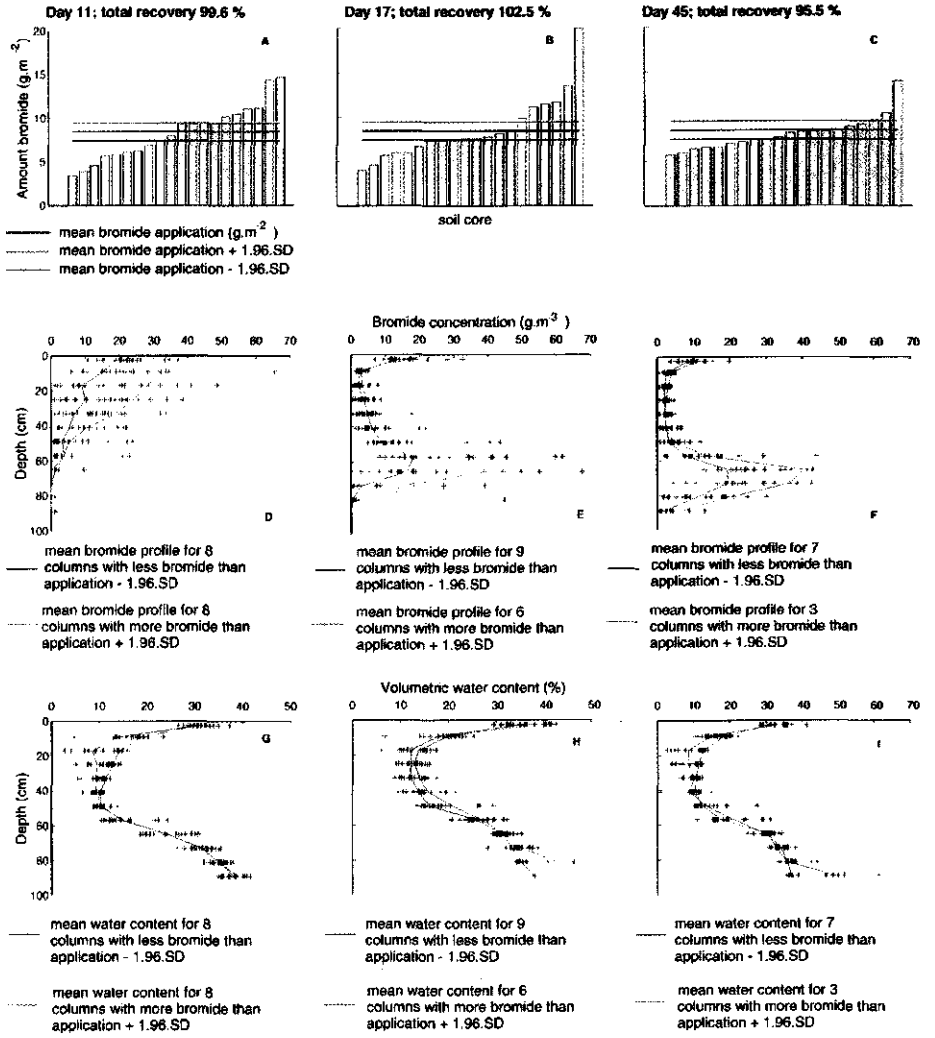

Fig. 3.1 *Quantities of bromide per unit surface area recovered in the soil cores (A, B, C), bromide concentrations (D, E, F) and volumetric soil water contents (G, H, I) at the Ouddorp experimental field for the sampling days 11, 17 and 45. Mean bromide concentration profiles and mean soil water content profiles are shown for the groups of cores containing more and less bromide than the upper and lower 95% confidence limits of the amount of tracer applied.*

cores contained more bromide than the upper confidence limit of 9.47 $g.m^{-2}$ and eight cores contained less bromide than the lower confidence limit of 7.47 $g.m^{-2}$. Therefore, it can be concluded that in 80% of the soil cores sampled, lateral inflow or outflow of bromide increased or decreased the total bromide quantities significantly during these 11 days. Mean bromide concentrations and mean volumetric soil water contents versus depth are shown for two groups of soil cores. One group showed significantly higher quantities than applied, while the other showed significantly lower bromide quantities than those applied. In those cores containing more bromide than the upper confidence limit, bromide had advanced slightly deeper into the profile (Fig. 3.1D). The reason was that the profiles of these cores in the water repellent zone, to a depth of approximately 45 cm, were wetter (Fig. 3.1G). On day 17, six of the 20 cores sampled contained significantly more bromide, and nine contained significantly less bromide than applied (Fig. 3.1B). Mean bromide concentration and soil water content profiles for these two groups of soil cores confirmed the observations of day 11. In those cores with high quantities of bromide, bromide reached greater depths than in the other group of cores (Fig. 3.1E), due to the wetter conditions in the former group (Fig. 3.1H).

On day 45, three cores contained higher quantities of bromide than the upper confidence limit, while seven cores contained lower quantities than the lower confidence limit (Fig. 3.1C). Higher mean bromide concentrations were found in the bottom part of the profile for the group of cores containing more bromide than the upper confidence limit (Fig. 3.1F). These cores were slightly wetter throughout the profile than those with significantly lower bromide quantities (Fig. 3.1I). The bromide peak descended by some 10-15 cm between days 17 and 45 (Fig. 3.1E versus Fig. 3.1F). *It can be concluded that lateral displacement of bromide was indeed observed within the Ouddorp experimental site. Water and solutes apparently concentrated in wetter areas within the experimental field, causing bromide to reach greater depths at these locations.*

3.3.2 Analysis of correlative patterns

With respect to the spatial distribution of water and solutes in the top layer, the question arose which conditions were regulating this process at the Ouddorp experimental site. An additional sampling campaign was therefore carried out to

measure soil water contents, dry bulk densities, and the degree of potential water repellency of the 0-2.5 cm soil layer in a rectangular sampling grid of 10 by 20 steel cylinders (see Chapter 3.2.2). Before sampling of the selected site (1.2 m by 0.6 m)

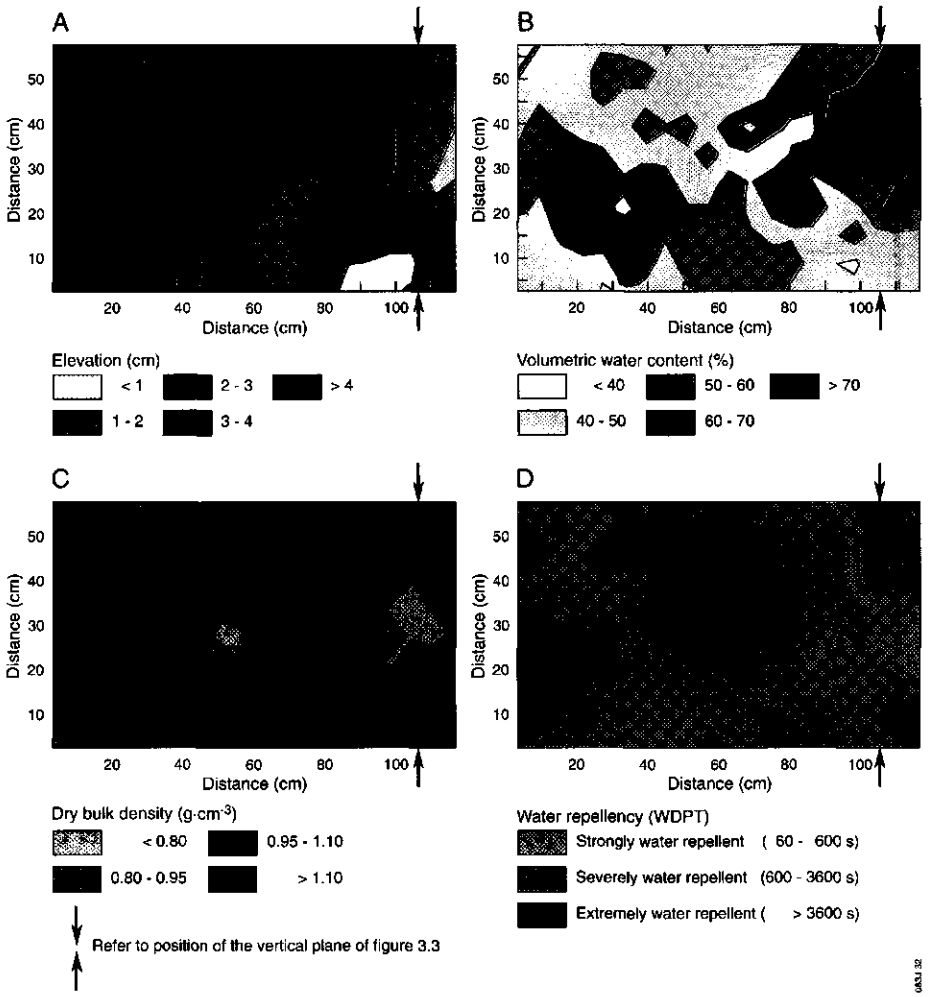

Fig. 3.2 *Contour plots showing soil surface elevations of the intensively sampled 1.2 m by 0.6 m area selected within the Ouddorp experimental field (A), and the spatial distribution of volumetric soil water content (B), dry bulk density (C), and potential water repellency (D) of the 0-2.5 cm depth soil layer. Each plot is based on 200 measurements.*

repellency is less severe than in the surrounding areas. Infiltration and vertical transport are facilitated at these sites.

3.4 DISCUSSION

That the process of distribution flow has so far been neglected as a serious research topic is probably mainly caused by the fact that the process is extremely difficult to identify under actual field conditions, while in laboratory studies, distribution flow is even less recognizable as a significant process.

It was, and often still is, common practice in soil laboratory studies to remove the upper soil layers to a depth of at least 10-20 cm, as the general opinion is that this layer, due to its internal heterogeneity etc, would prevent the collection of reliable measurements or disturb a straightforward interpretation of the data obtained.

Additionally, a serious limitation of soil laboratory studies is the restricted lateral dimension of the columns used, which usually range from a few cm to some dm (Wierenga and Van Genuchten, 1989). Water applied to such columns is actually forced to infiltrate and flow in the vertical direction, while under comparable field conditions this might have happened to a lesser extent or not at all. This problem was already indicated for field lysimeter studies by Miller (1963) and Sanchez et al. (1987).

In field experiments, the installation of permanent tensiometers or other measuring devices in the upper mm/cm of the soil is extremely difficult due to the loose structure of this layer, and therefore has often been avoided or neglected. In studying the water flow pattern in the top layer of soils, the most effective method to determine the process of distribution flow and its effects on displacing water and solutes is, in our opinion, the use of tracers. In tracer studies, the lateral distribution of water and solutes which occurs between two measuring campaigns can be approximated and related to the original tracer application rate when use is made of the volumetric soil core sampling method, as this allows tracer balances to be easily quantified.

3.5 CONCLUSIONS

Water which is on route from atmosphere to groundwater is deflected from its vertical path in the top layer, i.e. the distribution layer, of soils. Here, distribution flow

displaces water and solutes horizontally towards regions where vertical infiltration actually dominates. *Distribution flow is inextricably linked to the distribution layer.* The distribution layer in water repellent soils is generally very thin, of the order of mm to cm. The distribution layer may vary in thickness for different soils, due to differences in structural and textural properties of the top layer.

In leveled terrains, such as the one at Ouddorp, where elevation differences only occur at the microscale, distribution flow had a major impact on the spatial concentration of water and solutes at specific sites. Concentration of water and solutes was found at those locations in the 0-2.5 cm layer with the lowest degree of potential water repellency. At these sites, preferential flow paths formed through the entire water repellent layer. Deeper in the profile, in the wettable zone, lateral redistribution may occur due to diverging flow.

CHAPTER 4

TWO-DIMENSIONAL FINGERED FLOW PATTERNS

Adapted version of 'How water moves in a water repellent sandy soil 2. Dynamics of fingered flow' by C.J. Ritsema and L.W. Dekker, published in Water Resources Research 30:2519-2531, 1994.

4 TWO-DIMENSIONAL FINGERED FLOW PATTERNS

Abstract

Two-dimensional fingered flow patterns were studied in a water repellent sandy field soil by sampling ten, 5.5 m long and 0.5 m deep, trenches during a one-year cycle. In dry soil, fingers originated in those places in the top layer which had the lowest degree of potential water repellency. Finger diameters generally varied between 10 and 20 cm, and sporadically reached values of 25 cm. The fingers were wet in the top layer and became drier with depth. In none of the trenches sampled were any serious indications found of finger merging. Actually water repellent soil volumes between fingers were detected in all ten trenches. The temporal and spatial variability of these actually water repellent soil volumes is illustrated.

4.1 INTRODUCTION

Nowadays it is generally accepted that in most soils, water and solutes sometimes bypass large volumes of the unsaturated zone. This phenomenon seriously accelerates the transport of water and surface-applied solutes towards the saturated zone, and consequently increases the risk of contaminating groundwater reservoirs. In drained agricultural areas, preferential flow may lead to an increase in the contamination risk of surface waters. So far, however, no reliable observations have been published on where and when preferential flow may be expected in field situations. From a management point of view, this knowledge is essential for the development of consistent strategies to minimize environmental risks to groundwater and surface waters.

As long as half a century ago, field evidence was reported of water flowing through channels in the unsaturated zone of a water repellent sandy soil (Jamison, 1942, 1945 and 1946). Jamison mainly focused on the problems arising from this phenomenon, i.e. the decline in citrus groves and the inefficiency of irrigating such soils. To restore the wettability of these soils, Jamison suggested tilling to a depth of three inches prior to the summer rainy season, and/or mixing wettable alumino-silicate and phosphatic clays with the upper inch of the surface layer, followed by alternate irrigation and cultivation,

and/or spraying wetting agents.

In the sixties and seventies, research on water repellent soils shifted from the practical point of view towards more fundamental attempts to unravel the causes of water repellency. Water repellency has been attributed to specific microflora in soils (Bond, 1964; Savage et al., 1969b), specific vegetation covers (Gilmour, 1968; Scholl, 1971; Abbott and Robson, 1981), and to organic coatings of soil particles (Wander, 1949; Van 't Woudt, 1959; Krammes and Debano, 1965).

Over the last decade, research related to water repellent soils has focused on the increasing risks of runoff (McGhie, 1980; Burch et al., 1989; Witter et al., 1991; Crockford et al., 1991; Jungerius and Dekker, 1990), and on the phenomenon of preferential flow (Van Dam et al., 1990; Hendrickx and Dekker, 1991; Hendrickx et al., 1993).

In order to develop a simulation model predicting water and solute transport in water repellent sandy soils, Ritsema et al. (1993) executed a detailed tracer experiment to describe, explain and illustrate the mechanism of preferential flow (see Chapters 2 and 3). The results of this study indicated the occurrence of fingers below the humous layer in the water repellent zone at depths between 5 and 45 cm. In the wettable zone, starting at a depth of around 45 cm, no fingers were detected. The diameters of the fingers ranged from 10 to 20 cm, and the size of the dry areas in between were often somewhat larger.

However, it is assumed that the occurrence of fingers is subject to temporal and spatial variations. So far, there has been no information on fingered flow patterns in sandy soils under field conditions at different times of the year. The objectives of the present study were to

- present extensive information about fingered flow patterns in a water repellent sandy soil;
- relate observed finger patterns with the actual and potential water repellency of the soil;
- compare the observed 'field fingers' with 'laboratory fingers' previously reported in the literature.

4.2 MATERIALS AND METHODS

4.2.1 Soil and meteorological conditions

The field experiment was carried out on the same water repellent sandy soil in the western part of the Netherlands, near the village of Ouddorp, which was used in the studies described in Chapters 2 and 3.

Precipitation on the experimental field was measured weekly. Daily rainfall and evaporation rates were derived from measurements taken at a nearby meteorological station. Groundwater levels were measured in observation tubes in the experimental field. Fig. 4.1 shows precipitation and potential evaporation rates, and groundwater levels during the experiment. A total precipitation of 645 mm was measured between the first and last sampling campaign. The groundwater level fluctuated between 70 and 155 cm below the soil surface.

4.2.2 Field experiment

Between April 1988 and March 1989, ten 5.5 m long and 0.5 m deep trenches were sampled in a 0.05 ha experimental field. For each transect, 100 samples (diameter 5 cm; height 5 cm) were collected at depths of 5-10, 15-20, 25-30, 35-40 and 45-50 cm. Over the entire study, a total of 5000 soil samples were collected. Each sample was used to determine soil water content, dry bulk density, and degree of actual and potential water repellency. The degree of water repellency was measured using the water drop penetration time and alcohol percentage tests (see Chapter 2; Dekker and Ritsema, 1994).

In addition samples were taken from the 25-35 cm layer at three locations within the experimental field to determine the soil water retention and hydraulic conductivity functions, using Wind's evaporation method (Boels, 1978).

4.2.3 Data analysis

All data of each sampling campaign were used in an interpolation procedure aimed at obtaining soil water content contours, in order to visualize the fingers in vertical cross-

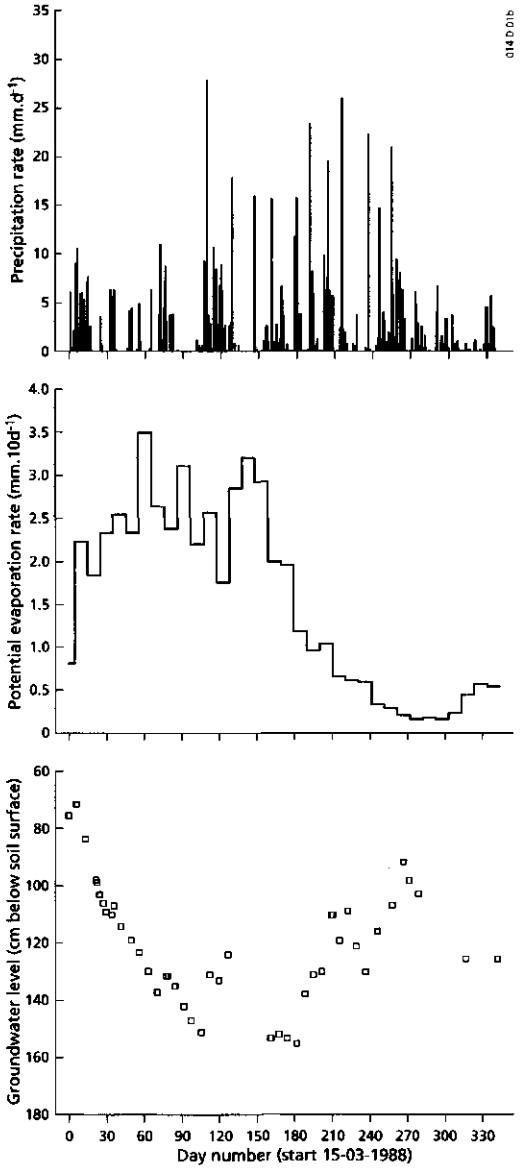

Fig. 4.1 *Precipitation rate, potential evaporation rate and measured groundwater levels during the experiment.*

sections of the soil. The results of the ten sampling campaigns were compared and evaluated with respect to the prevailing weather conditions.

4.3 RESULTS

4.3.1 Soil water content and actual water repellency patterns

Fig. 4.2 shows the volumetric water contents measured, plotted against depth, for the ten sampling dates. In general, considerable spatial variability was found on all the sampling dates. For instance, on December 13 the volumetric water content of the top layer varied between 1.9% and 23.8%. In most cases, the middle part of the profile was relatively dry compared with the top and bottom layers. The largest variations in water content were found in the top layer. The variation in soil water content in the deeper part of the profile was relatively small during the experiment. The minimum volumetric water content was 0.6%, measured in the 15-20 cm layer on June 21, while the maximum value was 33.9%, measured in the 5-10 cm layer on April 8 (Table 4.1). The standard deviation ranged from 0.2% to 5.7%, while the coefficient of variation varied between 8.0% and 80.8%, which is relatively high compared with values found in bare dune sands (Ritsema and Dekker, 1994a).

Table 4.1 *Volumetric soil water content at five depths (n=100) for all trenches, showing minimum, maximum, mean, standard deviation (SD) and coefficient of variation (CV).*

Depth (cm)	Minimum (%)	Maximum (%)	Mean (%)	SD (%)	CV (%)
		April 8, 1988			
5-10	11.1	33.9	19.4	4.7	24.2
15-20	8.8	15.4	12.2	1.3	10.5
25-30	8.7	13.9	11.5	1.0	8.7
35-40	8.3	12.2	10.4	0.8	8.0
40-45	9.2	24.4	17.9	3.7	20.9
		May 24, 1988			
5-10	2.1	10.5	4.5	1.4	31.4
15-20	1.1	14.7	2.8	2.3	80.8
25-30	1.6	13.1	3.2	1.8	55.5
35-40	3.2	13.6	5.6	1.6	28.0
45-50	4.5	9.7	7.4	1.0	13.2
		June 21, 1988			
5-10	1.6	4.4	3.1	0.5	16.3
15-20	0.6	2.2	1.7	0.2	10.1

25-30	1.0	2.2	1.6	0.2	12.0
35-40	1.2	4.9	2.7	1.0	36.0
45-50	1.8	6.9	4.9	1.3	26.3
		July 12, 1988			
5-10	3.2	24.2	9.7	5.1	52.6
15-20	1.8	15.6	5.7	3.1	53.2
25-30	1.7	12.3	5.6	2.5	44.7
35-40	1.6	10.0	4.3	2.1	47.9
45-50	4.1	10.3	7.7	1.2	16.0
		August 30, 1988			
5-10	2.5	15.5	5.1	2.9	57.7
15-20	1.1	12.7	4.4	2.9	66.3
25-30	1.5	10.4	3.9	2.1	54.0
35-40	1.6	7.1	3.0	1.3	44.3
45-50	1.4	7.5	3.5	1.4	38.8
		October 4, 1988			
5-10	4.0	21.1	11.3	3.4	29.6
15-20	1.9	10.5	6.6	2.3	35.2
25-30	1.7	9.8	6.8	1.9	29.6
35-40	5.0	8.9	7.2	0.9	11.9
45-50	7.1	11.0	8.8	0.7	8.3
		October 11, 1988			
5-10	3.8	26.0	12.7	5.7	45.1
15-20	2.1	16.5	8.0	4.1	51.8
25-30	1.8	14.0	6.5	3.2	49.6
35-40	2.8	12.3	8.6	2.1	24.5
45-50	8.2	15.2	11.1	1.3	12.0
		November 10, 1988			
5-10	3.1	18.2	9.7	3.4	34.6
15-20	2.1	9.8	5.9	2.2	37.7
25-30	1.5	8.0	4.5	1.8	40.3
35-40	2.2	8.4	5.0	1.3	26.6
45-50	6.4	10.1	8.2	0.7	9.0
		December 13, 1988			
5-10	1.9	23.8	13.9	4.6	33.1
15-20	1.9	14.3	7.5	3.3	43.2
25-30	1.6	12.0	5.8	2.8	48.6
35-40	1.6	12.4	6.8	2.7	40.4
45-50	8.1	13.7	11.2	1.4	12.1
		February 22, 1989			
5-10	8.1	21.3	16.0	3.0	18.7
15-20	3.0	15.1	9.3	2.6	28.1
25-30	2.2	12.6	7.5	2.5	33.0
35-40	2.6	11.8	6.4	1.9	30.0
45-50	5.8	9.7	8.2	1.0	11.7

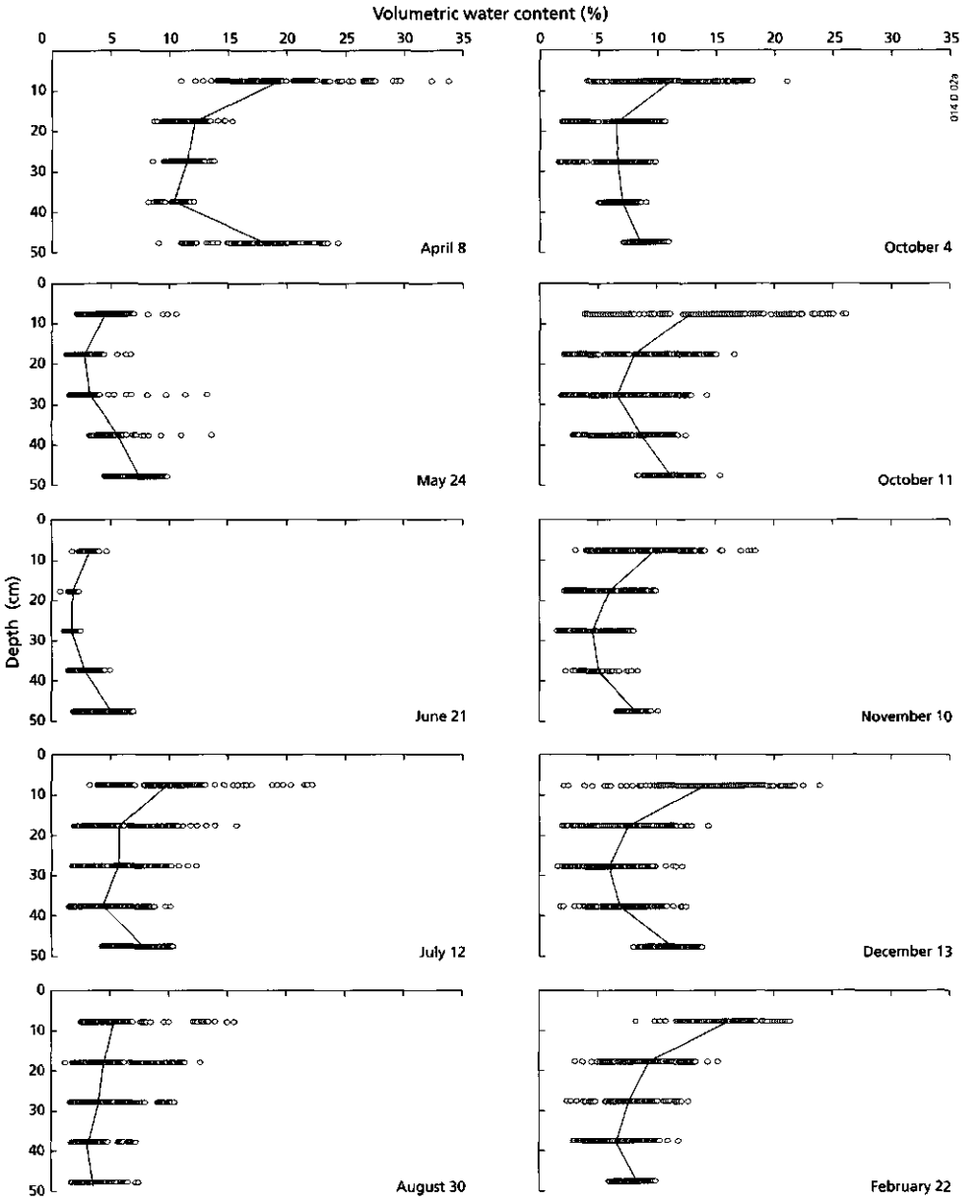

Fig. 4.2 *Volumetric water contents versus depth, and average profile for all trenches.*

Fig. 4.3 shows the spatial distribution of soil water content in the vertical plane for all trenches, together with the actually water repellent soil regions (the black dotted areas). The critical volumetric soil water contents below which the Ouddorp soil becomes water repellent (see Chapter 2) at depths of 5-10, 15-20, 25-30, 35-40, and 45-50 cm were approximately 4.75%, 3.0%, 2.5%, 2.0% and 1.75%, respectively (Dekker and Ritsema, 1994). Differences in soil water content between the trenches are mainly caused by differences in weather conditions between the excavations, since the spatial variability in soil texture, soil cover, potential water repellency, etc. within the experimental field is small (Dekker and Ritsema, 1994).

The wettest situation was observed on April 8, around the end of the winter. Soil water distribution at that moment showed only slight variations (see also coefficients of variation in Table 4.1). Some drier soil areas were visible in the middle part of the profile (Fig. 4.3), but none of them were actually water repellent (Table 4.2).

Between April 8 and May 24, the profile dried out due to low rainfall and increased evaporation (see Fig. 4.1), resulting in a distinct increase in the percentage of actually water repellent soil (Fig. 4.3 and Table 4.2). In this period, the groundwater level dropped from around 1 m to 1.4 m depth. On May 24, some wet soil patches could still be seen in the middle section of the profile. These wet patches were not connected with wet areas in the top layer and were therefore assumed to represent remnants of wet soil within the drying soil profile. June 21 saw the driest situation, with soil water contents ranging from 0.6% to 6.9%, resulting in an almost completely water repellent soil to a depth of approximately 35 cm (Fig. 4.3 and Table 4.2). The drying process resulted in a relatively uniform water distribution within the soil profile (see also coefficients of variation in Table 4.1).

Between June 21 and July 12, more than 75 mm of rainfall was recorded, which resulted in the development of vertically directed fingers and a decrease in actually water repellent soil. The fingers were wet at the top of the profile and became drier with depth (Fig. 4.3). They alternated with dry (< 5%) soil areas of various sizes. These dry areas generally occurred within the water repellent zone at depths between 10 and 40-45 cm, and had widths of 20 to 40 cm (Fig. 4.3).

From July 12 until the end of August, the weather was relatively dry (see Fig. 4.1). At the end of August, groundwater levels of about 155 cm below soil surface were recorded. Only a few fingers were visible in the trench sampled on August 30.

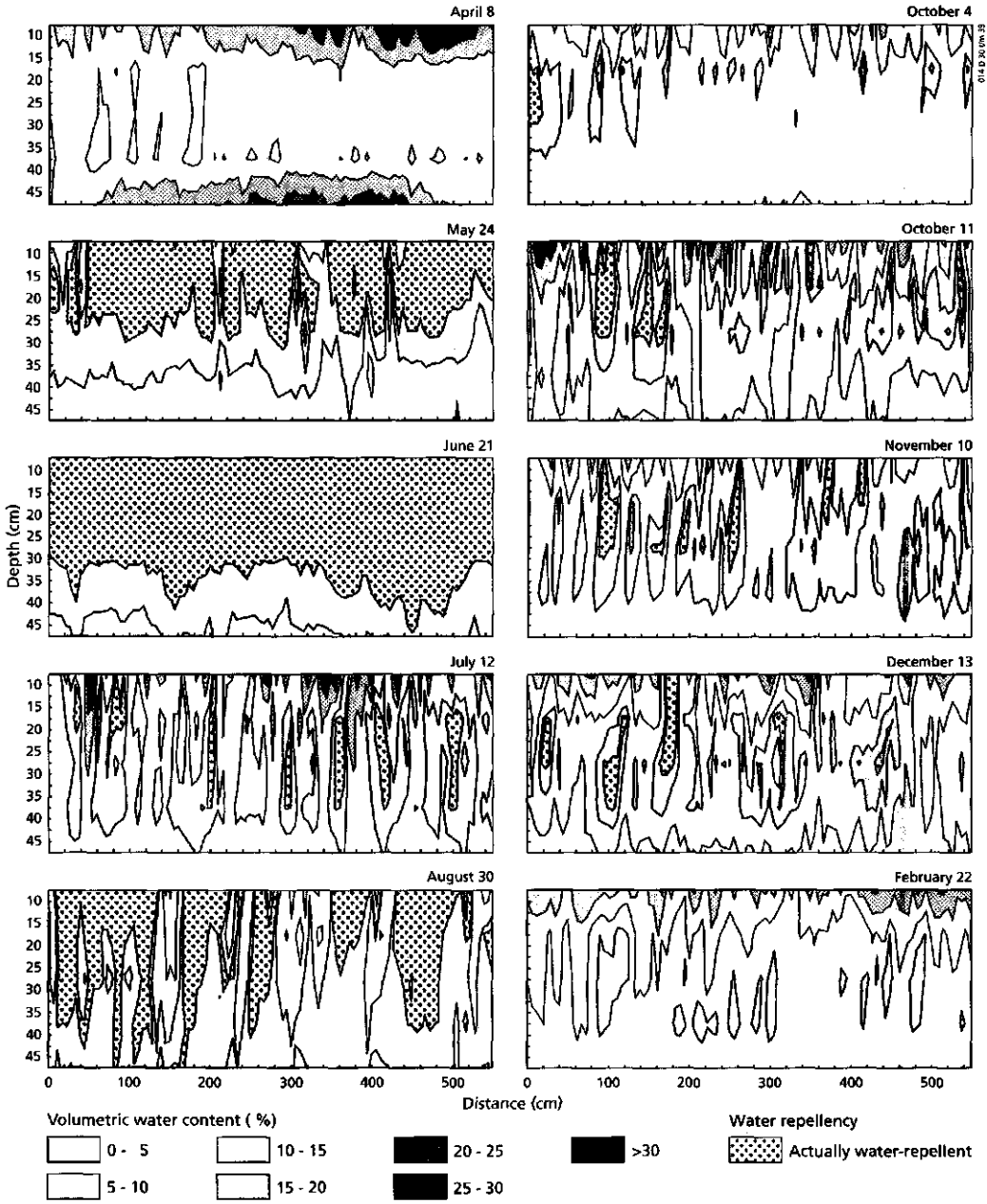

Fig. 4.3 *Contour plots showing the spatial distribution of volumetric water content and actual water repellency for all trenches.*

Compared with the trench sampled on July 12, these fingers were drier and were imbedded in drier, more actually water repellent soil material.

Between August 30 and October 4, more than 105 mm of rainfall was recorded. On October 4, soil water contents within the trench as a whole were higher than at the end of August. Dry soil areas and actual water repellency were still present in the middle of the profile, whereas small fingers were visible at the top of the profile. On the whole, soil water contents showed less variation with depth than those found on July 12 and August 30.

Within one week after October 4, almost 50 mm of rainfall was measured. The fingers advanced downwards (compare October 11 with October 4 in Fig. 4.3), and were clearly connected with a wet zone at the bottom of the profile. Simultaneously, the groundwater level rose from 130 cm to 110 cm below the soil surface (Fig. 4.1). Finger diameters seemed to increase compared with the midsummer situation (see July 12 in Fig. 4.3).

The period between October 11 and November 10 (autumn) was characterized by only 46 mm of rainfall. The soil profile dried out significantly, leading to an increase in the proportion of actually water repellent soil. Some slightly wetter fingers were present in the upper part of the soil.

Table 4.2 *Percentage of samples for the five depths in all trenches which were actually water repellent.*

	Depth				
Date	5-10 (cm)	15-20 (cm)	25-30 (cm)	35-40 (cm)	45-50 (cm)
April 8	-	-	-	-	-
May 24	76	85	34	-	-
June 21	100	100	100	29	-
July 12	9	22	15	8	-
August 30	68	53	33	23	5
October 4	3	10	5	-	-
October 11	6	14	13	-	-
November 10	11	17	17	-	-
December 13	5	11	18	4	-
February 22	-	1	1	-	-

From November 10 until December 13, 117 mm of rainfall was recorded, causing the profile to wet again (Fig. 4.3). Some fingers were seen to be connected with wet soil areas deeper in the profile. The groundwater level rose simultaneously from 130 cm to 98 cm depth. However, the pattern of vertical fingers alternating with dry, partly actually water repellent, soil areas remained largely unchanged. Until February 22, another 66 mm of rainfall was recorded. The upper and middle parts of the profile became wetter than the trench sampled on December 13, while the deeper part was slightly drier. However, on February 22 dry soil areas were still present in the profile, none of them actually water repellent (Fig. 4.3 and Table 4.2).

4.3.2 Potential water repellency

The potential water repellency of a soil (see Chapter 2) is assumed to be a more or less time-independent parameter, which can only vary from place to place due to variations in local vegetation type and cover, and/or the quantity and nature of organic matter in the soil. Dekker and Ritsema (1994) described in detail the spatial distribution of the potential water repellency of the trenches. Potential water repellency, based on the alcohol test (see Chapter 2), was high down to a depth of approximately 40-45 cm and almost absent in the deepest layers of the trenches (Dekker and Ritsema, 1994). Although the top layers of all trenches had a very high level of potential water repellency, slight variations occurred at each depth (Dekker and Ritsema, 1994).

At a specific depth, soil regions with high degrees of potential water repellency may be expected to have generally lower water contents than those with lower degrees of potential water repellency. This means that the spatial distribution of soil water within a trench may be expected to be at least partly determined by the spatial distribution of the potential water repellency. Fig. 4.3 indicates that the fingers originated within the top layer of the soil, so it may be assumed that this zone is characterized by a relation between the position of the fingers and the degree of potential water repellency in these places.

Fig. 4.4 shows graphs for the June 21 and July 12 trenches. The graphs plot for each depth, the mean water content of soil samples versus the degree of potential water repellency of these samples. The June 21 trench, the driest trench sampled, showed no relation between the two parameters; mean soil water content was independent of the

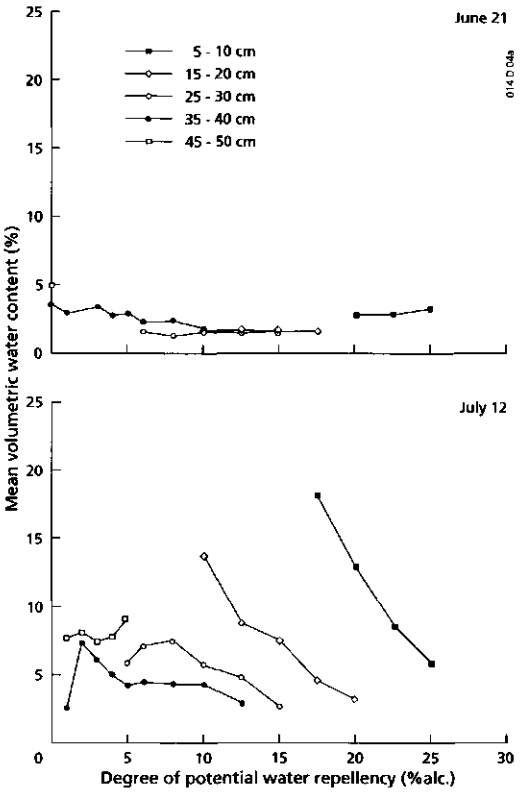

Fig. 4.4 *Mean volumetric water content versus degree of potential water repellency for all layers of the June 21 and July 12 trenches.*

degree of potential water repellency of the samples. The second graph shows the same relation for the July 12 trench, which was sampled after more than 75 mm of rainfall. This graph reveals a distinct relation, especially in the top layer, between the degree of water repellency of soil samples and their mean water contents. Water contents were higher in samples with lower degrees of potential water repellency. This relation became weaker with depth, indicating that water was indeed distributed within the surface layer towards positions with lower potential water repellency, where fingers were either present or could develop. Analysis of the other trenches yielded comparable

results as is shown for the July 12 trench in Fig. 4.4. *Hence, it may be concluded that in a horizontal plane, the wettest areas, i.e. the origins of the fingers, are those with the lowest degree of potential water repellency.* As the degree of potential water repellency is more or less constant in time, this implies that after periods of drought these fingers should recur in the same places. The permanent or semi-permanent character of these fingers also seems to be indicated by Fig. 4.5, which shows a horizontal cross-section through two fingers at a depth of 30 cm. The fingers, which have a circular cross-section, are clearly visible thanks to iron precipitates on the boundary between the wet fingers and the surrounding dry soil (reduction-oxidation zone).

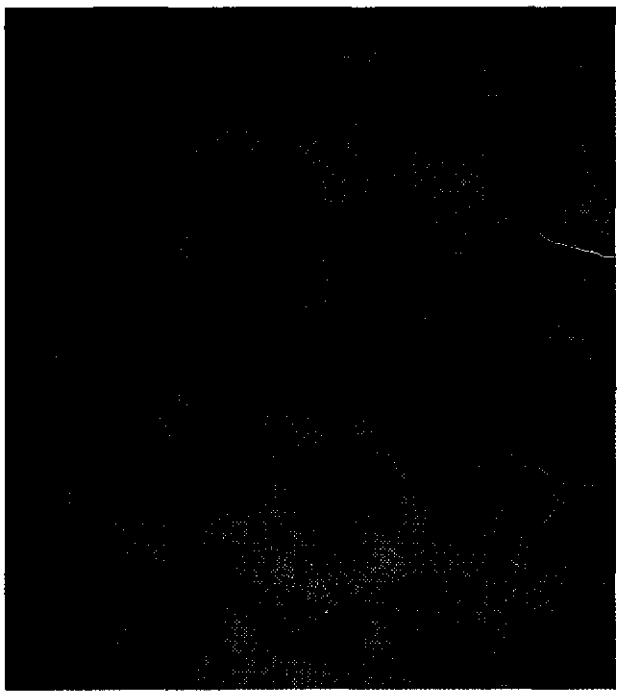

Fig. 4.5 *Horizontal cross-section through two fingers with diameters of 10-15 cm at a depth of 30 cm, with iron precipitates on the boundary between the wet fingers and the surrounding dry soil.*

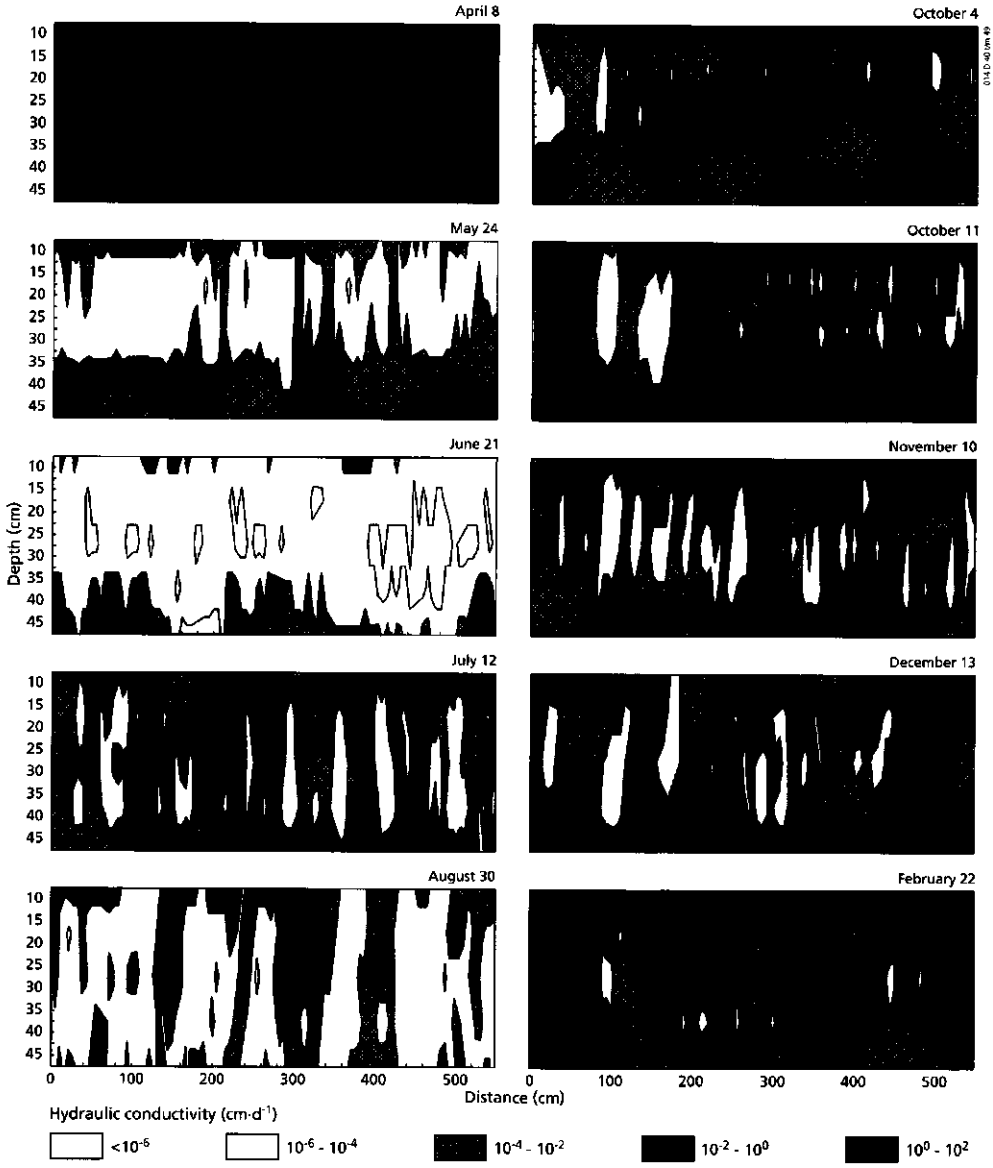

Fig. 4.6 *Contour plots showing the spatial distribution of actual hydraulic conductivity for all trenches.*

4.3.3 Hydraulic conductivity

Water is distributed laterally through the top layer towards the vertical fingers (Ritsema et al., 1993). The differences in soil water content between fingers and the surrounding dry soil areas lead to considerable spatial differences in actual hydraulic conductivity. Measured water contents were converted into hydraulic conductivity values by using the k-θ function determined in the laboratory. Contour plots of the actual hydraulic conductivities are given in Fig. 4.6 for all trenches. The plots show that the spatial patterns are roughly similar to those of the water content distributions in Fig. 4.3. Differences between wet and dry areas are exaggerated in Fig. 4.6 due to the log-normal dependence of hydraulic conductivity on water content. Actual hydraulic conductivity was low, viz., less than 10^{-4} cm.d^{-1} in the dry soil areas, reaching values up to 60 cm.d^{-1} in the wet areas.

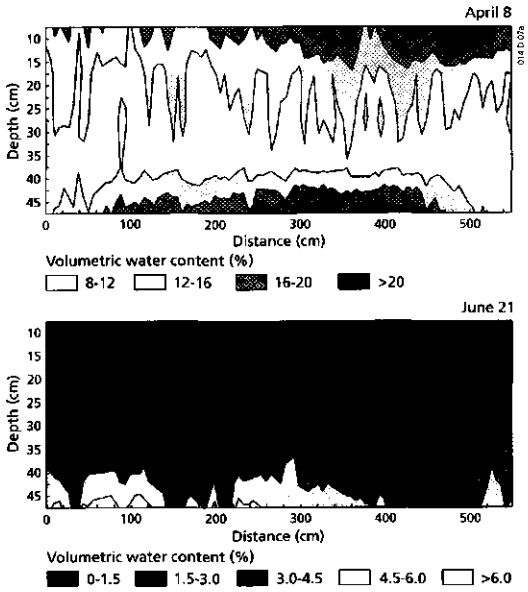

Fig. 4.7 *Contour plot showing the spatial distribution of volumetric water content in a fine range of classes for the April 8 and June 21 trenches.*

These spatial differences in actual hydraulic conductivity will cause the soil to behave anisotropically with respect to water flow. If rainfall occurs, the relatively wet soil areas are most easily infiltrated by water, consolidating and even intensifying spatial differences in soil water content within the soil profile. Due to hysteresis large variations in water content may occur and persist within a soil layer. If pressure head differences occur within a specific soil layer, dry soil areas may become wetter, although this may be expected to be a very slow process, due to the actually water repellent character and the related low actual hydraulic conductivities of the dry soil areas. The dry soil areas probably never reach soil water contents similar to those in the fingers, because these two types of areas are unequally supplied with water too. Even in the most uniform soil water content distributions observed, i.e. the April 8 and June 21 trenches, differences in soil water content were visible. Fig. 4.7 shows the soil water content distributions for these two trenches with a finer range of contour classes than that used in Fig. 4.3. This figure clearly shows that even under these conditions, soil water content differs from place to place.

4.3.4 Dry bulk density

It has often been suggested that soil water content differences are related to differences in dry bulk density (Nimmo and Akstin, 1988; Miles et al., 1988). Higher bulk densities flatten the shape of the soil water retention curve, resulting in more water being retained at low pressure heads. Table 4.3 lists some statistical parameters concerning the bulk density measured for the ten trenches.

The minimum dry bulk density was 1.12 $g.cm^{-3}$, for the top layer of the July 12 trench, while the maximum value was 1.62 $g.cm^{-3}$, for the 25-30 cm layer sampled on December 13. In general, the soil layers from depths of 5 to 10 cm had the lowest dry bulk densities, as they were, at least partly, intermediate layers between the humous layer and the underlying dune sand. Mean dry bulk density values for all trenches were 1.33 and 1.49 $g.cm^{-3}$ for the 5-10 cm layer and the underlying sand, respectively. Standard deviations ranged from 0.04 to 0.06 $g.cm^{-3}$ in the top layer, and from 0.02 to 0.03 $g.cm^{-3}$ in the underlying sand. The coefficient of variation ranged from 3.2% to 4.6% in the 5-10 cm layer, and from 1.3% to 2.3% in the rest of the profile. The correlation coefficient between dry bulk density and soil water content is also presented

Table 4.3 *Dry bulk density at five depths (n=100) for all the trenches, listing minimum, maximum, mean, standard deviation (SD), coefficient of variation (CV) and the correlation coefficient (r) for the relationship between bulk density and volumetric soil water content.*

Depth (cm)	Min ($g.cm^{-3}$)	Max. ($g.cm^{-3}$)	Mean ($g.cm^{-3}$)	SD ($g.cm^{-3}$)	CV (%)	*r* (-)
			April 8, 1988			
5-10	1.17	1.44	1.34	0.05	3.7	-0.42
15-20	1.37	1.54	1.48	0.03	2.3	+0.00
25-30	1.41	1.58	1.50	0.02	1.6	+0.00
35-40	1.47	1.56	1.52	0.02	1.3	+0.00
45-50	1.45	1.57	1.52	0.02	1.5	-0.30
			May 24, 1988			
5-10	1.20	1.47	1.32	0.05	4.1	-0.13
15-20	1.41	1.53	1.48	0.02	1.6	-0.16
25-30	1.41	1.57	1.51	0.03	1.8	+0.27
35-40	1.47	1.59	1.52	0.03	1.7	+0.10
45-50	1.46	1.56	1.51	0.02	1.3	-0.11
			June 21, 1988			
5-10	1.16	1.43	1.35	0.04	3.2	-0.53
15-20	1.39	1.53	1.46	0.03	1.9	+0.01
25-30	1.44	1.56	1.49	0.02	1.5	+0.00
35-40	1.41	1.55	1.49	0.03	1.8	+0.51
45-50	1.37	1.52	1.47	0.03	1.9	+0.51
			July 12, 1988			
5-10	1.12	1.45	1.29	0.05	4.1	-0.11
15-20	1.35	1.52	1.45	0.03	2.1	+0.04
25-30	1.41	1.55	1.48	0.03	1.8	+0.33
35-40	1.35	1.55	1.48	0.03	2.1	+0.34
45-50	1.38	1.52	1.47	0.03	1.7	+0.05
			August 30, 1988			
5-10	1.15	1.47	1.36	0.05	3.8	-0.17
15-20	1.39	1.50	1.45	0.03	1.7	+0.17
25-30	1.41	1.51	1.46	0.02	1.6	+0.33
35-40	1.42	1.52	1.48	0.02	1.5	+0.38
45-50	1.43	1.53	1.48	0.02	1.4	+0.21
			October 4, 1988			
5-10	1.16	1.38	1.29	0.04	3.3	-0.24
15-20	1.40	1.53	1.47	0.03	1.8	+0.23
25-30	1.45	1.57	1.52	0.03	1.7	+0.34
35-40	1.45	1.58	1.53	0.02	1.6	+0.04
45-50	1.40	1.55	1.50	0.02	1.7	-0.05
			October 11, 1988			
5-10	1.18	1.44	1.30	0.05	4.2	-0.14
15-20	1.38	1.53	1.47	0.03	1.9	+0.17
25-30	1.43	1.57	1.51	0.02	1.6	+0.39
35-40	1.46	1.55	1.51	0.02	1.3	+0.39

45-50	1.43	1.55	1.50	0.02	1.5	-0.10
			November 10, 1988			
5-10	1.15	1.46	1.35	0.06	4.6	-0.20
15-20	1.40	1.53	1.48	0.03	1.9	+0.19
25-30	1.39	1.57	1.51	0.03	1.8	+0.32
35-40	1.44	1.56	1.51	0.02	1.6	+0.27
45-50	1.45	1.55	1.50	0.02	1.4	+0.16
			December 13, 1988			
5-10	1.22	1.45	1.34	0.05	3.8	-0.35
15-20	1.40	1.54	1.49	0.03	1.7	+0.43
25-30	1.42	1.62	1.52	0.03	1.9	+0.58
35-40	1.43	1.57	1.51	0.03	1.9	+0.44
45-50	1.42	1.55	1.49	0.02	1.6	+0.34
			February 22, 1989			
5-10	1.22	1.44	1.36	0.05	3.4	-0.54
15-20	1.42	1.54	1.49	0.02	1.5	+0.24
25-30	1.45	1.56	1.51	0.02	1.3	+0.24
35-40	1.47	1.57	1.51	0.02	1.3	+0.05
45-50	1.44	1.54	1.49	0.02	1.4	-0.19

in Table 4.3. It varies between -0.54 for the top layer sampled on February 22 and +0.58 for the 25-30 cm layer sampled on December 13. For the 5-10 cm layers, negative correlations were always found between bulk density and soil water content, and the opposite was generally true for the underlying dune sand. This suggests that water in the top layer is mainly concentrated in places with relatively low dry bulk densities, while that in the deeper layers concentrate in places with higher densities. On the whole, however, the correlation coefficients are low, indicating weak or no correlation between the two parameters. This is illustrated in Fig. 4.8, which shows the spatial distributions of the volumetric and gravimetric soil water contents in the December 13 trench, together with the measured dry bulk density. It is obvious that the volumetric and gravimetric soil water content patterns were similar, and that the spatial differences in dry bulk density were of minor or no importance with respect to the differences in soil water content. The spatial distribution of the dry bulk density shows a more or less horizontal layering in the upper part of the soil, and a vertical pattern below it (Fig. 4.8). These vertical patterns have also been found for a variety of bare dune sand soils sampled in two contrasting climatic zones (Ritsema and Dekker, 1994a), and are probably somehow related to the successive formation of vertical preferential flow paths.

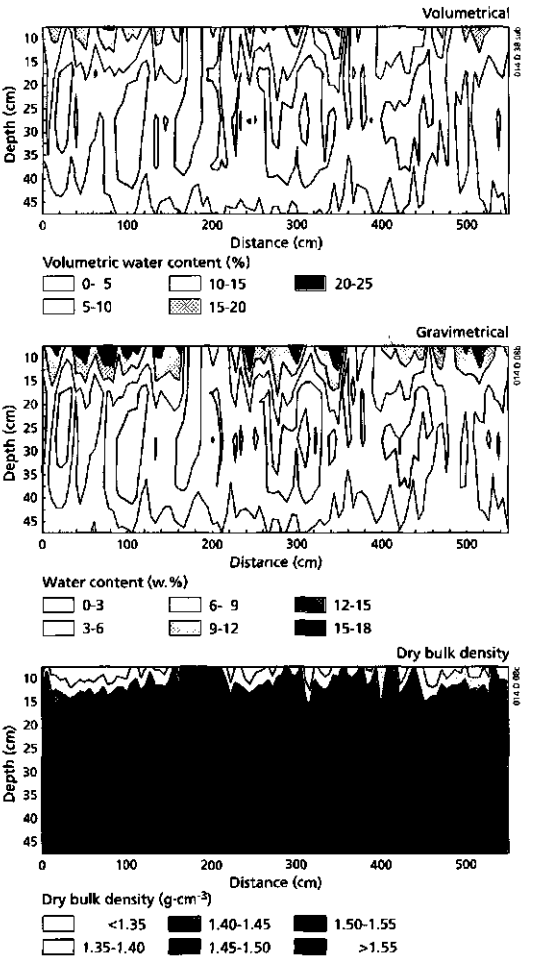

Fig. 4.8 *Contour plots showing the spatial distributions of volumetric and gravimetric water content, and dry bulk density for the December 13 trench.*

4.4 DISCUSSION

4.4.1 Finger diameters

A variety of studies describing and predicting finger diameters have been published

(Parlange and Hill, 1976; White et al., 1976; Glass et al., 1989b; Selker et al., 1989, 1991, 1992a). The theory for predicting finger diameters was originally developed for (wettable) layered soils (Glass et al., 1989a and 1989b), and has since then also proved to be applicable to homogeneous soils without layering (Selker et al., 1992a). According to this theory, finger diameters depend on the characteristic soil texture and a specific flux ratio, which is defined as the system flux divided by the saturated hydraulic conductivity (Selker et al., 1991 and 1992a). Common finger widths found for wettable, relatively coarse-textured sandy soils are of the order of centimetres (Glass et al., 1989c; Selker et al., 1989, 1992a). In initially dry, bare, wettable, dune sand, with a grain fraction comparable to that at the Ouddorp experimental site, Ritsema and Dekker (1994a) detected fingers with diameters between 5 and 15 cm.

Selker et al. (1991) presented a graph showing the expected finger diameters versus soil texture for different flux ratios for water infiltrating into dry soil. From this graph, the Ouddorp sandy soil, with its median particle size of around 0.17 mm, would be expected to show finger widths of the order of 10 cm. Fingers detected in the trenches sampled during the present study varied in width from 10 to 15 cm when the soil was dry (see for instance the July 12 trench), increasing their diameters in periods of abundant rainfall up to around 20 to 25 cm (see for instance the October 11 trench, Fig. 4.3). Thus the graph of Selker et al. (1991) predicted the finger width in dry sand quite well if we consider the findings in the July 12 trench. It is also worth noting that the scale of the fingers observed in the July 12 trench is very well comparable with those found in initially dry, wettable dune sands (Ritsema and Dekker, 1994a). Due to the water repellency of the Ouddorp experimental field, dry soil areas may be expected to be more persistent here than in the case of the wettable sand (Ritsema and Dekker, 1994b). Recently, Liu et al. (1994a,b) showed that fingers in initially wet sand are wider (by a factor of 3) than those found in dry sand, which is in accordance with the present field finger observations. *Thus, diameters of fingers in the field may show some expansion or shrinkage, depending on the sequence of weather conditions.*

4.4.2 Water distribution within fingers

Several authors have described the initial development of fingers in laboratory experiments (Glass et al., 1989c; Selker et al., 1992b). It was shown that the tip of the

advancing finger is generally saturated with water, while decreasing water contents were observed behind it. Our field results, however, showed a different pattern of water distribution. Fig. 4.9 shows two field fingers from the July 12 and October 11 trenches in detail, with their measured soil water content distributions. The wettest zone within the finger was found in the top layer, and the soil water content decreased with depth. This is typical of fingers in the experimental field, and has also been found to occur in bare, wettable dune sands (Ritsema and Dekker, 1994a). In the laboratory studies, saturated finger tips only occurred during water application. Saturated finger tips were

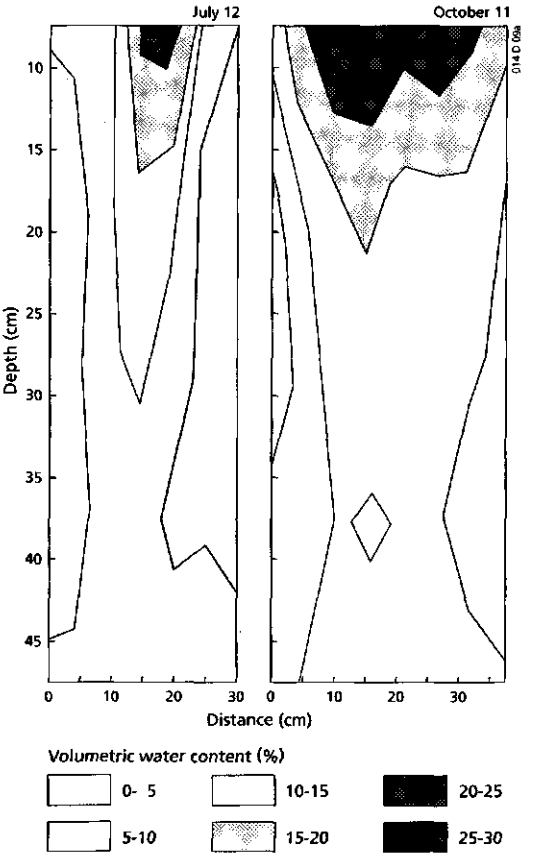

Fig. 4.9 *Typical examples of soil water distribution within preferential flow paths observed in the experimental field.*

not found in the sampled trenches, as sample collection always took place one or more days after a rainfall event, so the water had time to redistribute, leading to soil water contents decreasing with depth.

4.4.3 Finger merging

Various laboratory studies have found finger merging to be an important process, reducing the number of fingers with depth (Glass et al., 1989b; Selker et al., 1989 and 1991). A 35% decrease in the number of fingers and the wetted area over a depth of 30 cm was observed by Selker et al. (1992a) in three-dimensional laboratory experiments. Based on the work of Kung (1990a,b), Selker et al. (1989) as well as others have stated that '*in the field we should expect finger merging to be a dominant process*'. The field results of our study clearly show, however, that finger merging is not as relevant as Selker et al. (1989) suggested. None of the trenches showed any indications of intensive finger merging. What we did find is that in some trenches the depth of finger penetration varied from place to place, most probably due to differences in the total amount of water directed towards individual fingers. Corresponding results without finger merging in laboratory experiments have been presented by Tamai et al. (1987), White et al. (1977) and Hill and Parlange (1972).

4.5 CONCLUSIONS

The experimental results show that fingered flow is an important phenomenon in grass-covered water repellent sandy soils. At the end of June, a relatively uniform dry situation was met in the experimental field. Thereafter, fingers developed relatively quickly, starting in July with finger diameters of 10 to 15 cm, increasing to 20 to 25 cm in October. Initial finger diameters were the same as expected on the basis of the graph presented by Selker et al. (1991), showing the relation between finger diameter and particle size for water infiltrating into dry soil. At the end of the winter, the profile showed a more or less uniformly wet pattern. *Short-term variations in the number and size of fingers were related to the succession of weather conditions during the experimental period. As sampling was executed just after or in between two successive rain events, the fingers were wet in the topsoil and became drier with depth. The data*

presented suggest that finger merging is an irrelevant process in the experimental field, contradicting laboratory findings by Selker et al. (1992a) and Glass et al. (1989b). Percentages of actually water repellent soil were quantified, and related to spatial soil water content distributions in individual trenches. The positions of the fingers seem to be determined by slight variations in the degree of potential water repellency of the top layer, the fingers being located in places with the lowest degree of potential water repellency. *The presence of the fingers result in large spatial differences in actual hydraulic conductivity, causing the soil to behave anisotropically with respect to water flow. Hysteresis tends to magnify this phenomenon, as it is one of the major causes of the long term persistence of fingers. Spatial differences in bulk density do not seem to be important for the differences in soil water content.*

CHAPTER 5

THREE-DIMENSIONAL FINGERED FLOW PATTERNS

Adapted version of 'Three-dimensional fingered flow patterns in a water repellent sandy field soil' by C.J. Ritsema, L.W. Dekker and A.W.J. Heijs, published in Soil Science 162:79-90, 1997.

5 THREE-DIMENSIONAL FINGERED FLOW PATTERNS

Abstract

Water flow and solute transport through the vadose zone of water repellent field soils mainly take place through preferred flow paths. For modeling purposes, it is essential to know when and where fingers can be expected, and what the average dimensions of the fingers are. Therefore, samples were taken from ten soil blocks, each with a length of 1.2 m, a width of 0.6 m, and a depth of 0.52 m, in the Ouddorp water repellent sandy field soil. Sampling took place according to a predefined spatial grid, with 200 (100 cm^3) cylinders being sampled at 7 depths, yielding a total of 1400 samples per soil block. Each sample was used to determine soil water content, and some of the samples were used to determine the degree of potential and actual water repellency. Data were used to visualize the three-dimensional water content patterns and water repellency distributions. Fingered flow patterns were clearly present in soil blocks sampled after distinct rain events. Finger positions were related to places with relatively low degrees of potential water repellency in the upper part of the soil. Soil blocks sampled between rain events showed only remnants of fingerlike wetting patterns as a result of drainage, redistribution and evaporation. Water contents were less heterogeneously distributed in these soil blocks, as was also the case for a very wet soil block sampled after an abundant rainfall.

5.1 INTRODUCTION

During the last decades, it has become obvious that water and solutes often move preferentially through sandy soils (Hill and Parlange, 1972; Raats, 1984; Selker et al., 1991). This process might be due to internal soil heterogeneity, leading for instance to funneled flow over inclined coarse sandy layers (Kung, 1990a,b), or unstable flow in situations with a fine over a coarse (Hillel and Baker, 1988; Baker and Hillel, 1990) or a dense over a loose layer (Ritsema and Dekker, 1994a). Unstable flow might be induced in apparently homogeneous soils as well (Selker et al., 1989), for instance due to air entrapment (Glass et al., 1990) or water repellency (Ritsema et al., 1993).

Water repellency of a soil is generally caused by the presence of organic materials,

and by humic substances (Bisdom et al., 1993; Wallis and Horne, 1992). Water repellency is plant-induced and therefore occurs in many soils. In the Netherlands, water repellency has been found in sand (Dekker and Jungerius, 1990), in loam (Dekker and Ritsema, 1995), in peaty clay and clayey peat (Dekker and Ritsema, 1996a), and in heavy basin clay soils (Dekker and Ritsema, 1996b). Outside the Netherlands, the occurrence of soil water repellency has been reported in Australia (McGhie, 1987), Spain (Imeson et al., 1992), the USA (Jamison, 1969) and many other countries (DeBano, 1981; Wallis and Horne, 1992). In sandy soils with low organic matter content, water repellent humic substances are the main cause of water repellency. Individual sand grains are coated by these water repellent substances, and these coatings generally persist for very long periods.

The effect of water repellency on water flow depends on the actual water content of the soil (Dekker and Ritsema, 1994). Under dry conditions, the effect of water repellency is most pronounced, causing water infiltration into the soil to be inhibited or retarded at first. In hilly regions, this process may lead to serious runoff during the first rain events after dry periods (Burch et al., 1989; Jungerius and Dekker, 1990; Crockford et al., 1991). With prolonged rainfall, however, the soil will start to wet, generally resulting in a very wet surface layer on top of a still dry subsoil. This process enhances lateral flow components in the top layer, causing water and solutes to move laterally to places where vertical infiltration is easiest. This process has been referred to as distribution flow (Chapter 3), and is confined to the distribution layer (Ritsema et al., 1993; Ritsema and Dekker, 1995). After some time, the infiltrating wetting front will break up into vertically directed preferential flow paths, facilitating the rapid downward movement of water and surface-applied solutes. Ritsema et al. (1993) presented evidence of this typical preferential flow mechanism, based on a detailed bromide tracer experiment in a water repellent sandy soil (Chapter 2). However, no information is so far available on the three-dimensional structure of preferred flow paths in water repellent field soils. Therefore, the objectives of the present study were to

- present three-dimensional water content distributions in a water repellent sandy field soil at various times during a one year cycle;
- relate these water content patterns to potential water repellency patterns;
- indicate the effect of soil water content on the occurrence of water repellency.

5.2 MATERIALS AND METHODS

5.2.1 Soil block sampling and weather conditions

In order to obtain three-dimensional soil water content patterns, ten soil blocks, each with a length of 1.2 m, a width of 0.6 m and a depth of 0.52 m, were sampled at the Ouddorp experimental site during a one year cycle. The ten soil blocks were sampled on October 28 and November 20, 1991, and on January 6, March 3, April 8, May 25, June 6, July 15, September 1 and November 2, 1992. Daily rainfall and evaporation rates were obtained from a nearby meteorological station. Cumulative rainfall minus cumulative potential evaporation is shown in Fig. 5.1 for the entire experimental period. Cumulative rainfall minus cumulative potential evaporation amounted to slightly more than 400 mm, with the most pronounced infiltration events occurring just before the sampling of the November 20, June 6, September 1, and November 2 soil blocks.

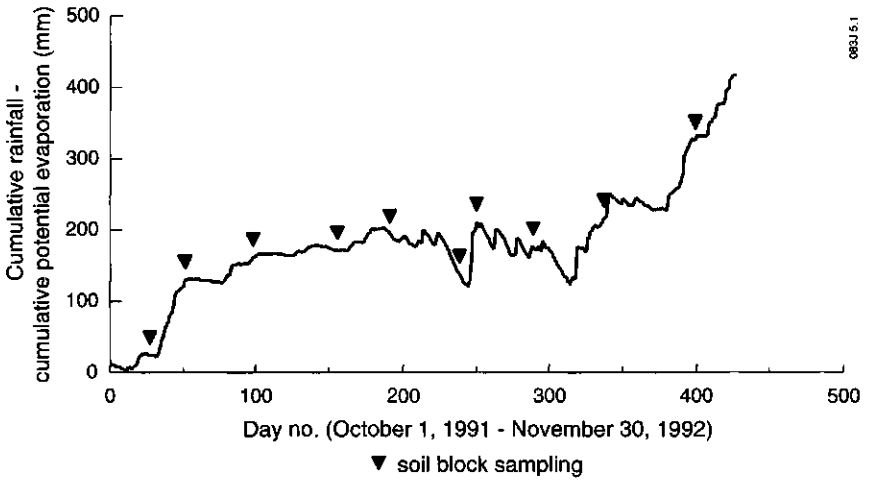

Fig. 5.1 *Cumulative rainfall minus cumulative potential evaporation during the experimental period. Major infiltration events occurred before the sampling of the November 20, June 6, September 1, and November 2 soil blocks.*

Each soil block was sampled using 5 cm wide and 5 cm high (100 cm^3) steel cylinders. Sampling took place in a regular grid, with 20 by 10 samples per layer. A

total of 7 layers were sampled per soil block, at depths of 0-5, 7-12, 14.5-19.5, 22-27, 29.5-34.5, 39-44 and 47-52 cm, yielding a total of 1400 samples per block. The sampling grid applied was designed on the basis of previous experiences within the same experimental field during attempts to optimize sampling strategies for detecting preferential flow paths (Ritsema and Dekker, 1996a). The first soil block, sampled on October 28, 1991, consisted of 4 layers only, yielding 800 samples for this block. The last soil block, sampled on November 2, consisted of 8 layers, as the samples from the 0-5 cm layer were split up into two parts, one from 0 to 2.5 and one from 2.5 to 5 cm depth. A total of 13,600 samples were collected during the sampling campaigns.

5.2.2 Measurements

All samples were used to determine volumetric soil water content (oven-drying method), while some of the samples (the July 15 and November 2 soil blocks) were used to determine the degree of potential water repellency. The latter was determined using the Water Drop Penetration Time test (WDPT test) on oven-dried (65^{0}C) soil samples using ten classes of water repellency (see Chapter 2).

Additionally, all field-moist samples originating from the June 6, July 15, September 1 and November 2, 1992 soil blocks, were used to determine the actual water repellency (see Chapter 2), using the same WDPT test. Based on these measurements, critical soil water contents could be derived for each layer. The critical soil water contents were used to define whether field moist samples from other soil blocks were actually wettable or actually water repellent at the moment of sampling.

5.2.3 Three-dimensional visualization

Sample coordinates and data on the related soil water contents, the actual wettable or water repellent status and, if relevant, the degree of potential water repellency were tabulated for each soil block. These data sets were used as the basis for visualizing the water content patterns and water repellency distributions. Visualization was done using the IRIS Explorer modular visualization software environment, on a SGI Indigo (R4000XZ) workstation (Heijs et al., 1996; Ritsema et al., 1997). Techniques used included the visualization of three-dimensional iso-surfaces, combined with intersecting

horizontal planes. Typical soil water content iso-surfaces were visualized for each soil block, in order to reveal fingered flow patterns most distinctly. Combinations of these iso-surfaces with color mapping of the soil water content data in horizontal cutting planes yielded the images presented below. Visualization of water repellency patterns was achieved in a similar way.

5.3 RESULTS

5.3.1 Fingered flow patterns

For each of the ten soil blocks, the minimum, maximum and mean water content values per soil layer are listed in Table 5.1, together with the standard deviations and coefficients of variation.

Table 5.1 shows that the driest soil block was sampled on May 25, and the wettest on November 2. For all soil blocks, mean volumetric soil water content varied between 6.6% and 42.2% for the 0 to 5 cm layer and between 5.5% and 10.9% for the 47 to 52 cm layer. Soil water content variations generally decreased with depth. The largest absolute soil water content differences per unit of depth were found in the November 20 soil block, except for the 29.5 to 34.5 cm soil layer, where the largest differences were found in the January 6 soil block. For all soil blocks, standard deviations ranged from 0.6% to 7.1%, and coefficients of variation from 7.1% to 88.2%.

Fig. 5.2 shows the three-dimensional soil water content distributions for each soil block. Each visualization is based upon 1400 soil water content measurements, except those of the soil blocks sampled on October 28 and November 2, which are based upon 800 and 1600 soil water content measurements, respectively. Each image shows a specific soil water content iso-surface, depicting the fingered flow process most clearly. Furthermore, two horizontal planes have been visualized for each image, at depths of 17.0 cm and 49.5 cm below the soil surface. These depths coincide with the centres of the 14.5-19.5 and 47-52 cm soil layers. From Fig. 5.2, it can be seen that fingerlike flow patterns were present in those soil blocks sampled after pronounced infiltration events, like those sampled on October 28 (Fig. 2A), November 20 (Fig. 2B), June 6 (Fig. 2G) and September 1 (Fig. 2I). Fingers always started at a depth of around 10 cm.

Table 5.1 *Volumetric soil water content and measured actual water repellency for each depth (n=200) in all ten soil blocks. SD, CV and AWRS denote standard deviation, coefficient of variation and actual water repellent soil, respectively.*

Depth (cm)	Minimum (%)	Maximum (%)	Mean (%)	SD (%)	CV (%)	AWRS (%)
			October 28, 1991			
0-5	21.1	36.3	30.5	3.2	10.5	7.5
7-12	2.1	13.5	4.5	2.5	55.6	48.5
14.5-19.5	1.2	10.2	2.7	1.8	66.7	73.5
22-27	1.3	9.4	3.0	1.9	63.3	61.0
			November 20, 1991			
0-5	19.5	52.4	41.0	6.0	14.6	1.5
7-12	1.6	20.0	6.7	4.8	71.6	40.0
14.5-19.5	0.6	17.4	5.0	4.2	84.0	49.0
22-27	1.4	16.4	5.2	3.8	73.1	39.0
29.5-34.5	1.1	11.0	4.0	2.7	67.5	38.0
39-44	1.2	13.7	3.9	2.7	69.2	29.5
47-52	1.2	13.9	5.6	2.9	51.8	4.0
			January 6, 1992			
0-5	33.1	55.5	42.2	3.6	8.5	0.0
7-12	3.2	17.5	11.0	3.1	28.2	1.5
14.5-19.5	1.5	13.7	6.7	2.9	43.3	12.5
22-27	1.7	13.3	7.4	2.7	36.5	5.5
29.5-34.5	1.8	13.7	7.4	2.4	32.4	1.5
39-44	1.5	10.2	5.7	2.0	35.1	4.5
47-52	2.2	10.4	6.5	1.8	27.7	0.0
			March 3, 1992			
0-5	38.6	43.8	34.7	2.5	7.2	0.0
7-12	4.6	15.4	10.9	2.0	18.3	0.0
14.5-19.5	1.8	14.3	7.3	2.1	28.8	6.5
22-27	1.5	10.8	5.9	2.0	33.9	8.0
29.5-34.5	1.5	8.7	4.8	1.8	37.5	12.0
39-44	1.9	8.2	4.7	1.6	34.0	0.0
47-52	2.8	8.7	5.8	1.2	20.7	0.0
			April 8, 1992			
0-5	38.9	50.2	35.6	3.4	9.6	0.0
7-12	6.5	17.6	11.7	2.1	17.9	0.0
14.5-19.5	2.3	13.1	7.3	2.0	27.4	4.0
22-27	1.6	12.0	6.0	2.0	33.3	5.5
29.5-34.5	1.7	11.0	5.0	1.9	38.0	8.0
39-44	1.7	9.4	4.5	1.7	37.8	1.5
47-52	2.4	9.2	5.5	1.5	27.3	0.0

			May 25, 1992			
0-5	4.4	10.9	6.6	1.1	16.7	100.0
7-12	1.7	6.8	3.4	1.2	35.3	76.0
14.5-19.5	1.9	8.0	3.7	1.2	32.4	30.5
22-27	2.1	7.2	4.4	0.9	20.5	2.0
29.5-34.5	3.1	7.2	4.9	0.8	16.3	0.0
39-44	3.5	6.8	5.0	0.6	12.0	0.0
47-52	3.6	6.8	5.4	0.6	11.1	0.0
			June 6, 1992			
0-5	19.2	37.8	26.6	3.9	14.7	36.0
7-12	2.0	12.3	4.9	2.2	44.9	45.0
14.5-19.5	1.9	11.0	6.2	2.2	35.5	8.0
22-27	2.0	9.7	6.4	1.6	25.0	1.5
29.5-34.5	3.9	9.0	6.0	1.4	23.3	0.0
39-44	3.1	9.8	6.5	1.2	18.5	0.0
47-52	4.2	10.5	7.2	1.2	16.7	0.0
			July 15, 1992			
0-5	11.0	34.1	19.2	4.1	21.4	89.5
7-12	1.7	11.9	2.9	1.6	55.2	87.5
14.5-19.5	1.2	11.3	2.6	2.0	76.9	77.0
22-27	0.7	12.9	3.3	2.2	66.7	53.5
29.5-34.5	0.8	11.2	4.9	2.0	40.8	5.5
39-44	2.6	9.2	5.6	1.5	26.8	0.0
47-52	3.5	9.1	5.8	1.1	19.0	0.0
			September 1, 1992			
0-5	22.5	44.8	34.2	4.2	12.3	2.0
7-12	1.5	17.5	4.4	3.5	79.5	66.5
14.5-19.5	1.0	15.3	3.9	3.4	87.2	62.0
22-27	1.2	12.6	5.0	3.5	70.0	38.5
29.5-34.5	1.7	11.9	5.7	2.7	47.4	5.5
39-44	3.6	9.6	6.8	1.3	19.1	0.0
47-52	3.5	10.3	7.5	1.3	17.3	0.0
			November 2, 1992			
0-2.5	37.6	78.0	51.6	7.1	13.8	0.0
2.5-5	17.0	43.6	30.2	4.3	14.2	10.0
7-12	3.5	20.8	12.7	2.6	20.5	1.0
14.5-19.5	6.4	13.7	10.3	1.2	11.7	0.0
22-27	6.7	11.4	9.3	0.8	8.6	0.0
29.5-34.5	6.7	11.4	8.7	0.8	9.2	0.0
39-44	7.1	12.4	9.7	0.9	9.3	0.0
47-52	8.3	15.1	10.9	1.2	11.0	0.0

Soil blocks with less pronounced fingered flow patterns (Figs. 2C-F and 2H) were those which had been sampled in between major rain events (see also Fig. 5.1). For these soil blocks, actual soil water content distributions depended to a large extent on

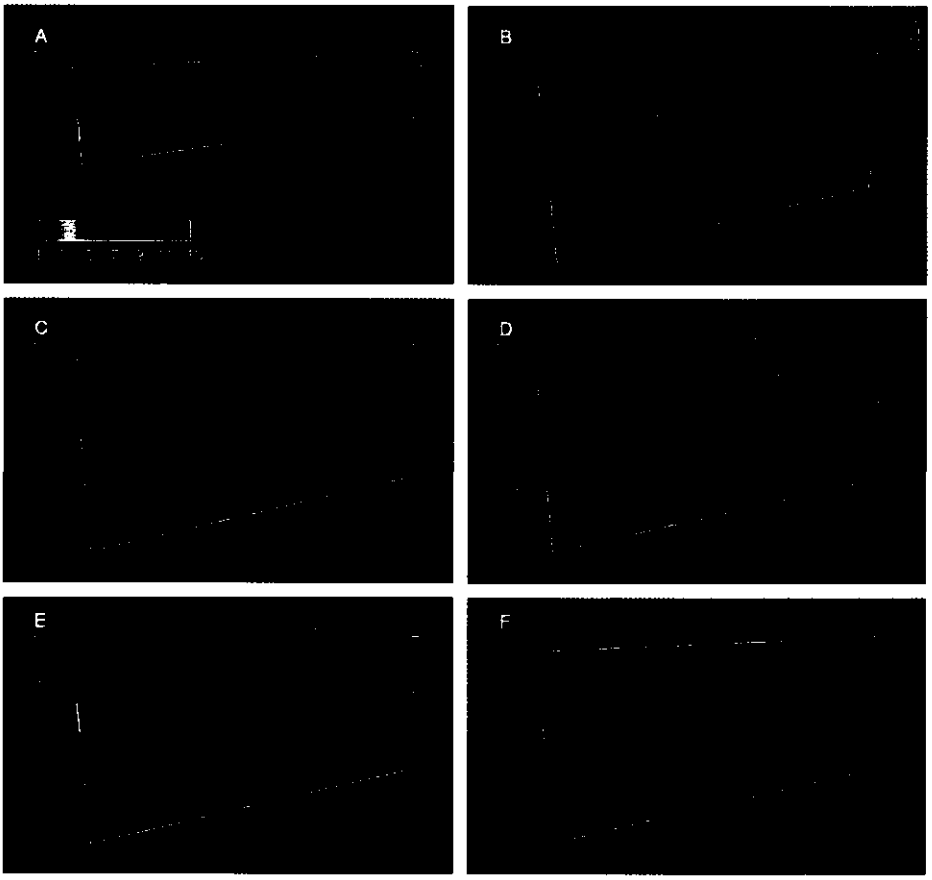

Fig. 5.2 *Spatial distribution of volumetric soil water content in 10 grass-covered sand blocks, each with a length of 1.2 m, a width of 0.6 m and a depth of 0.52 m, sampled during 1991 and 1992 at Ouddorp. Three-dimensional iso-surfaces and two-dimensional horizontal cutting planes at depths of 17 and 49.5 cm have been visualized. Each image is based upon 1400 measurements of soil water contents, except those for the soil blocks sampled on October 28 and November 2, which are based on 800 and 1600 samples, respectively. Soil blocks were sampled on October 28, 1991 (A), November 20, 1991 (B), January 6, 1992 (C), March 3 (D), April 8 (E), May 25 (F), June 6 (G), July 15 (H), September 1 (I), and November 2 (J).*

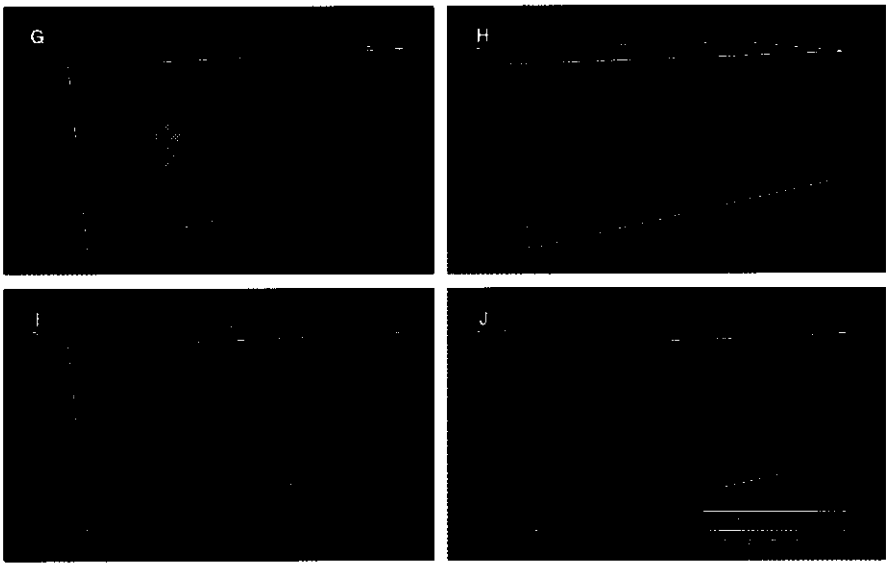

Fig. 5.2 *Continued.*

the time between the last major rain event and the moment of sampling. As time progresses after a major rain event with finger formation, fingered flow patterns gradually become irregular or even unrecognizable due to on-going processes like drainage, redistribution of the water and evaporation. In the long term, soil water content differences between sites with and without fingers become minimal. By contrast, fingered flow patterns may also disappear or become unclear after large amounts of rainfall, as is shown by the November 2 soil block (Fig. 2J). In this extremely wet soil block, water contents were less heterogeneously distributed than in the other soil blocks. Only some vague remnants of fingerlike patterns could be distinguished (Fig. 2J).

5.3.2 Actual water repellency

A critical soil water content exists, above which a water repellent soil layer becomes wettable (Chapters 2 and 4). These critical soil water content values were determined for each layer on the basis of the complete set of individual WDPT measurements

carried out on field-moist samples originating from the June 6, July 15, September 1, and November 2 soil blocks. For each soil layer, samples were divided into actually wettable and actually water repellent ones, and, by combining this with the related soil water contents, critical soil water contents could be established. For the 0-5, 7-12, 14.5-19.5, 22-27, 29.5-34.5, 39-44 and 47-52 cm soil layers, critical volumetric soil water contents were approximately 25.0%, 4.0%, 3.0%, 2.6%, 2.25%, 1.85%, and 1.7%, respectively. In a previous study of the same experimental site, critical soil water contents had been derived for the soil layers at depths of 5-10, 15-20, 25-30, 35-40, and 45-50 cm (see Chapter 4). A complete overview of the critical soil water contents versus depth for the Ouddorp soil is shown in Fig. 5.3. To the left of the line, the soil is water repellent, to the right it is wettable. This graph clearly indicates that *the occurrence of water repellency strongly depends on the actual water content of the soil, and that it varies with depth.* Therefore, water repellency will affect water flow mainly in initially dry soil, and its influence will be less significant under wetter soil conditions.

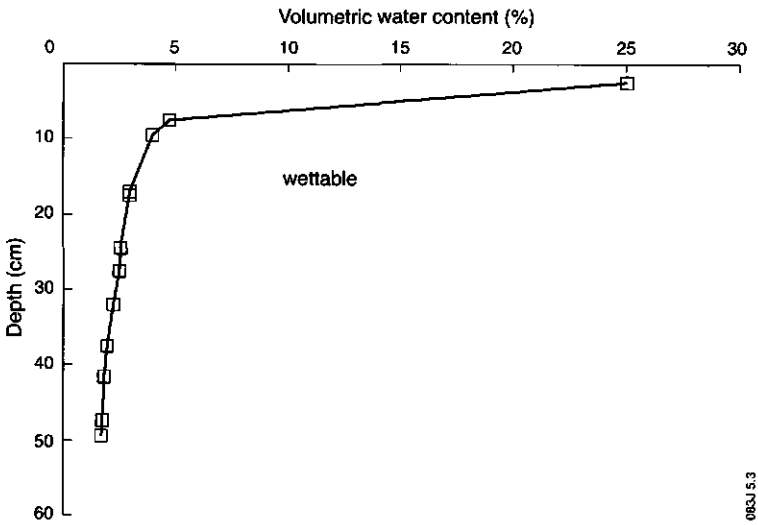

Fig. 5.3 *Critical soil water contents versus soil depth for the Ouddorp experimental field, indicating actually wettable soil to the right, and actually water repellent soil to the left of the line.*

The critical soil water content values were used to determine the percentages of actually water repellent soil for each of the soil blocks, which have been summarized in Table 5.1. Actually water repellent soil was mainly confined to the top three or four soil layers, and rarely (for instance in the November 20 soil block) reached down to greater depths. Actually water repellent soil was mainly found in the upper part of the soil profile, due to the combined effect in this zone of more severe drying and the highest critical soil water contents.

If some areas of the soil are actually water repellent, water will infiltrate most easily in the other areas, i.e. those with actually wettable soil. Areas with actually water repellent soil will inhibit or retard vertical water infiltration. In these areas, distribution flow will cause water and solutes to move mainly laterally toward actually wettable places, where vertical infiltration dominates. Fig. 5.4 shows top views of two of the soil blocks, indicating places with and without actually water repellent soil. Places with

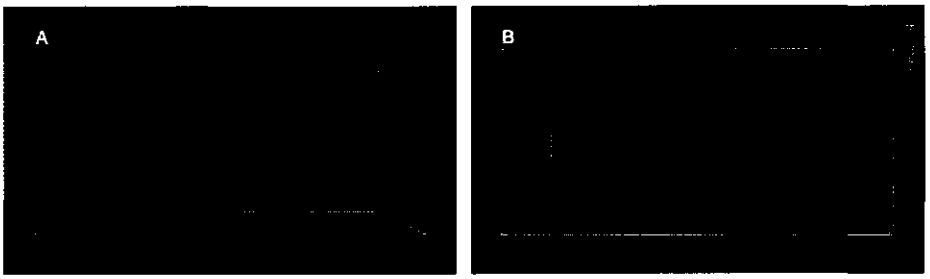

Fig. 5.4 *Top views of actually water repellent (red), and actually wettable (black) soil areas at the time of sampling of the November 20 (A) and June 6 (B) soil blocks at Ouddorp.*

wettable soil are potential locations for finger occurrence or finger formation, as these places are most accessible to water infiltration. Fig. 5.2 shows that fingers were indeed found in the wettable zones of the two soil blocks pictured in Fig. 5.4. Under wetter soil conditions, with water contents above the critical value, as was the case for instance in the November 2 soil block, fingerlike wetting patterns might disappear or become unrecognizable due to substantial lateral diffusion, leading to less heterogeneously distributed water contents per depth.

5.3.3 Potential water repellency

Information about the spatial variation in the degree of potential water repellency was obtained by applying the WDPT test on oven-dried (65°C) soil samples. Spatial variations in the degree of potential water repellency might be caused by a heterogeneous distribution of water repellent humic substances within the soil. In contrast with the actual water repellency, which might change rapidly in time due to changing water contents of the soil, potential water repellency is a more or less time-independent soil property, since much time is needed to change the quantity and/or quality of the water repellent humic substances within a volume of soil.

The degree of potential water repellency was measured in samples from the July 15 and November 2 soil blocks. The average degree of potential water repellency for the different soil layers is depicted in Fig. 5.5. This diagram illustrates that the most extreme potential water repellency was found in the 7 to 12 cm soil layer. The humous layer above was less water repellent, and the water repellency of the dune sand underneath decreased with depth. Potential water repellency disappeared at a depth of

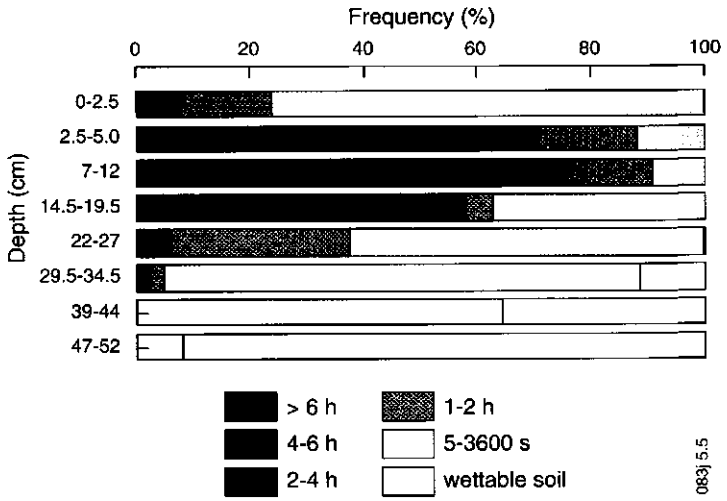

Fig. 5.5 *Diagram showing relative frequencies of varying degrees of potential water repellency for each soil layer in the Ouddorp experimental field. The diagram is based upon WDPT measurements of oven-dried samples of the soil blocks sampled on July 15 and November 2, 1992.*

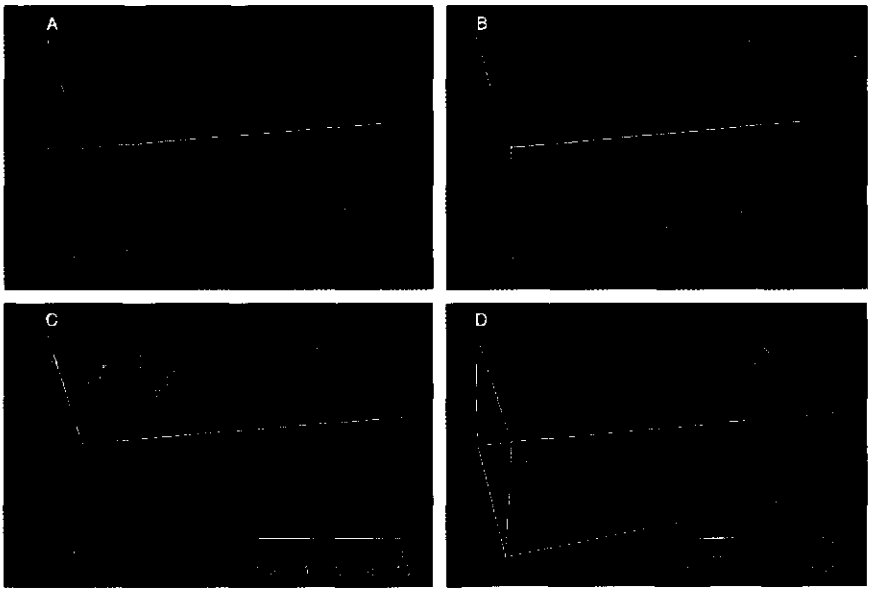

Fig. 5.6 *Images showing two-dimensional potential water repellency (A, C) and soil water content (B, D) patterns in the 7 to 12 cm layer of the July 15 (A, B) and November 2 (C, D) soil blocks. Places with relatively low degrees of potential water repellency coincide with places with relatively high soil water contents. In the very wet November 2 soil block, dry soil was found only in places with the highest degree of potential water repellency.*

approximately 50 cm. It seems likely that the most water repellent soil layer, i.e. the 7 to 12 cm soil layer, obstructs infiltrating wetting fronts most effectively, causing instability at this depth. However, the diagram depicted in Fig. 5.5 reveals that for a specific depth, the degree of potential water repellency varies from place to place as well. This indicates that each layer consists of areas with relatively high and those with relatively low degrees of potential water repellency. For a 'uniformly' dry soil, finger formation might therefore be expected in areas with a relatively low degree of potential water repellency, as resistance to wetting is lowest there.

Fig. 5.6 shows potential water repellency and soil water content distributions for the

7 to 12 cm layer of the soil blocks sampled on July 15 and November 2. For the July 15 soil block, these images reveal that the highest soil water content values were indeed found in those places with the lowest degree of potential water repellency. Similar patterns of wet and dry soil were often visible during sampling, an example of which is shown in Fig. 5.7. For really wet conditions, such as those which occurred in the soil block sampled on November 2, the images in Fig. 5.6 clearly indicate that remnants of dry soil were restricted to places with the highest degree of potential water repellency. The patterns shown in Fig. 5.6 support the idea that the water flow patterns in this particular soil were related to, or regulated to a large extent by, the spatial differences in potential soil water repellency.

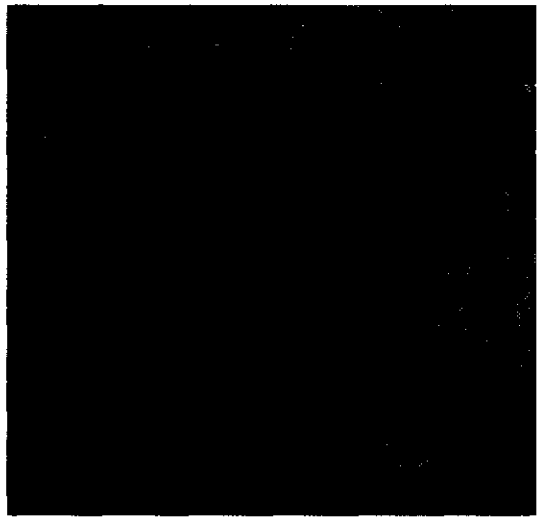

Fig. 5.7 *Top view of wet (dark areas) and dry (light areas) soil in a horizontal plane during the sampling of one of the soil blocks.*

5.4 DISCUSSION

The soil block sampling method applied in the present study is a destructive method, yielding only one three-dimensional soil water content distribution per block. In our

opinion, it was the only feasible method to obtain three-dimensional information about soil water content patterns in a field soil at such a fine spatial resolution. Installation of permanent measuring devices in a spatial grid comparable to that used in the destructive soil block sampling campaigns is impossible with current measurement techniques.

Interpretation of the three-dimensional water content distributions in the soil indicated that the fingered flow patterns might become less clear during periods of excessive rain or during prolonged droughts. Therefore, future studies on fingered flow in water repellent soils should focus on water dynamics during and just after rain events. Only then can information be gathered on how fast fingers appear during rain events and disappear after rainfall ceases. This type of information is especially crucial for studies dealing with the prediction of transport velocities of surface-applied agrichemicals.

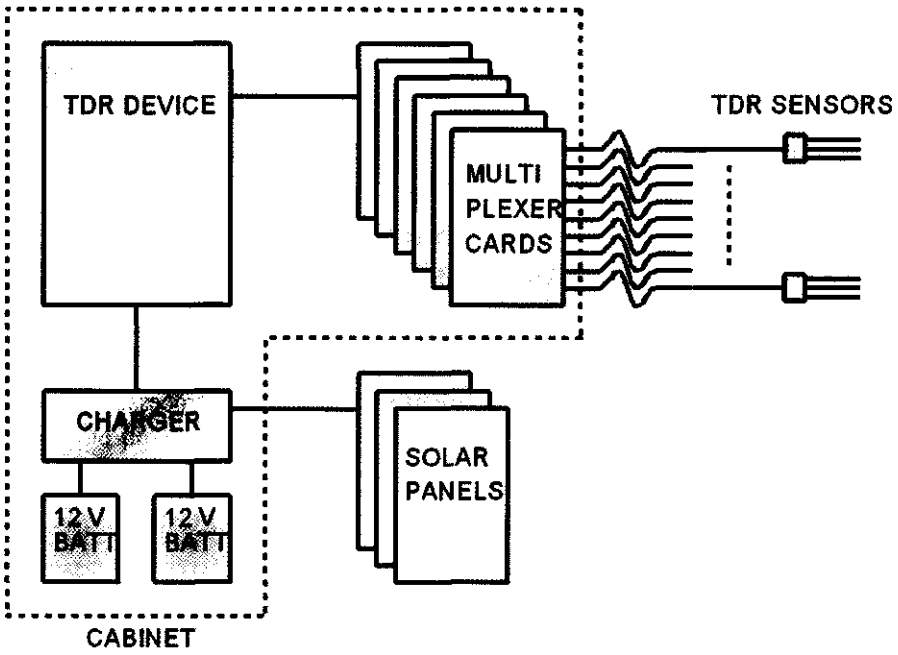

Fig. 6.1 *Schematic set-up of the stand-alone TDR measurement device used to monitor water content changes in the water repellent soil near Ouddorp, the Netherlands.*

This geometry allowed calculation of the volume that holds 95% of the electrical energy, i.e. the approximate measuring volume, using the model introduced by Knight et al. (1994). The imaginary elliptical envelope around the rods of the sensors holding 95% of the radiated energy was about 7.2 cm in vertical diameter and 6.4 cm in horizontal diameter, if the rods were placed horizontally. This elliptical envelope covered an area of about 36 cm^2. The length of the rods was 20 cm, yielding a measuring volume of about 720 cm^3 per probe. In combination with the measuring grid used, which had horizontal distances of 15 cm and vertical distances of 8, 10 or 15 cm between adjacent probes, this guaranteed sufficient spatial resolution to detect any occurrence of fingered flow pathways (Ritsema and Dekker, 1996a).

Solar power supply

Since the system was placed in a remote area, it was powered by two parallel 12 V, 50 Ah batteries. The entire measuring system consumed about 1.4 Ah per 24-hour period. This battery capacity enabled the system to remain operational for at least four weeks without being recharged. This guaranteed continuous operation even during the winter period. The batteries were charged by a set of three Siemen's 50 W solar panels, using a Siemen's charging regulator. The solar panel size was such that the batteries could be recharged within three sunny days. The power supply system caused no problems during the entire measuring period.

Data processing

During the 8 months experimental period, almost 200,000 volumetric soil water content values were recorded, which were used to construct two-dimensional water content distributions for every 3 hour time-step. In all, around 2,000 graphs were made, a selection of which is presented in the present study.

6.2.2 Precipitation, potential evaporation and groundwater level

Precipitation was measured using an automatically recording tipping bucket system, with an accuracy of 1 mm. Daily potential evaporation rates were obtained from a nearby meteorological station. The groundwater level was measured using an automated groundwater level logger, based on a water level pressure sensor. The measuring range of this water level logger was 1500 mm. Data from both devices were retrieved by a laptop PC every three weeks during the visits to the site.

6.3 RESULTS

Values of precipitation, potential evaporation, mimimum net infiltration (precipitation rate minus potential evaporation rate) and groundwater level measured in the course of the experiment are shown in Figs. 6.2A, 6.2B, 6.2C and 6.2D, respectively. Most rainfall was recorded in the second half of the experimental period (Fig. 6.2A), the total rainfall registered being around 500 mm. Daily potential evaporation ranged from 0 to 5 $mm.d^{-1}$, with highest amounts occurring in summer, at the start of the experiment

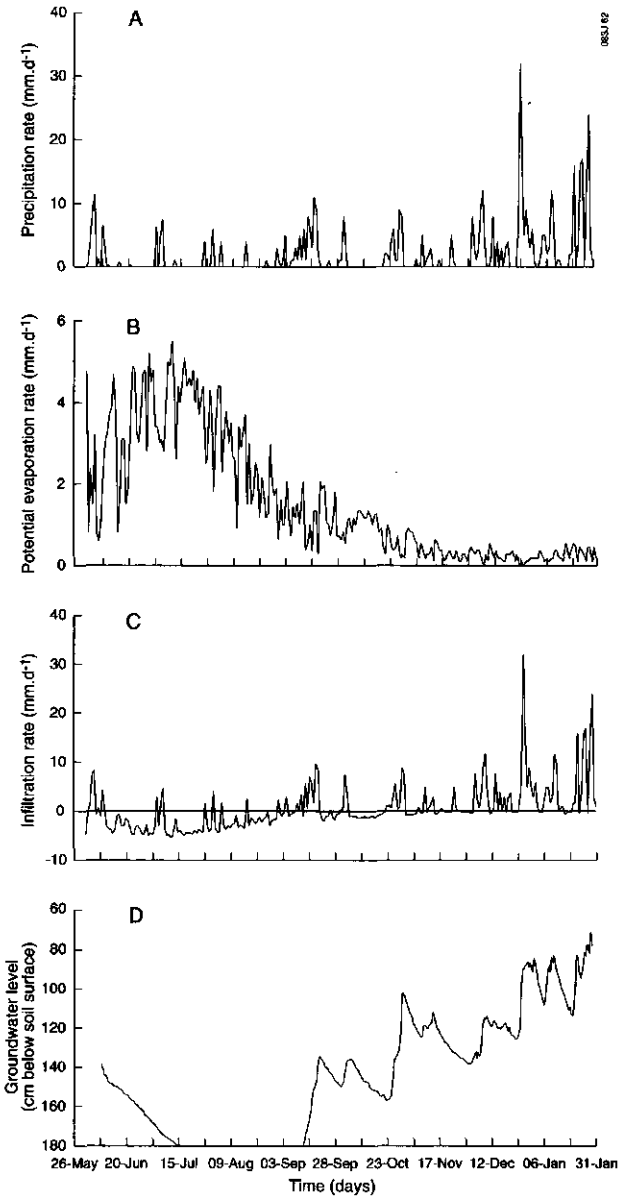

Fig. 6.2 *Precipitation rate (A), potential evaporation rate (B), minimum net infiltration rate (C), and groundwater level (D) measured at Ouddorp during the 8 months measurement campaign.*

(Fig. 6.2B). Fig. 6.2C shows that several major infiltration events occurred during the experiment, particularly between September 1994 and the end of January 1995. These events were accompanied by sharp rises in the groundwater level (Fig. 6.2D), indicating rapid downward transport of water during such events.

Fig. 6.3 shows examples of soil water contents measured by three TDR probes placed above each other at depths of 4, 30 and 70 cm. Data for a three week period in July 1994 were lost due to a computer breakdown. The probe at 4 cm (Fig. 6.3A) responded very quickly to rain events (see also Figs. 6.2A and 6.2C), and volumetric water contents varied between 3% and 30%. The probe at 30 cm showed a similar, but less pronounced, response to rain events (Fig. 6.3B). There was little or no delay in wetting compared to the probe at a depth of 4 cm. Volumetric water contents measured by the probe at 30 cm varied between 4% and 20%. Even at a depth of 70 cm within the profile, direct volumetric water content rises occurred during rain events (Fig.

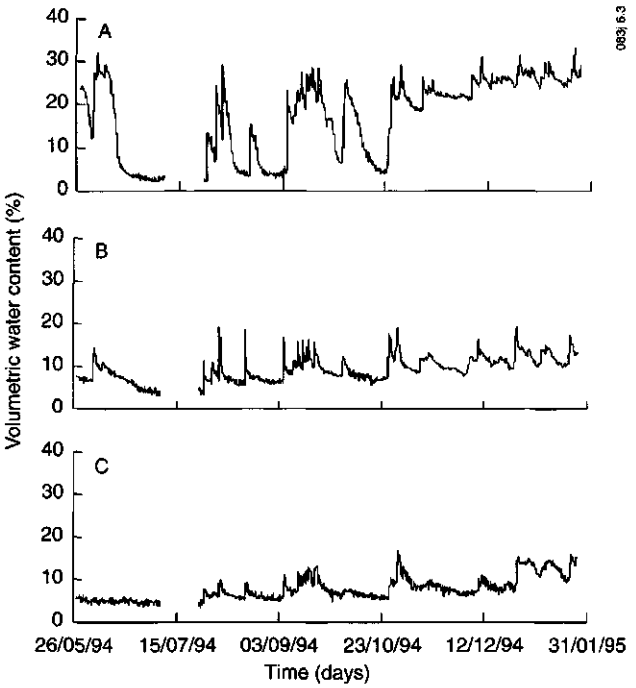

Fig. 6.3 *Examples of soil water content values measured by three TDR probes arranged in a vertical line at depths of 4 (A), 30 (B) and 70 (C) cm.*

6.3C), and the pattern showed a close resemblance to those observed by the other two probes. Water content variations at this depth were, however, less pronounced, and varied between 4% and 15% only.

In order to illustrate the process of finger formation and finger recurrence, a selection was made of the seven most pronounced rainy periods during the experimental period. Table 6.1 summarizes information about these seven rainy periods. The duration of the rainy periods was between 8 and 11 days, and the total rainfall ranged from 34 to 81 mm per event. Subtraction of the potential evaporation from the rainfall quantities yielded a conservative estimate of the amount of infiltrated water during the selected periods. Estimated net infiltration varied between 13 and 79 mm (Table 6.1), with the most distinct events during the months of December and January. The cumulative rainfall, potential evaporation, and mimimum net infiltration, as well as the course of the groundwater level during the selected rainy periods are depicted in Fig. 6.4. The groundwater level responded to each event, except for the period in June (missing data) (Fig. 6.4B).

Table 6.1 *Rainfall duration and quantity, potential evaporation, and minimum net infiltration for the seven most pronounced rainy periods during the period June 1994 until January 1995 at the Ouddorp experimental site.*

Rainy period	Rainfall duration (days)	Rainfall amount (mm)	Potential evaporation (mm)	Minimum infiltration (mm)
1	11	36	23	13
2	10	47	11	36
3	10	34	3	31
4	8	40	3	37
5	10	81	2	79
6	8	39	2	37
7	8	57	3	54

For each rainy period, the soil water content distributions measured within the TDR transect are shown just before, during (twice), and at the end (or after cessation) of the rainfall (Fig. 6.5). Volumetric soil water contents before the rain events (Fig. 6.5, left hand side) were generally between 0% and 10% for the water repellent subsoil, and up

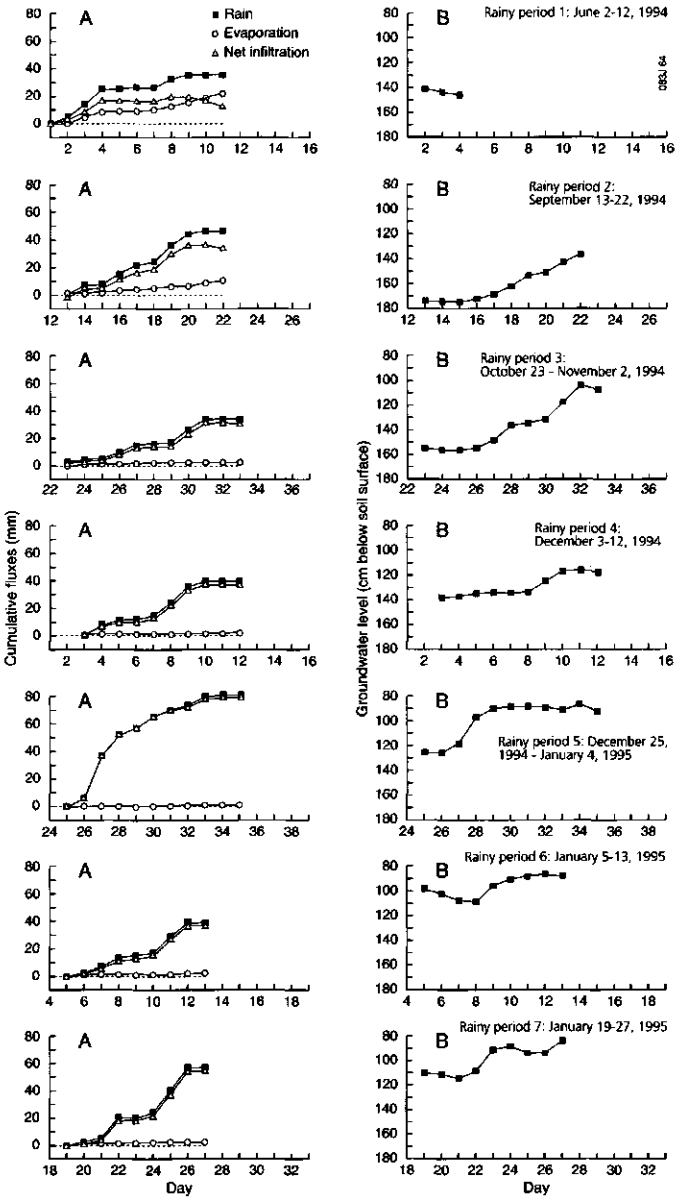

Fig. 6.4 *Cumulative rainfall, potential evaporation, and mimimum net infiltration (A), and course of the groundwater level (B), for the selected rainy periods.*

to 10% to 25% for the humous layer, although there were some differences. No fingered flow patterns were present before the start of the rain events, but these emerged during all rainy periods. The most distinct ones were monitored under conditions of heavy rainfall with initially slightly wetter topsoil (rainy periods 3, 5, 6, and 7). During the rainy periods 1, 2 and 4, fingered flow patterns emerged as well, but with less evidence of protrusion of fingers to the deepest layers of the TDR transect. However, the groundwater level evidently rose during events 2 and 4 (Fig. 6.4), indicating downward flow to the groundwater in both cases.

Based upon the arrangement of the TDR probes within the transect, the soil profile can be divided into seven layers, namely the 0-8, 8-16, 16-25, 25-35, 35-47.5, 47.5-62.5 and 62.5-77.5 cm layers. If we assume that the TDR probes monitor soil water content changes for each of these layers, a soil water balance can be made for the entire TDR transect. Table 6.2 shows the estimated water balance for the entire transect for each of the selected rainy periods. Mimimum net infiltration was derived by subtracting potential evaporation from rainfall, while changes in the water content in the soil in the transect down to a depth of 77.5 cm were determined using the individual TDR measurements. These two values were used to estimate the mimimum amount of deep drainage to the soil region below 77.5 cm.

From the amounts summarized in Table 6.2, one can conclude that deep drainage was most evident during the December and January rain events. Based upon the measured hydraulic conductivity characteristic of the Ouddorp sand (Ritsema and Dekker, 1994b) (see Chapter 4), it might be concluded that water flowing along the fingered flow pathways provided the main contribution to deep drainage. Hydraulic conductivities at volumetric water contents of 5, 10, 15, 20 and 25% were 0.0002, 0.02, 0.2, 0.5, and 1.5 cm.day^{-1}, respectively. This indicates, for instance, that the hydraulic conductivity at a volumetric water content of 15% is a thousand times higher than that at a volumetric water content of 5%. According to Table 6.2, the emerging fingered flow pathways in the TDR transect during rainy periods 1 and 3 did not lead to considerable drainage below 77.5 cm depth. However, the observed groundwater level rise during rainfall period 3 does suggest the opposite, and most probably much more water infiltrated into the soil during this event than was estimated in Table 6.1.

The percentage of the infiltrating water per rainy period which was transported through the fingers to the deep subsoil could also be derived, and ranged from 0% to

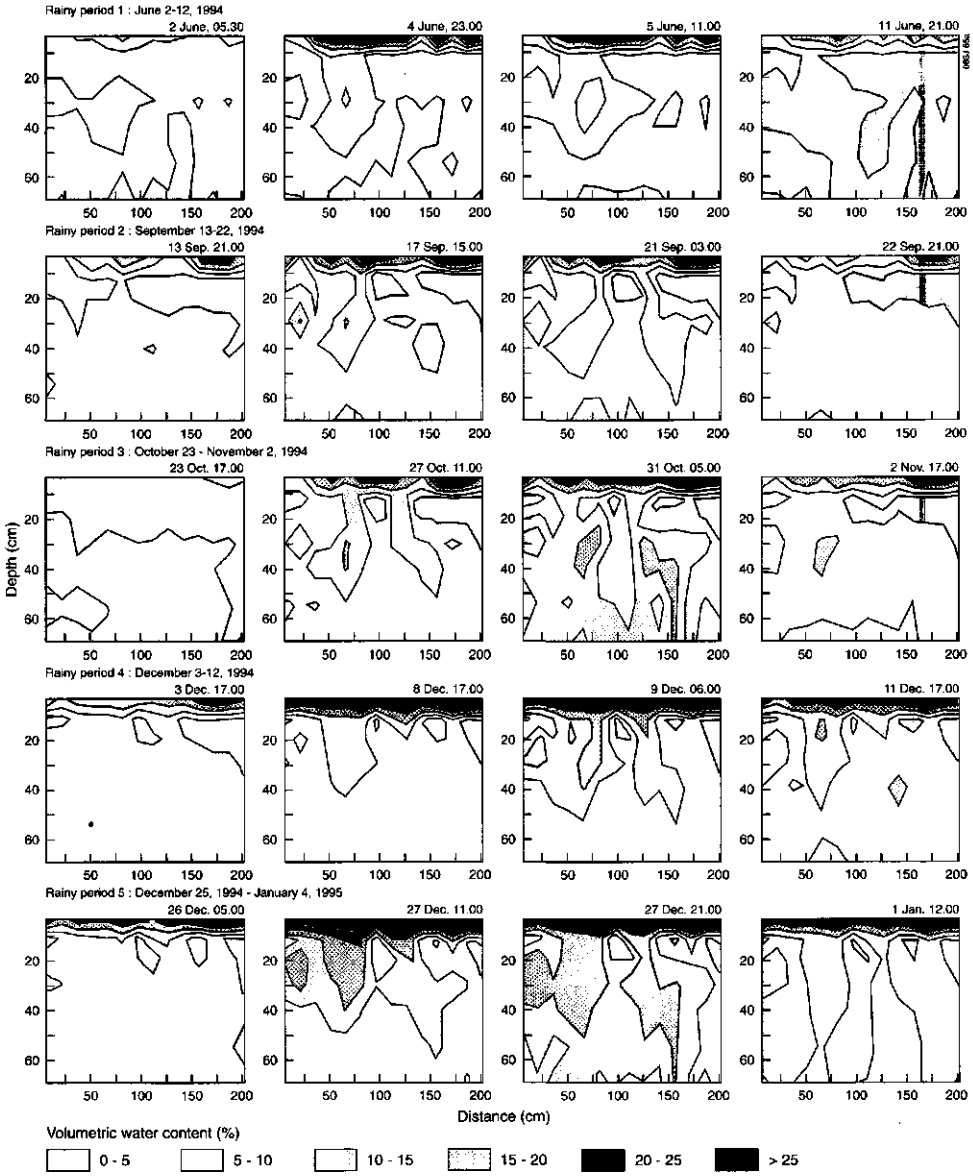

Fig. 6.5 *Spatial distributions of soil water content in the 2 m long and 0.7 m deep TDR trench before, during and after the selected major rainy periods.*

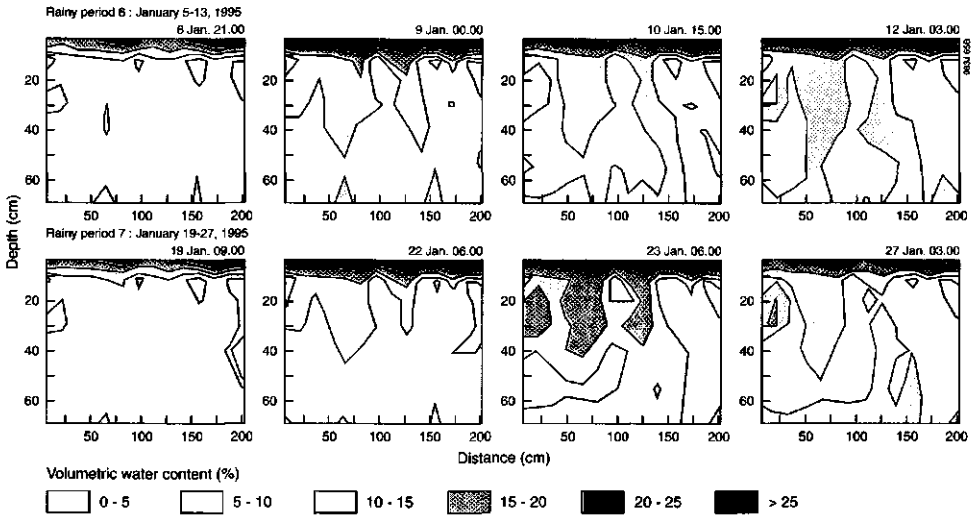

Fig. 6.5 Continued.

Table 6.2 *Estimated soil water balance for the 200 cm long and 77.5 cm deep TDR transect for the selected rainy periods.*

Rain event	Mimimum net infiltration (mm)	Change in water storage to a depth of 77.5 cm (mm)	Mimimum deep drainage below a depth of 77.5 cm (mm)	Part of infiltrating water flowing to depths below 77.5 cm (%)
1	13	13	0	0
2	36	21	15	42
3	31	31	0	0
4	37	20	17	46
5	79	16	63	80
6	37	11	26	70
7	54	24	30	56

80%, depending on the wetting history of the soil and the rainfall characteristics (see Table 6.2). The highest percentages occurred during the rainy periods in the winter (events 5, 6, and 7).

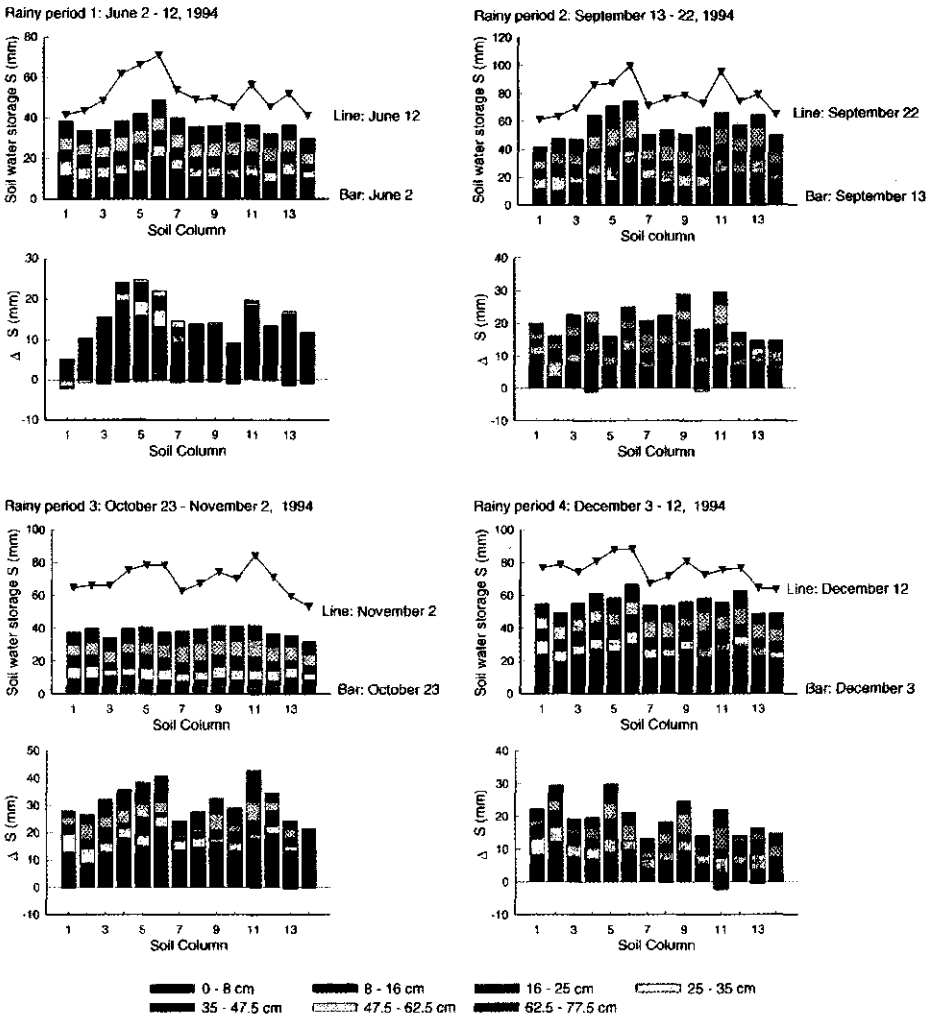

Fig. 6.6 *Calculated amounts of water stored in the soil just before and at the end of seven rainy periods in fourteen 77.5 cm deep soil columns located within the 2 m long TDR transect at Ouddorp. Also shown are storage changes for each soil layer.*

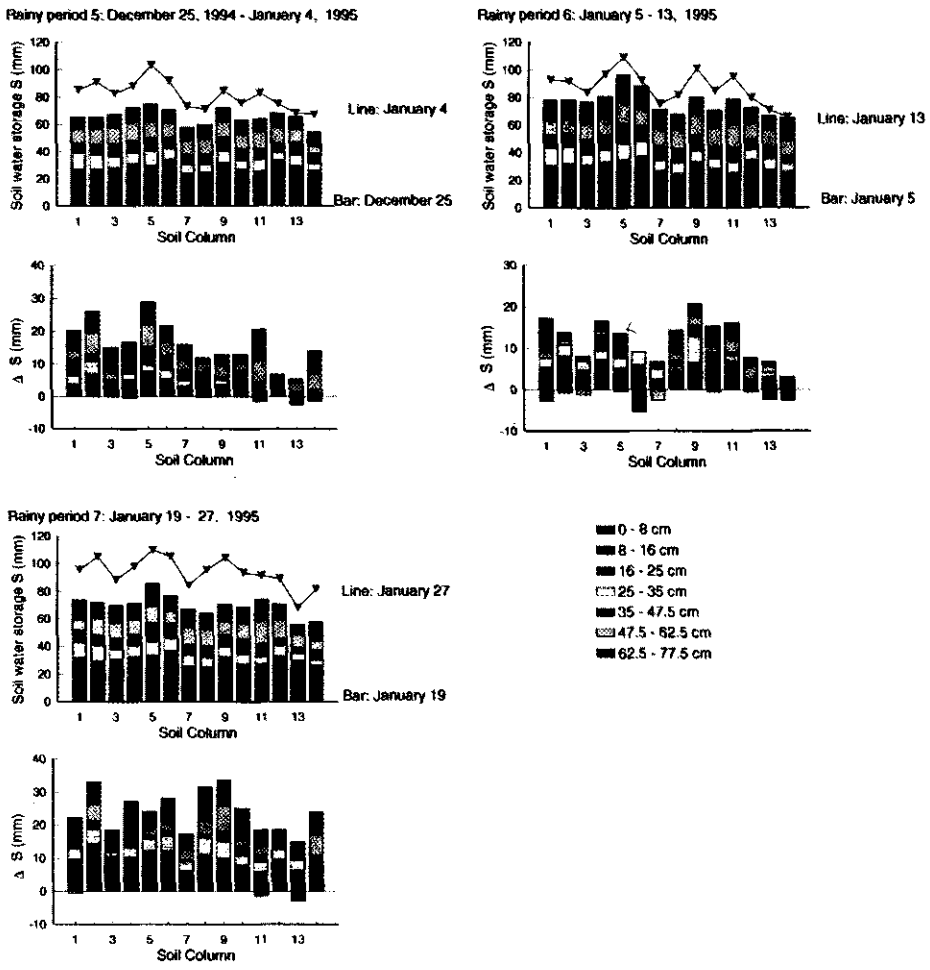

Fig. 6.6 *Continued.*

The set-up of the TDR transect, with 98 probes in a fixed spatial grid, enabled us to distinguish 14 vertical soil columns within the transect, each with probes at seven depths. If we assume that the various TDR probes measured soil water contents for the same representative soil layers, i.e. the layers 0-8, 8-16, 16-25, 25-35, 35-47.5, 47.5-62.5 and 62.5-77.5 cm, the total water storage can be estimated before and at the end of the rainy periods, as can the changes per layer for each soil column. Fig. 6.6 shows

the total soil water content down to a depth of 77.5 cm for all 14 soil columns at two times, namely just before the start of the rainy period and at the end. From the combined line-bar graphs in Fig. 6.6, it can be concluded that some places within the TDR transect were initially wetter and were (sometimes) wetted to a greater degree during the rainy periods than others. The general trend seems to be that initially wetter places remained more wet or received more water than initially drier places, although this was not always obvious from Fig. 6.6 (probably due to on-going processes like redistribution of soil water and/or deep drainage during the rainy periods). The single bar graphs in Fig. 6.6 depict the increase or decrease in the amount of soil water for each soil layer and soil column distinguished, for all selected rainy periods. These bars show that during the first rain events the infiltrating water was mainly used to increase the water content of the upper soil layers of the TDR transect, while later on, large proportions of the infiltrating water passed through to deeper soil regions, even below a depth of 77.5 cm (Table 6.2).

6.4 DISCUSSION

6.4.1 Resolution of measurements

A comparison of the two-dimensional soil water content distributions measured by the TDR device (Fig. 6.5) with those obtained via the intensive soil cylinder sampling method (Ritsema and Dekker, 1994b) (see Chapters 4 and 5) reveals that the resolution was slightly poorer for the TDR transect. This is not unexpected, as the soil cylinder sampling method uses 100 cm^3 soil samples in a dense array to determine water contents. The TDR set-up applied in the present study uses individual soil water content measurements which are representative of volumes of slightly more than 700 cm^3 of soil. Despite the high quality measurement results obtained in this study, resolution can be increased by using smaller TDR probes. In this way, more accurate information will be gathered with respect to maximum and minimum soil water content values. Future studies of the dynamic behavior of fingered flow processes would therefore benefit from using the smallest TDR probes available to maximize the measuring resolution. Using smaller probes would also allow the measuring grid to be refined.

6.4.2 Recurrence of flow fingers

The findings of the present study indicate that *fingers recur at the same locations during successive rain events.* It has been shown by Ritsema et al. (1998a,b) (see also Chapters 8 and 9) that the water retention function of the Ouddorp sand is extremely hysteretic, characterized by a steep main wetting branch. This is typical of water repellent materials, and explains why vertical fingers can exist in dry soil (Nieber, 1996). The recurrence of fingers at the same locations can be attributed to the hysteretic water retention character of the Ouddorp sand. After the cessation of rainfall, the water content of the soil decreases throughout the profile, within as well as outside the fingers. After a certain period of time, water content variations in previous locations with and without fingers decrease, but differences do remain, due to their different wetting history. *Even when the soil water content differences have become very small, water will still show a tendency to flow into the previous pathways, as the water content in these places is slightly higher than that in the immediate vicinity of the previous fingers. Even only slightly higher soil water content implies significantly larger hydraulic conductivities, as was illustrated by Ritsema and Dekker (1994b) (Chapter 4), promoting the flow of water through the wetter soil.* This process of finger recurrence in soils might continue for an unlimited period of time, except that human influence might change the pattern drastically. The particular grass-covered experimental site used in the present study had not been tilled for several decades. *If fields are used for the cultivation of crops, fingers might retain stable spatial positions for one growing season only.* In the following growing season, tillage treatments and seed bed preparation might cause fingers to occur at different locations than the year before. Therefore, *persistent spatial finger patterns like those found in the present study might develop in, for instance, untilled agricultural fields, nature reserves and forests.*

6.5 CONCLUSIONS

The TDR measurement device used in the present study is a suitable instrument for detecting finger formation and finger recurrence in soils. For future studies, we recommend the use of smaller TDR probes, allowing for denser measurement arrays and higher measurement resolution. Finger formation depends on the wetting history

of the soil and rainfall characteristics. *Fingers develop rapidly during severe rain storms, causing significant proportions of the infiltrating water to be preferentially transported through the fingers to the deeper subsoil.* Fingers recurred at the same sites during all rain events.

CHAPTER 7

FINGERED FLOW INDUCED BROMIDE DISTRIBUTIONS

Adapted version of 'Three-dimensional patterns of moisture, water repellency, bromide and pH in a sandy soil' by C.J. Ritsema and L.W. Dekker, published in the Journal of Contaminant Hydrology 31:85-103, 1998.

7 FINGERED FLOW INDUCED BROMIDE DISTRIBUTIONS

Abstract

Water repellency may lead to preferential flow of water and surface-applied solutes through the unsaturated zone of soils. To study this process in detail in the Ouddorp experimental field, a bromide tracer was applied to a 2.2 m by 0.4 m plot. The bromide application rate was 8 $g.m^{-2}$, and the plot was sampled using 100 cm^3 steel cylinders after 52 mm of rainfall in 12 days. A total of 7 soil layers were sampled, to a depth of 74 cm. Each layer was sampled at 240 locations in a grid of 40 by 6 samples. All samples were used to determine soil water content, degree of actual and potential water repellency, bromide concentration and pH. The spatial distributions of these properties were visualized three-dimensionally, and compared. The distribution of the degree of water repellency, bromide concentration, and pH bore close resemblance to the fingered flow induced soil water content distribution. The degree of potential water repellency was relatively low in places with fingers. Actual water repellency occurred at the dry spots between the fingers. Bromide was not found, or only in very low concentrations, in such places. Bromide depth profiles clearly indicated the occurrence of diverging flow in the wetter subsoil. Manuring activities during the last decades are likely to have resulted in relatively high pH values in the humous layer, as well as in the subsoil along the recurring fingered flow pathways.

7.1 INTRODUCTION

Water repellent soils are difficult to wet in the range below their critical soil water content, i.e. the soil water content above which a soil is wettable and below which it becomes water repellent (Dekker and Ritsema, 1994; Ritsema et al., 1997a). In initially dry soil, rainwater often percolates through specific paths which allow higher infiltration rates than the surrounding soil (Ritsema and Dekker, 1995). During rainy periods, preferential flow paths or fingers may form in such places, through which water and surface-applied solutes are transported rapidly to the subsoil and the underlying groundwater reservoirs. This may result in increased contamination risk if

agrichemicals or manure have been applied to the soil surface. Sometimes as much as 80% of the infiltrating water is transported in preferential flow paths to the deep subsoil during single rain events (Ritsema et al., 1997b) (see Chapter 6). During successive rain events, fingers may recur in the same places within a field. This phenomenon can be attributed to hysteresis in the water retention function of water repellent soils, causing places with fingers to be slightly wetter throughout the year, even after prolonged dry periods. Therefore, water infiltration will always be higher within fingers remaining from previous infiltration processes, as has been shown experimentally in the field (Ritsema et al., 1997b; Chapter 6) and in model studies (Nieber, 1996; Ritsema et al., 1998a; Chapter 8).

Transport of solutes through water repellent soils has been studied in some field tracer experiments (Van Dam et al., 1990; Ritsema et al., 1993). However, no detailed information on three-dimensional solute distributions has been obtained so far. Therefore, this study aimed to

- investigate three-dimensional fingered flow induced bromide distributions in a water repellent sandy soil;
- relate the bromide distribution to water content and water repellency distributions;
- indicate the effect of fingered flow on the spatial distribution of pH in the soil.

7.2 MATERIALS AND METHODS

7.2.1 Tracer experiment

The experimental plot was 2.2 m long and 0.4 m wide. A KBr tracer solution was applied manually to the soil surface with six nozzle sprinklers on November 15, 1995. The tracer application rate was determined by placing 24 small trays around the experimental plot. A total of 8.0 g bromide per m^2 was applied, with a standard deviation of 1.5 $g.m^{-2}$. On November 27, after 52 mm of rain, excavation of the experimental plot started, on the basis of a spatial grid of 40 by 6 by 7 samples, in the X, Y and Z directions, respectively, yielding a total of 1680 samples for the entire plot. Samples were taken with the help of steel cylinders (volume 100 cm^3, height and diameter 5 cm), which were carefully pushed into the soil. In the horizontal direction,

the distance seperating two adjacent samples was 0.5 cm. Seven soil layers were sampled at depths of 0-5, 9-14, 19-24, 30-35, 42-47, 55-60, and 69-74 cm. The samples were taken to the laboratory for the determination of their water content, degree of water repellency, bromide concentration and pH. Since the variation in the degree of water repellency in the upper soil layers is often large, samples originating from the 0-5 cm layer were split into a 0-2.5 and 2.5-5 cm sample, respectively.

Precipitation and groundwater levels were recorded automatically from November 15 to 27 (Fig. 7.1). A total of 52 mm of rain was recorded in this period, and the groundwater level rose slightly from around 174 to 170 cm below the soil surface.

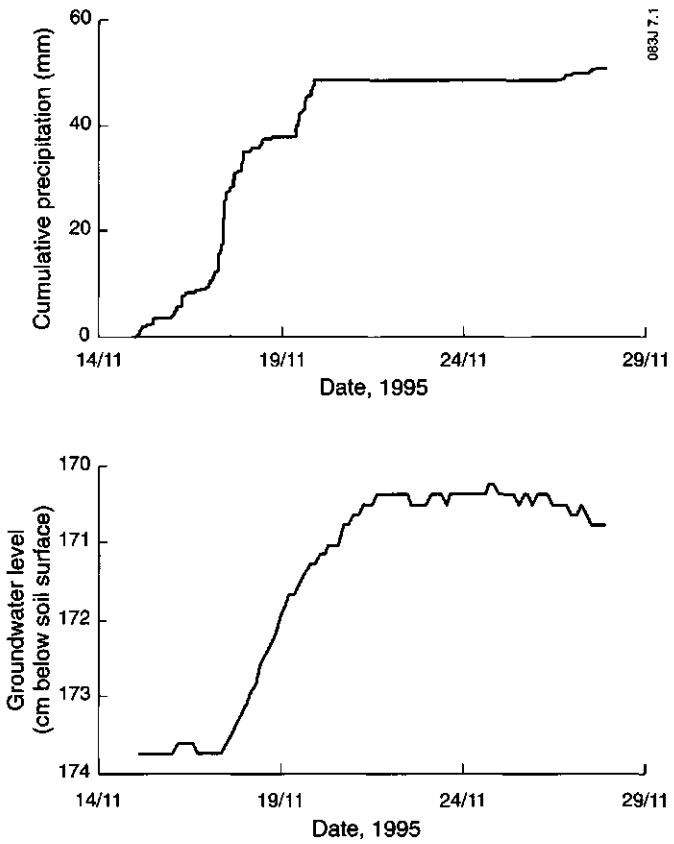

Fig. 7.1 *Measured precipitation and groundwater level between November 15 and 27, 1995, during the bromide tracer experiment at Ouddorp.*

7.2.2 Laboratory measurements

All field-moist soil samples were first weighed in the laboratory, and the degree of actual water repellency was determined using the WDPT test described in Chapter 2. Ten classes of water repellency were distinguished. Thereafter, samples were oven-dried at 65°C, and weighed again to determine the volumetric water content. After equilibration in the laboratory for three days, samples were used to determine the degree of potential water repellency, using the same WDPT test. The samples were then used to determine bromide concentrations. After water had been added to the samples, and the mixture had been shaken for a fixed period of time, bromide concentration in the solution was measured using the High Pressure Liquid Chromotography technique. Finally, the pH of the solution was determined using a standard pH electrode.

7.2.3 Three-dimensional visualization

The laboratory data on water content, water repellency, bromide concentration, and pH were used to obtain three-dimensional visualizations of each of these properties, using the Iris Explorer modular visualization software environment on a SGI Indigo workstation (Heijs et al., 1996; Ritsema et al., 1997a). Besides visualization of three-dimensional iso-surfaces, intersecting horizontal and vertical planes were also depicted in the graphs.

7.3 RESULTS

7.3.1 Soil water content distribution

The average soil water content profile, with 95% confidence intervals, indicates relatively high water contents in the surface layer and much lower values in the subsoil (Fig. 7.2A). The subsoil exhibited the lowest degree of variation in soil water content. The other components of Fig. 7.2, i.e. the bromide concentration and pH behavior, are discussed in paragraphs 7.3.3 and 7.3.4, respectively.

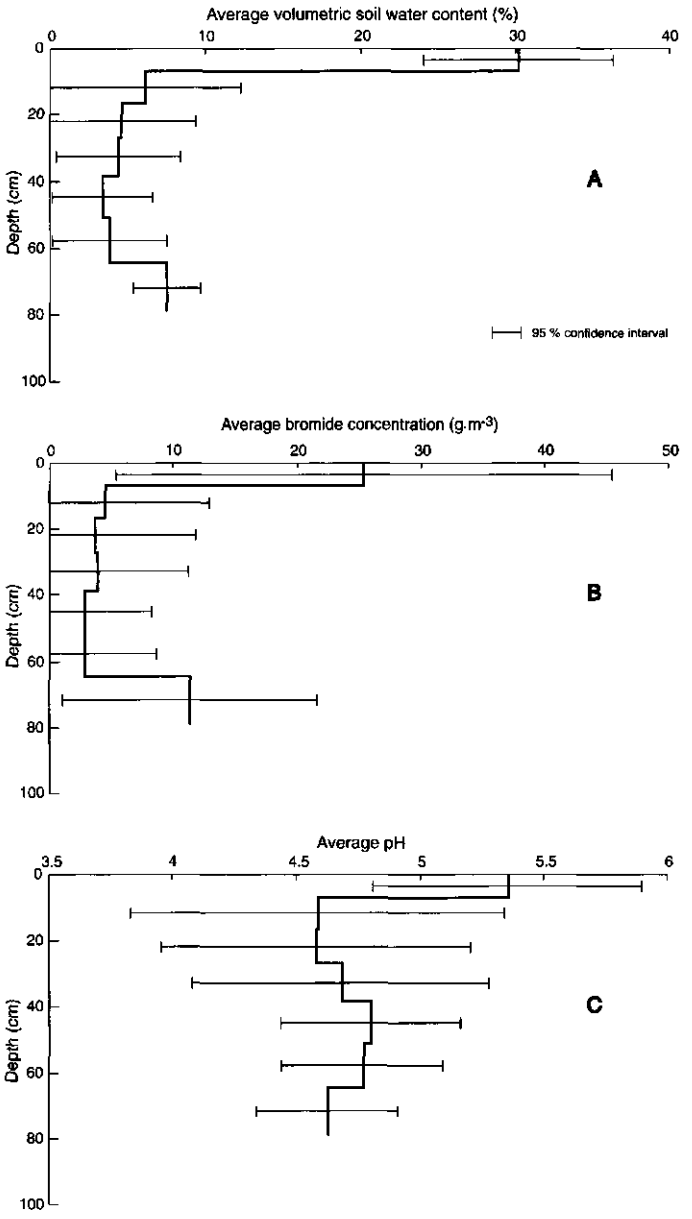

Fig. 7.2 *Average soil water content (A), bromide concentration (B), and soil pH (C) profiles, including the 95% confidence intervals, at the time of excavation.*

Based upon the sampling grid, the soil profile was divided into seven successive layers, i.e. the 0-7, 7-16.5, 16.5-27, 27-38.5, 38.5-51, 51-64.5 and 64.5-79 cm layers. On the assumption that the water contents measured across the 5-cm layers are representative of the slightly thicker layers listed above, 240 (79 cm long) individual soil cores can be distinguished for which the total amounts of soil water can be derived. The amount of water in each of the soil layers is shown for all 240 soil cores in Fig. 7.3A. Total water per column ranged from 4 cm to more than 8 cm. Wet columns were characterized by relatively large amounts of water in the soil layers below a depth of 7 cm, compared to the dry columns. This suggests a pattern of vertically directed preferred flow paths. Wet columns represent zones with, and dry columns zones without preferred flow paths. The occurrence of preferred flow paths at this particular experimental site had already been confirmed in a previous study by Ritsema et al. (1997b) using TDR probes (see Chapter 6).

The water content distribution within the sampled soil block was visualized three-dimensionally (Figs. 7.4A and 7.4B). Besides a volumetric water content iso-surface of around 6%, a horizontal (Fig. 7.4A) and a vertical (Fig. 7.4B) cutting plane were also visualized. In general, fingerlike patterns were present within the soil block, although they were not very distinct. This is most probably caused by the fact that sampling occurred around 7 days after the last major rain event (see Fig. 7.1). It has been shown by Ritsema et al. (1997a,b; Chapters 5 and 6) that after cessation of rainfall, fingered flow patterns vanish relatively rapidly due to deep drainage, water redistribution and evaporation processes. Therefore, the most pronounced fingered flow patterns can be expected during and just after major rain events. Some fingerlike patterns are still visible in the Figs. 7.4A and 7.4B, especially at the center and on the right-hand side of the block sampled. Outside areas with fingers, volumetric water contents were low, sometimes as low as 1% to 2% (Fig. 7.4B). The humous layer was relatively wet, and it can be seen that the wettest sites in this layer lay on top of zones with fingers. In the deepest part of the soil block, volumetric water contents increased to values between 6% and 10%. The highest water content values in this layer were found in the area directly below or in the vicinity of fingers.

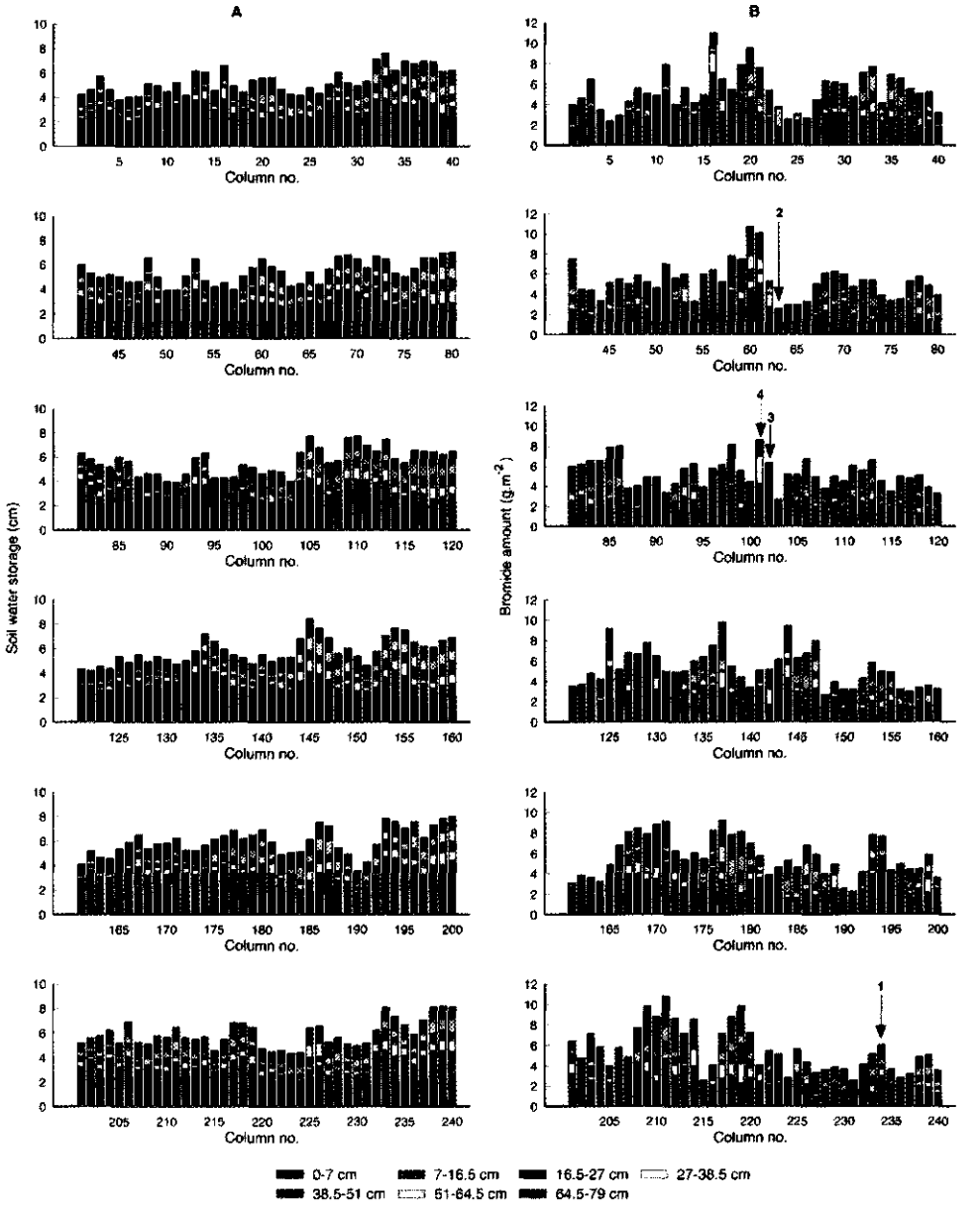

Fig. 7.3 *Measured soil water storage (A) and bromide (B) quantities in 240 soil columns (79 cm long) at the experimental site. The average bromide application rate was 8.0 g.m^{-2}.*

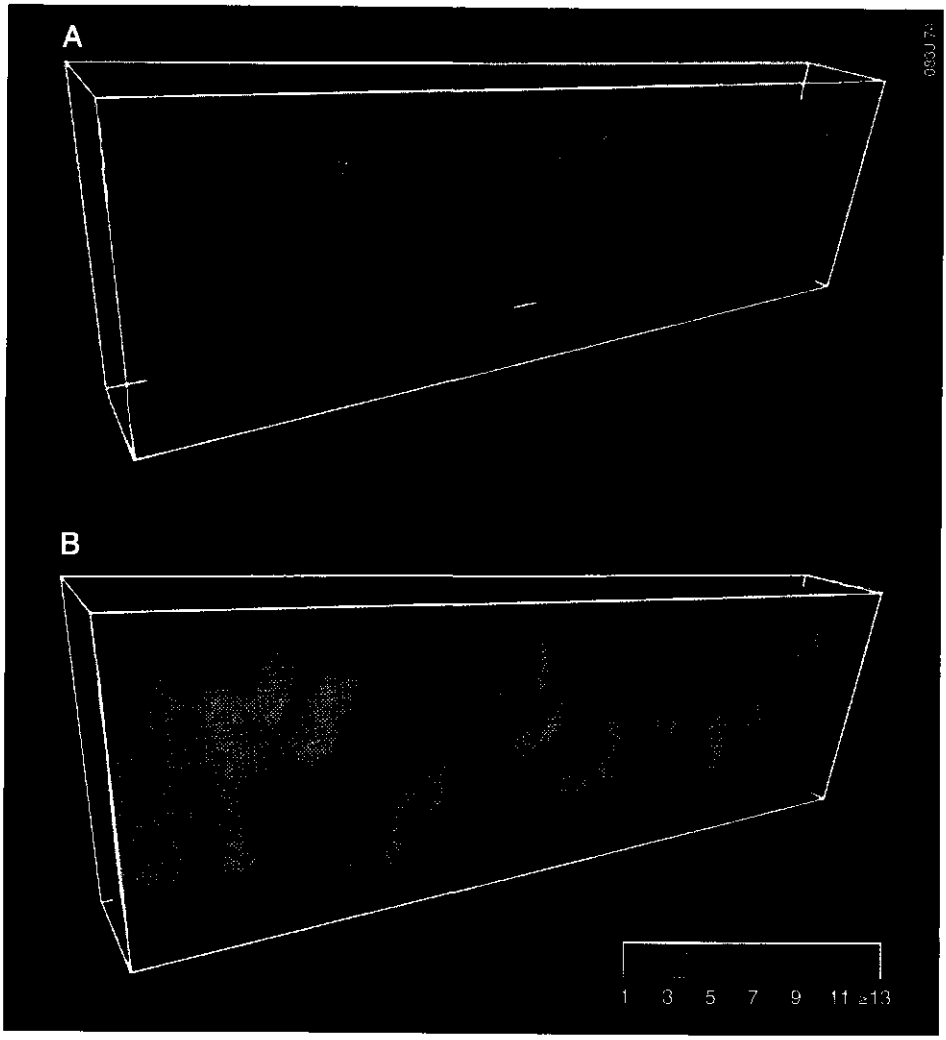

Fig. 7.4 *Three-dimensional soil water content distribution with intersecting horizontal (A) and vertical (B) planes in the excavated soil block. Values in the legend indicate volumetric soil water contents in %. The red color indicates dry soil with a volumetric water content of 1%, while the purple color refers to volumetric water contents equal to or higher than 13%.*

7.3.2 Soil water repellency distribution

All 1680 samples were used to determine the degree of water repellency for field-moist conditions (actual water repellency) and after drying at 65°C (potential water repellency).

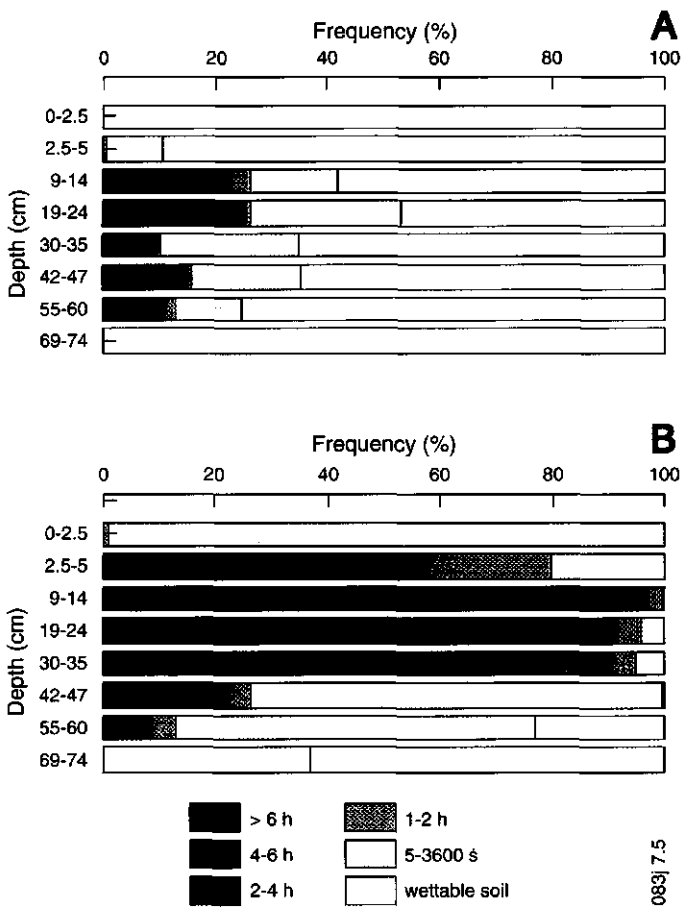

Fig. 7.5 *Relative frequencies of varying degrees of actual (A) and potential (B) water repellency. Actual water repellency was determined using the WDPT test on the field-moist samples, potential water repellency after drying the samples at 65°C.*

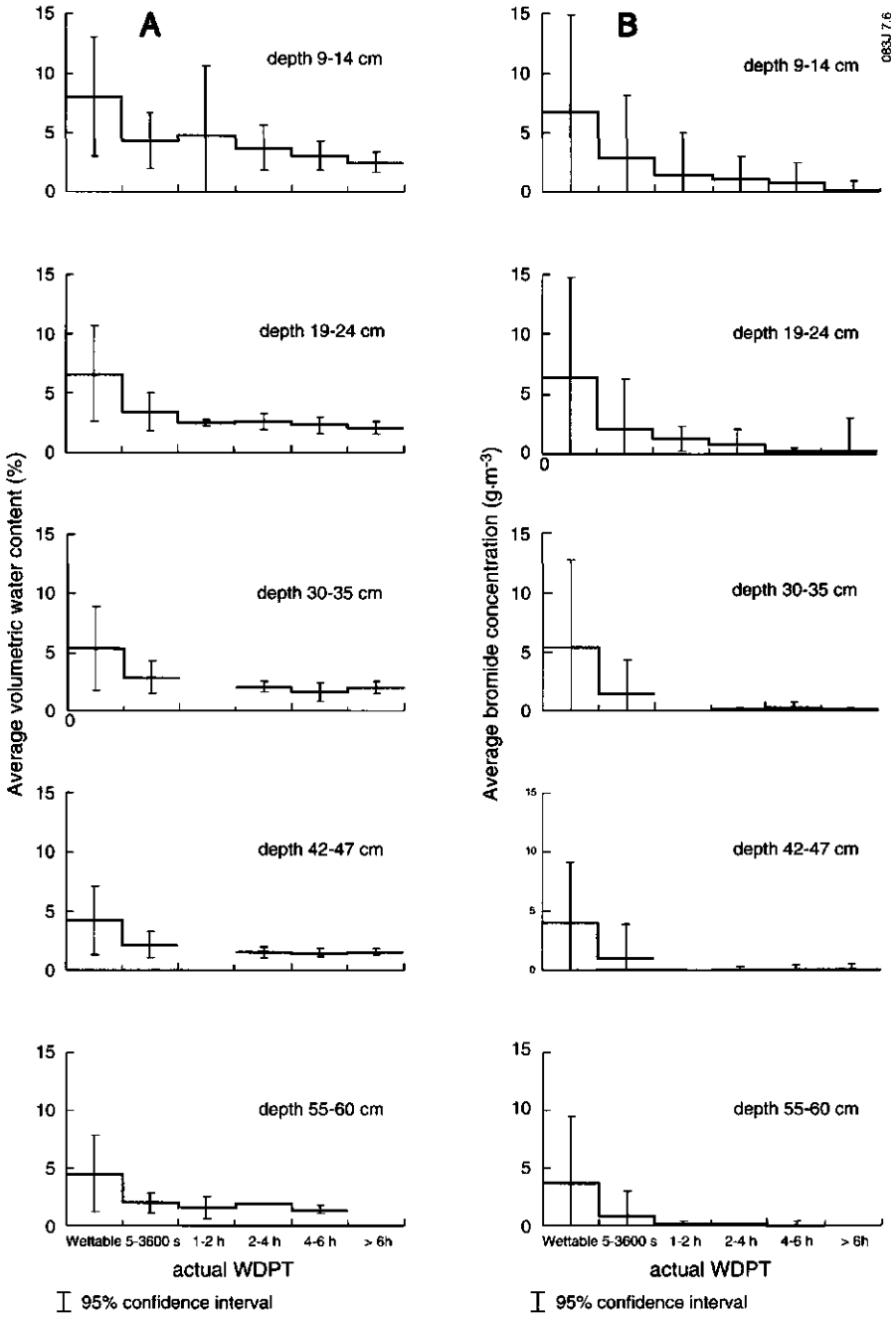

Fig. 7.6 *Average soil water content (A) and average bromide concentration (B), with 95% confidence intervals, for all actual water repellency classes for the 9-14, 19-24, 30-35, 42-47 and 55-60 cm soil layers.*

Fig. 7.5A shows the percentages of the soil with varying degrees of actual water repellency for all field-moist samples. It can be concluded that the 0-2.5 and 69-74 cm soil layers were wettable at the moment of sampling. All other layers showed actual water repellency, at least in some of the samples. The highest degree of actual water repellency was found in the 9-14 and 19-24 cm soil layers. Even at a depth of 55-60 cm, actual water repellency was distinct in approximately 60 of the 240 samples.

Soil zones showing actual water repellency were found between the areas with fingerlike wetting patterns. Fig. 7.6A shows average soil water contents and their 95% confidence intervals for each of the actual water repellency classes for the 9-14 through 55-60 cm soil layers. This figure clearly indicates that the driest soil regions can be found in places with the highest actual water repellency, while the opposite is true for the wet soil areas.

Fig. 7.5B summarizes the percentages of the soil with varying degrees of potential water repellency, using the same classes as Fig. 7.5A. This graph illustrates that under very dry conditions, extreme soil water repellency might occur in this soil. The highest potential water repellency was found in the 9 to 35 cm layer. Deeper in the profile, potential water repellency decreased, although it could still be detected in the 69-74 cm layer.

The iso-surface representing the potential water repellency class 3 to 4 hours is shown in Figs. 7.7A and 7.7B. The vertically directed patterns within this iso-surface indicate regions with a relatively low degree of potential water repellency within the 9-45 cm layer. These regions are the most likely sites for fingered flow formation, as water permeability will be the highest here. Between these zones, potential water repellency is more pronounced, as is shown by the horizontal (Fig. 7.7A) and vertical (Fig. 7.7B) cutting planes. Potential water repellency in the humous layer and the 45-74 cm layer is less severe, as is also shown in Fig. 7.5B.

Comparison of the iso-surfaces in Figs. 7.7A and 7.7B with those shown in Figs. 7.4A and 7.4B clearly shows that places with lower degrees of potential water repellency had fingerlike soil water content patterns, while places with high degrees of potential water repellency had dry, actually water repellent soil. It can be concluded from Fig. 7.8 that *the most severe actual water repellency occurred in places with the highest potential water repellency. Thus, actual and potential water repellency distributions are closely linked, the difference being that the actual water repellency*

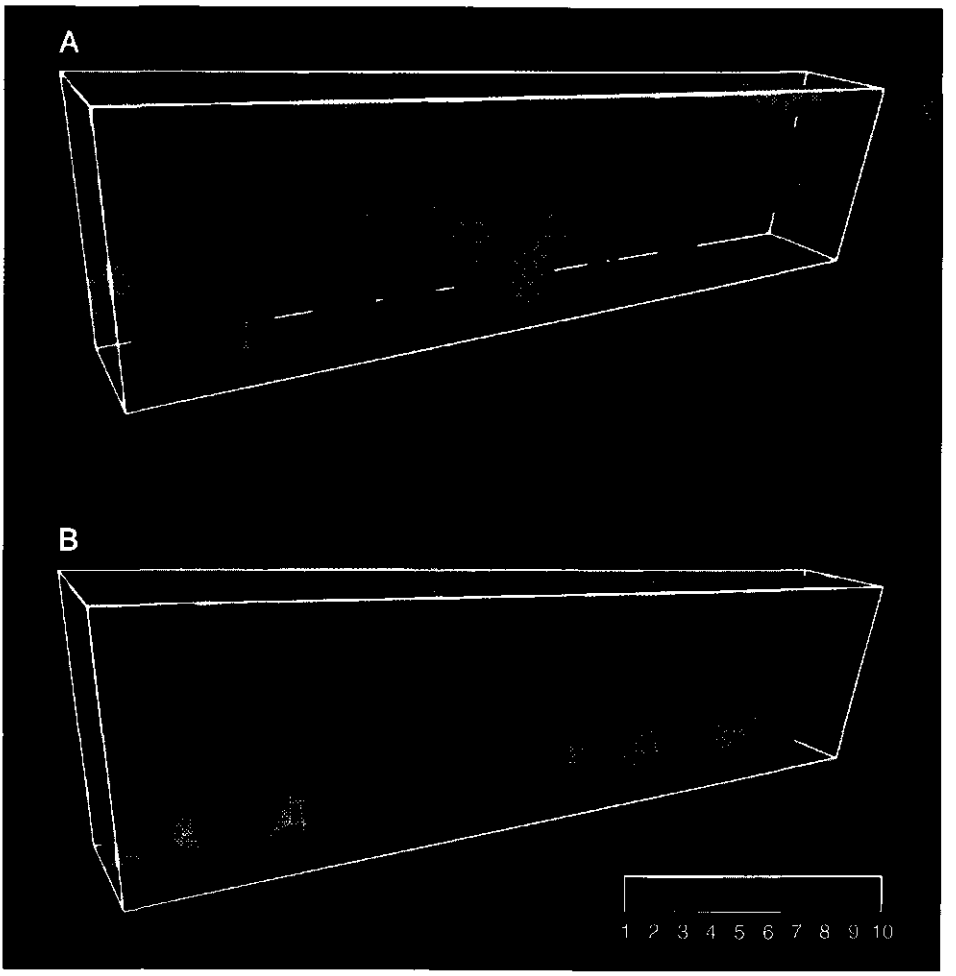

Fig. 7.7 *Three-dimensional potential water repellency classes with intersecting horizontal (A) and vertical (B) planes. Increasing values in the legend indicate increasing degrees of potential water repellency. The zero value (red color) represents potentially wettable soil, while the purple color refers to the potential water repellency class with water drop penetration times of > 6 h.*

distribution in a soil might vary from day to day, depending on the sequence of local weather conditions, while the potential water repellency distribution is a more constant property, which yields information about what might happen to the soil during a prolonged dry period.

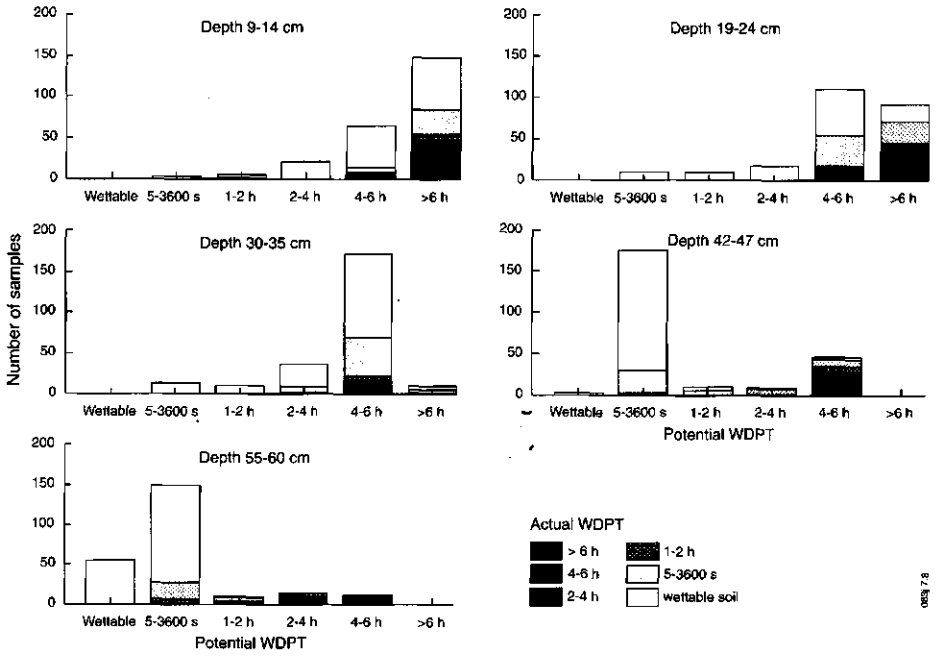

Fig. 7.8 *Distribution of actual water repellency classes for all samples belonging to a specific potential water repellency class, for the 9-14, 19-24, 30-35, 42-47 and 55-60 cm soil layers.*

7.3.3 Bromide distribution

Fig. 7.2B shows the average bromide concentration profile with 95% confidence intervals. Bromide concentrations were high in the humous layer and in the 64.5 to 79 cm layer, which also showed the greatest variation in bromide concentrations. Bromide concentrations in the soil layers with actually water repellent zones were much lower (Fig. 7.2B).

Fig. 7.3B shows bromide amounts for the same 240 (79 cm) soil cores used in Fig. 7.3A. The bromide application rate was 8.0 $g.m^{-2}$, and the average recovery down to depth of 79 cm was 5.4 $g.m^{-2}$, indicating that during the 12 days between tracer application and soil sampling around 32.5% of the applied bromide had leached to below this level. There was considerable variation in the bromide amounts in the columns, ranging from 2 to 11 $g.m^{-2}$ (Fig. 7.3B). Besides differences in total bromide amounts, Fig. 7.3B also shows that major differences existed in bromide depth profiles. In some soil columns, bromide could be detected in the humous layer only, while in others bromide was found down to the bottom of the soil profile. Furthermore, single-

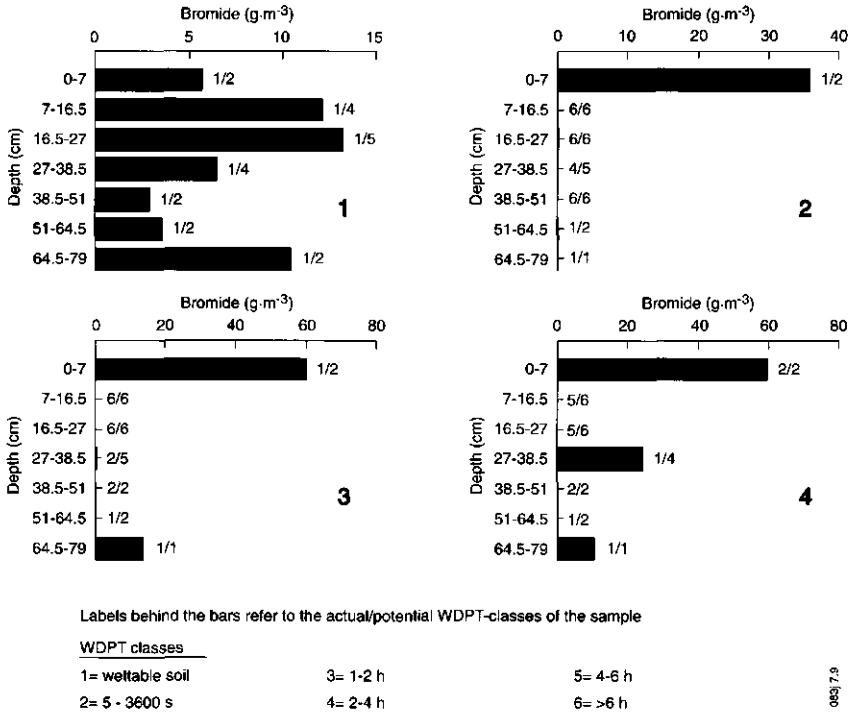

Fig. 7.9 *Some typical bromide depth profiles, and actual and potential water repellency classes. Numbers 1-4 refer to the soil columns indicated by arrows in Fig. 7.3.*

peaked, double-peaked and triple-peaked profiles were found (Fig. 7.9), indicating the occurrence of diverging flow in wetter (i.e. wettable) soil (Ritsema et al., 1993; see Chapter 2). *From the bottom end of fingers, water and bromide could diverge in a*

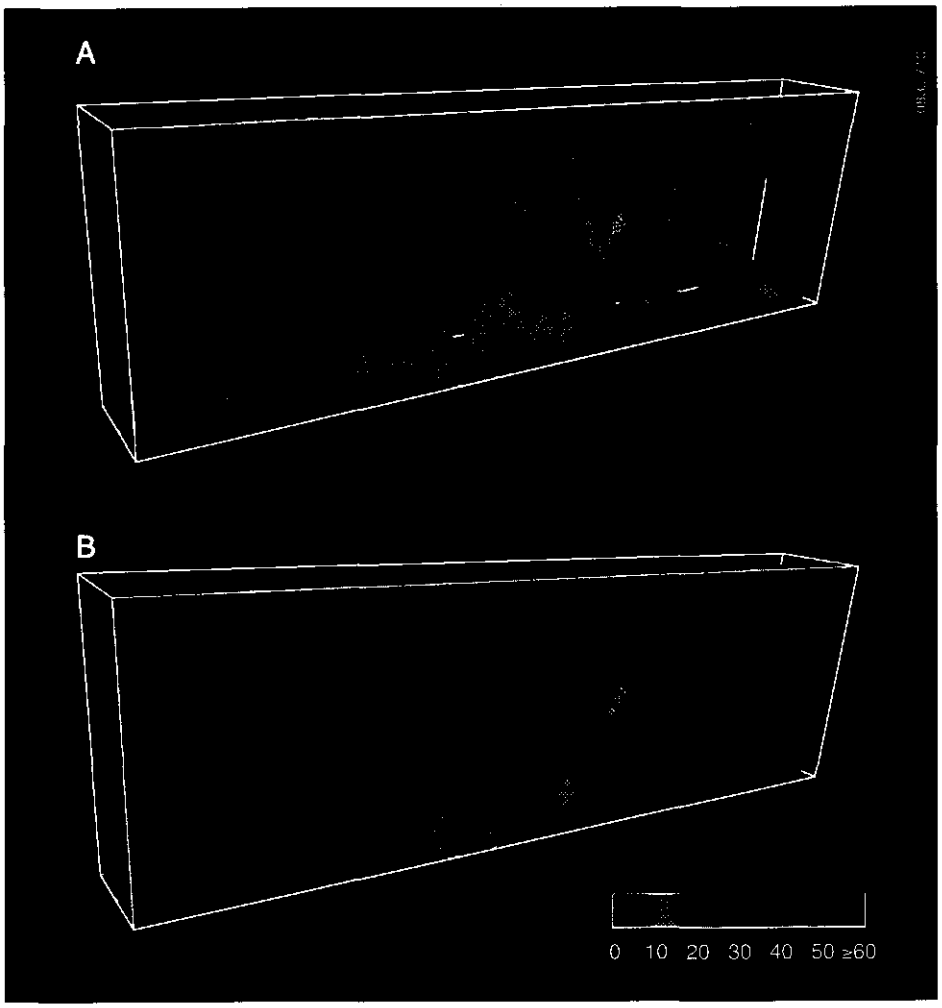

Fig. 7.10 *Three-dimensional bromide concentration distribution with intersecting horizontal (A) and vertical (B) planes. Values in the legend indicate concentrations in* $g.m^{-3}$.

radial direction toward zones below dry, actually water repellent soil regions. The typical bromide depth profiles in Fig. 7.9 appeared to be strongly related to the water repellency depth profiles (see labels in Fig. 7.9). Generally, bromide was found in the actually wettable layers, which often exhibited the lowest degree of potential water repellency as well (Fig. 7.9).

Bromide concentrations in the humous layer were relatively high, indicating that at least part of the bromide had been trapped in this layer in places from which it was apparently not quickly transported downward. *The humous layer acted as a bromide reservoir, from which bromide was released during successive rain events in small portions only.* This indicates that the assumption of full mixing within the distribution layer, made for instance by De Rooij (1996) in a model study simulating water flow through a water repellent soil, is not realistic in our case.

Figs. 7.10A and 7.10B show the spatial distribution of the measured bromide concentrations. An iso-surface, representing a bromide concentration of around 10 $g.m^{-3}$ was visualized, together with two intersecting horizontal (Fig. 7.10A) and vertical (Fig. 7.10B) planes. These figures indicate that bromide concentrations were relatively high in the humous layer and in the deepest soil layer, especially below regions with fingerlike pathways (see Figs. 7.4A and 7.4B). In the 9 to 64 cm depth range, bromide concentrations were relatively high in places with fingers (see Figs. 7.4A and 7.4B), whereas zones without any bromide could be detected between the fingers in the very dry, actually water repellent soil regions (Fig. 7.6B). This observation corresponds to the findings shown in Fig. 7.6B, indicating that the zones of highest actual water repellency were by-passed by the infiltrating water and bromide during the 12-day experiment.

7.3.4 Soil pH distribution

Fig. 7.2C shows the average pH profile of the soil, with 95% confidence intervals. The pH of the humous layer is clearly higher than that of the deeper layers in the profile. The greatest variations were found in the top four soil layers.

According to information obtained from the farmer, only manure had been applied to our experimental field for the last decades. From Figs. 7.11A and 7.11B it can be seen that the highest pH values were found in the humous layer and in the underlying

fingers (see also Figs. 7.4A and 7.4B). The higher pH values might be caused by the fact that manure, which normally has pH values of 7 or over, moved mainly through the wet humous layer and the wet fingers. It is highly likely that a lack of oxygen in these zones largely inhibited nitrification of manure compounds (like NH_4), causing the

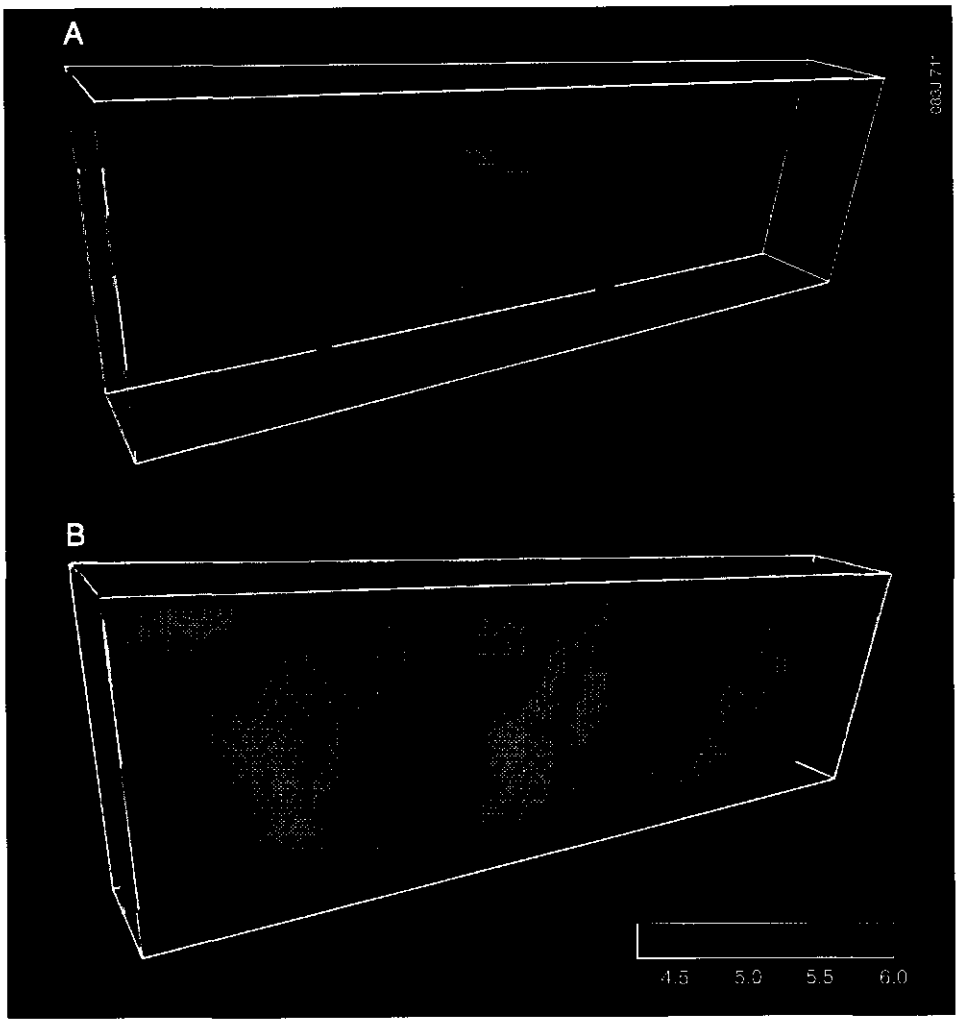

Fig. 7.11 *Three-dimensional soil pH distribution with intersecting horizontal (A) and vertical (B) planes.*

soil pH to increase instead of decrease in these areas. *Thus, if a soil is dominated by fingered flow, it can be expected that agrichemicals applied to it will move predominantly through the major flow path regions, i.e. through the surface layer and the fingered flow zones.* Residues of compounds applied might be found here, while little or no effect can be expected between the fingers. As the farmer had been applying manure for long periods, and from the similarities between the soil water content and pH distributions, it might be concluded *that the fingered flow pathways have already recurred for years in the same places during every major rain event.* This would explain the relatively large differences in soil pH found between places with and without fingers.

7.4 CONCLUSIONS

After 52 mm of rainfall, 32.5% of the applied bromide had leached to a depth below 79 cm. Distribution flow in the surface layer transported bromide to the vertically directed fingers. Indications were found that the distribution layer, i.e. the humous surface layer, acted as a bromide reservoir, releasing bromide in limited amounts during single rain events. In the actually water repellent soil zone, down to a depth of 64 cm, bromide was transported downwards through vertically directed fingers. Bromide could not be detected, or at very low concentrations only, in between the fingers, i.e. at the dry spots with the highest degrees of actual water repellency. The spots showing the highest actual water repellency were found in places with the highest degrees of potential water repellency. In the actually wettable zone, starting at a depth of around 64 cm, diverging flow from the fingers toward the surrounding areas caused bromide to be transported below dry, actually water repellent soil zones, resulting in double-peaked bromide profiles. Sporadically, triple-peaked bromide profiles were encountered, due to slightly wetter areas within the actually water repellent zone. Despite the process of diverging flow, the highest bromide concentrations within the actually wettable zone were found in places below fingers. Long term application of manure had increased soil pH values in the humous layer and underlying fingers. The dry, actually water repellent soil regions between the fingers were not affected by the manure applications. The observed soil pH distribution could only be explained by the long term recurrence of the fingered flow pathways during successive rain events.

CHAPTER 8

MODELING FINGER FORMATION AND FINGER RECURRENCE

Adapted version of 'Modeling and field evidence of finger formation and finger recurrence in a water repellent sandy soil' by C.J. Ritsema, L.W. Dekker, J.L. Nieber and T.S. Steenhuis, published in Water Resources Research 34:555-567, 1998.

8 MODELING FINGER FORMATION AND FINGER RECURRENCE

Abstract

With prolonged rainfall, infiltrating wetting fronts in water repellent soils may become unstable, leading to the formation of high velocity flow paths, the so-called fingers. Finger formation is generally regarded as a potential cause of the rapid transport of water and contaminants through the unsaturated zone of soils. Theoretical analysis and model simulations indicate that finger formation results from hysteresis in the water retention function, and the nature of the formation depends on the shape of the main wetting and main drainage branches of that function. Once fingers are established, hysteresis causes them to recur along the same pathways during subsequent rain events. Leaching of hydrophobic substances from these fingered pathways makes the soil within the pathways more wettable than the surrounding soil. In the long term, therefore, instability-driven fingers can become heterogeneity-driven fingers.

8.1 INTRODUCTION

In the unsaturated zone, water and solutes often move preferentially through paths that are usually wetter and carry more water per unit area than the surrounding dry soil (Gee et al., 1991; Jury and Flühler, 1992). These preferential flow paths can be heterogeneity- or instability-driven. Heterogeneity-driven flow paths generally occur in clay and peat soils with well-defined macropore or mesopore networks (Beven and Germann, 1982; White, 1985; Bronswijk et al., 1995), while instability-driven fingers can be found in water repellent soils (Hendrickx et al., 1993, Ritsema et al., 1993; Ritsema and Dekker, 1994b; Ritsema and Dekker, 1996b) and coarse grained soils (Glass et al., 1989a,b; Liu et al., 1993, 1994a).

Water repellent soils occur in many parts of the world, in all types of climates (Krammes and DeBano, 1965; DeBano, 1969; McGhie, 1987; Dekker and Jungerius, 1990), and can be found beneath different vegetation types, including forests, brushwood, heath, grassland, arable land, and golf courses (DeBano, 1981; Wallis and Horne, 1992). The degree of water repellency depends on the vegetation type.

Extremely water repellent soils can be found beneath grass, almost regardless of the type of soil (Dekker and Ritsema, 1996c).

Water infiltration in initially dry, water repellent soils is slower than infiltration in wet soils (Wallis et al., 1991), causing water to be retained in the top layer at first. With prolonged rainfall, minor perturbations in an originally planar infiltrating wetting front may grow into fingers. Although rapid transport through fingers in water repellent soils has been reported recently (Van Dam et al., 1990; Hendrickx et al., 1993; Ritsema et al., 1993; Ritsema and Dekker, 1995, 1998), the mechanisms of finger formation and finger recurrence have remained unclear.

The objectives of the study described in this Chapter were to

- explain the mechanism of finger formation and finger recurrence;
- simulate finger formation and finger recurrence using a numerical solution of coupled water and air flow in a two dimensional domain;
- propose a hypothesis for the effect of finger recurrence on formation of heterogeneity in soil water retention properties.

8.2 MECHANISM FOR FINGER FORMATION AND FINGER RECURRENCE

Fingered flow of water in soils is induced by the instability of the wetting front of the infiltrating water (Glass et al., 1989a; Selker et al., 1992a). Unstable conditions prevail for infiltrating water if the pressure gradient for the water phase is opposite (upward) to the direction of flow (downward). Raats (1973) explained that unstable flow can occur in water repellent soils, in soils with steep wetting retention curves, or when air pressure increases significantly above ambient atmospheric pressure ahead of the wetting front.

The initial formation of the fingered flow pathways and their reformation can be described in terms of the water retention and hydraulic conductivity properties of the soil (Glass et al., 1989b; Liu et al., 1994a; Nieber, 1996). Such a description is given in Fig. 8.1, which shows the water retention function for a soil along with an inset (left one) of a finger being formed. The water retention function is hysteretic, and both main wetting and main drainage branches, as well as two (boundary) wetting branches are shown. The very steep water retention function for the main wetting branch is similar

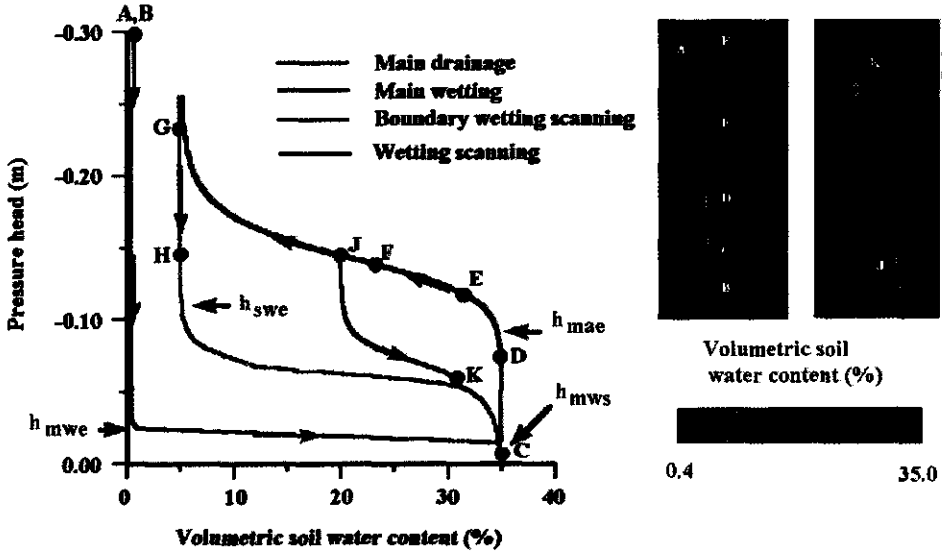

Fig. 8.1 *Graphic explanation of the mechanism of finger formation during the first wetting cycle into dry soil, and finger recurrence during subsequent drainage/wetting cycles. The shape of the hysteretic water retention function is typical of uniformly coarse soils and water repellent soils. The critical parameters in the water retention function are the water-entry pressure head (h_{mwe}) on the main wetting branch, and the air-entry pressure head (h_{mae}) on the main drainage branch. The inset illustrates the conditions during the second wetting cycle following a drainage period.*

to that for a water repellent soil. The graph shows several letters referring to points on the inset of the finger. Point A is situated beside the finger, while point B lies just ahead of the advancing saturated tip. Points C-F are situated inside the finger, with point C having a saturated water content and near zero pressure head, while points D, E and F show progressively lower pressure heads and lower water contents.

Several important parameters are indicated on the water retention graphs, i.e. the water-entry pressure head (h_{mwe}) and the saturation pressure head (h_{mws}) on the main

wetting branch, the water-entry pressure head (h_{swe}) on the boundary wetting branch, and the air-entry pressure head (h_{mae}) on the main drainage branch.

The mechanism of initial finger formation can be described starting at point B. Initially, B is on the main wetting curve at a low pressure head. As the saturated tip of the finger approaches B, the pressure head at that point increases until it reaches (h_{mwe}), at which point water can move into the porous medium at point B. With further downward movement of the saturated tip, the pressure head at point B rapidly increases to (h_{mws}), and the pores at B become saturated. As the tip of the finger continues to move downward, away from B, the pressure head at B decreases and the point progressively experiences the same pressure heads experienced by points C, D, E and F. *Thus the soil at B is initially dry, then becomes saturated when the finger tip reaches it, and then becomes progressively drier as the finger tip moves downward from B.*

The fact that the water in the finger shows no appreciable lateral diffusion can be explained by considering the soil at point A, beside the finger. Like the soil at point B, the soil at A is initially dry and conditions at that point correspond to the main wetting branch. *For water to enter the soil at A, it would be necessary for the pressure head in the finger to increase to above the h_{mwe} value prevailing at A. However, the pressure head in the finger above point C is seen to be lower than h_{mwe}. Therefore, water will not diffuse laterally and will be confined to the preferential path formed by the finger.*

If the water supply ends after a finger has been formed, the water in the finger will drain until a particular level of water content is reached. Consider, for instance, a situation in which the finger is drained to a uniform water content shown by point J in Fig. 8.1 (right inset). *If water is applied again at a rate less than or equal to the rate at which the finger was formed, it will enter the finger pathway at the top and will move preferentially down the finger because the initially moist pathway wets more easily than the surrounding dry soil.* As the new wetting front approaches any point J, the soil at that point will experience an increase in pressure head according to the wetting branch J-K. The highest pressure head reached inside the finger is that shown by point K on the diagram, which is lower than the h_{mwe} for point A. Once again, therefore, there will be no lateral diffusion of the water and the initial finger pathway will persist. *Note that if the water is applied at a higher rate than the rate at which*

the finger was formed, then the pressure head at K might increase above h_{mwe}, and limited lateral diffusion will occur in this situation.

It should be noted that there are many conditions under which fingers do not form. For instance, no fingers are formed in soils with $h_{mwe} < h_{mae}$, because the pressure head within a finger will be higher than h_{mwe} and moisture will diffuse laterally. Another example is a situation in which the entire soil is initially uniformly moist (even if $h_{mwe} > h_{mae}$ for the soil) at, say, the residual moisture content. During wetting, a point in the soil then wets along the pathway G-H indicated in Fig. 8.1. The water-entry pressure head for this wetting process is h_{swe}, and since this is below the air-entry pressure (h_{mae}), appreciable lateral diffusion of moisture occurs (Lu et al., 1994). This will be explained in more detail in Chapter 9.

8.3 MATHEMATICAL DESCRIPTION OF FINGERED FLOW

The mass balance equations for coupled two-dimensional flow of water and air in an unsaturated soil are expressed as

$$\frac{\delta M_w}{\delta t} = \frac{\delta}{\delta x}\left(\rho_w K_w \frac{\delta h_w}{\delta x}\right) + \frac{\delta}{\delta z}\left(\rho_w K_w \frac{\delta h_w}{\delta z}\right) + \frac{\delta(\rho_w K_w)}{\delta z} \tag{1}$$

$$\frac{\delta M_a}{\delta t} = \frac{\delta}{\delta x}\left(\rho_a K_a \frac{\delta h_a}{\delta x}\right) + \frac{\delta}{\delta z}\left(\rho_a K_a \frac{\delta h_a}{\delta z}\right) \tag{2}$$

where:

$M_w = \Phi \rho_w S_w$ = mass of the water phase per unit volume of the porous medium (kg.m^{-3}),
$M_a = \Phi \rho_a S_a$ = mass of the air phase per unit volume of the porous medium (kg.m^{-3}),
Φ = porosity of the porous medium (-),
S_w, S_a = degree of saturation for the water and air phases, respectively (-),

h_w, h_a = pressure heads for the water and air phases, respectively (m),

K_w, K_a = hydraulic conductivities for the water and air phases, resp. ($m.min^{-1}$),

ρ_w, ρ_a = densities for the water and air phases, respectively ($kg.m^{-3}$),

x, z = cartesian coordinates (m), and

t = time (min).

Note that both fluid compressibility and porous medium compressibility are included implicitly in these equations.

These equations are augmented by the relations

$$h = h_a - h_w \tag{3}$$

$$\rho_w = \rho_w (h_w) \quad \rho_a = \rho_a(h_a), \quad \Phi = \Phi (h_w, h_a) \tag{4}$$

$$\theta_w = (\theta_{w_s} - \theta_j) \left(\frac{1}{1+(\alpha_j h)^{n_j}} \right)^{1-\frac{1}{n_j}} + \theta_j \quad j = md, mw \tag{5}$$

$$S_{w_e} = \frac{S_w - S_r}{1 - S_r} = \frac{\theta_w - \theta_r}{\theta_s - \theta_r} \tag{6}$$

$$S_a = 1 - S_w \tag{7}$$

$$K_w = K_{w_s} S_{w_e}^{1/2} \left[1 - \left(1 - S_{w_e}^{\frac{n_j}{n_j - 1}} \right)^{1-\frac{1}{n_j}} \right]^2, \; s_{w_e} > 0 \quad j = md, mw \tag{8}$$

$$K_w = 0 \qquad S_{w_e} \leq 0 \tag{9}$$

$$K_a = K_{a_s}(1 - S_{w_e})^{1/2}\left(1 - S_{w_e}^{\frac{n_j}{n_j-1}}\right)^{2-\frac{2}{n_j}} \qquad j = md, mw \tag{10}$$

where h is the pressure head (m), K_{w_s} and K_{a_s} are the saturated hydraulic conductivities (m.min^{-1}) for the water and air phases, respectively, S_{w_e} is the effective saturation degree (-) of the water phase, θ_w is the volumetric water content (m^3.m^{-3}), θ_{w_s} is the saturated volumetric water content (m^3.m^{-3}), θ_r ($=\theta_{md}$) is the residual water content (m^3.m^{-3}) on the main drainage function, θ_{mw} is the air-dry water content (m^3.m^{-3}) on the main wetting function and α_j (m^{-1}) and n_j (-) are porous media dependent parameters for the main wetting function ($j=mw$), and the main drainage function ($j=md$). Note that although the fluid retention and hydraulic conductivity relations proposed by Van Genuchten (1980) were used in the above descriptions, alternative empirical formulae could be used as well.

The hydraulic conductivity equations for water given above are consistent with the notion that the water phase hydraulic conductivity will be zero if the water content is below the residual water content. That the water phase hydraulic conductivity is indeed zero at the wetting front of an initially air-dry porous medium has been shown experimentally by Lu et al. (1994) using photomicroscopic imaging of glass bead media. They showed that the wetting front moved by erratic advances into the initially air-dry media.

As was described in the previous section, the process of capillary hysteresis is important in the formation of fingers and their recurrence. A number of alternative models could be applied to describe capillary hysteresis. This paper uses the independent domain model developed by Mualem (1974), and the application is limited to modeling just a first-order wetting scanning function because only a single sequence of wetting/drainage/wetting is considered.

8.4 NUMERICAL APPROACH

The numerical solution of the two-phase flow problem is achieved using the finite element method with bilinear finite elements and a fully implicit time discretization scheme. The modified Picard procedure for the two-phase flow equations, as described by Celia and Binning (1992) has been applied to solve the nonlinear step of the solution process. In addition, the nodal hydraulic conductivity weighting scheme introduced by Dalen (1976) and described by Huyakorn and Pinder (1978) was used. The formulation of the numerical solution for the two-phase flow equations is similar to that presented by Nieber (1996) for Richard's equation, but here we also account for medium and fluid compressibility, and the dynamics of the air phase.

For a proper modeling of the formation of fingers and their recurrence it is essential that the associated sharp gradients in moisture content be maintained. This requirement is difficult to meet, since most numerical schemes will produce some dissipation of sharp moisture fronts. Nieber (1996) showed that when hydraulic conductivities for water are upstream weighted, this can lead to artificial dissipation of an initial perturbation or of a nascent finger. However, he demonstrated that if the nodal hydraulic conductivities are downstream weighted, then the sharp front can be maintained. The rules for assigning the hydraulic conductivity weighting factor have been summarized by Nieber (1996). In his study, these rules were applied only to the water phase, but they can be applied to the air phase hydraulic conductivities as well.

The finite element solution was implemented in FORTRAN-77 language on an SGI ONYX computer. The numerical solution uses a diagonally preconditioned conjugate gradient method (Pini and Gambolati, 1990) to solve the matrix equations. Automatic time step adjustment of the solution and determination of nonlinear solution convergence were achieved with the procedures described by Kaluarachchi and Parker (1989). For the present study, the relative and absolute errors in the fluid pressure heads were set at 0.0001 and 0.0001 m respectively. An additional criterion for determining nonlinear solution convergence was the testing of the change in fluid saturation, with the maximum allowable change between iterations set at 0.0001.

As mentioned above, the process of capillary hysteresis was modeled using the independent domain model developed by Mualem (1974), following two procedures. In each of these procedures, the pressure head at each node point is checked at the end of

solution convergence to assess whether a change in the water retention function is warranted. The first procedure applies to modeling the retention function for points starting with an air-dry condition. In this procedure, the main wetting curve is followed until the pressure head reaches h_{mws}. Points that reach this pressure head then switch to the main drainage curve. The second procedure applies to points with pressure head - saturation lying on or between the main drainage curve and the boundary wetting scanning curve. In this procedure, the Mualem (1974) independent domain model of capillary hysteresis was used to model pressure head - saturation pathways.

8.5 RESULTS

8.5.1 Simulation of finger formation and finger recurrence

The purpose of the numerical simulations described below is to demonstrate the process of finger formation and recurrence without matching any field conditions exactly. Simulation of the observed field data is the subject of two other papers (Hung et al., 1998a,b).

To illustrate the process of finger formation and recurrence, a vertical flow domain was considered with a height of 0.5 m and a width of 0.2 m. The top boundary has a boundary condition with a specified water flux and a specified air pressure of zero. During water applications, the application rate is 1/6 of the saturated water hydraulic conductivity of the soil. The bottom boundary is a seepage boundary for water. Air pressure is specified to be zero along the bottom boundary until it becomes saturated with water, at which time a condition of zero air flux is specified. The vertical boundaries are assumed to be impermeable to both water and air. Initially, the entire region is air-dry, except for a small saturated region at the top, with a perturbed front. This saturated region corresponds to the wetted domain which exists just prior to the destabilization of the wetting front. The perturbed front corresponds to the destabilization process. Alternatively, the perturbed front could also correspond to a larger scale perturbation caused by a wavy interface between textural horizons as observed at the Ouddorp site. For the cases shown here the perturbed front was generated using a summation of 20 sine waves of equal amplitude and frequency but randomly generated phase. For the finite element solution, the flow domain was discretized using a node spacing of 0.005 m in each coordinate direction.

Two porous media were treated in the numerical simulations. One of the porous media, referred to as porous medium A, has properties that will promote finger growth and recurrence, while the other, porous medium B, will tend to dissipate any initial perturbations or finger formation. The common parameters for the two porous media are given as

$$\Phi = \text{constant} = \theta_s = 0.35$$

$$\theta_r = 0.05, \quad K_{w_s} = 0.1 \text{ m.min}^{-1}$$

$$K_{a_s} = 6.0 \text{ m.min}^{-1}$$

$$\theta_{mw} = 0.005$$

$$\rho_w = 1000(1 + 4.3x10^{-6}h_w) \text{ kg.m}^{-3}$$

$$\rho_a = 1.24(1 + 0.1h_a) \text{ kg.m}^{-3}$$

Note that a linear function has been applied for the variation in water density (Freeze, 1971) and air density (Celia and Binning, 1992) with respect to the corresponding fluid pressure. Also, the porous medium has been treated as incompressible (Φ = constant).

The differences between the two porous media are manifested in the main wetting and main drainage retention functions. The parameters for these functions for porous media A are

$$\alpha_{mw} = 50 \text{ m}^{-1}, \; n_{mw} = 20$$
$$\alpha_{md} = 7 \text{ m}^{-1}, \; n_{md} = 10$$

while those for porous media B are

$$\alpha_{mw} = 15 \text{ m}^{-1}, \; n_{mw} = 3$$
$$\alpha_{md} = 5 \text{ m}^{-1}, \; n_{md} = 3$$

The growth and persistence of fingered flow paths in porous medium A are illustrated in Fig. 8.2, which shows a sequence of images representing the distribution of water content in a soil profile during an event in which water was applied for 30 minutes, then stopped for 90 minutes, and applied again for 30 minutes.

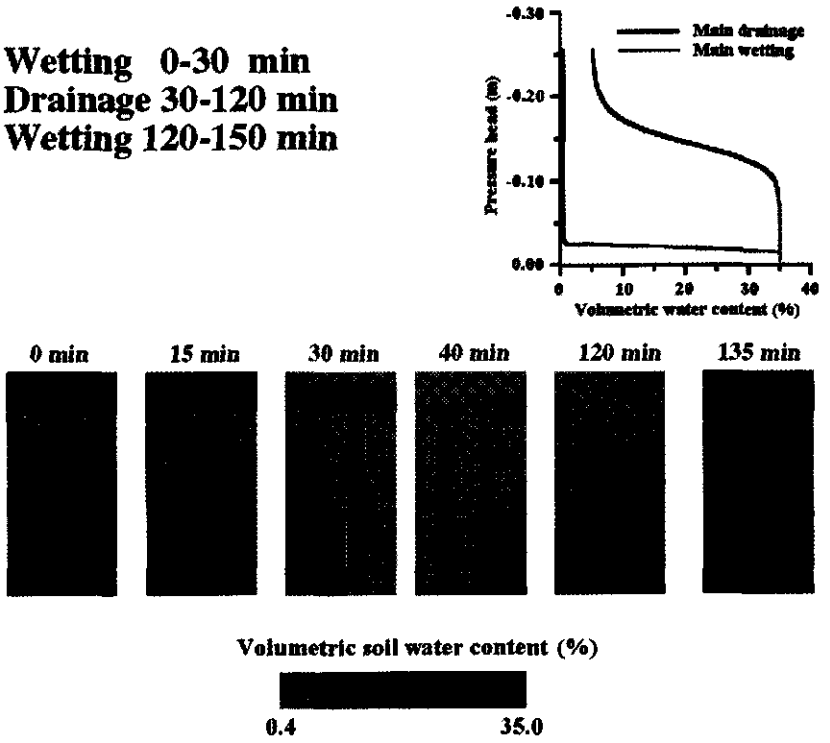

Fig. 8.2 *Illustration of fingered flow in a soil during the first wetting cycle, first drainage cycle and second wetting cycle. The fingers emanate from an initial perturbation in the wetting front at 0 minutes. The flow domain is 0.2 m wide and 0.5 m deep. The main wetting and main drainage branches of the water retention function for the soil are illustrated by the graphic inset. During wetting, water is applied uniformly across the top of the flow domain at a rate of 1/6 of the saturated hydraulic conductivity of the soil. Water is applied for the first 30 minutes and then ceases for the next 90 minutes. At 120 minutes the same water application rate is reinitiated for the next 30 minutes.*

The inset in the figure shows the main wetting and main drainage retention functions for the parameters associated with porous medium A. These curves have characteristics similar to those for water repellent horizons. In this case, $h_{mwe} > h_{mae}$, so it is expected that fingers will form in this soil, growing from perturbations in the wetting front. The flow patterns shown in Fig. 8.2 show that fingers form during the first water application period and are drained after the cessation of water application. Although large moisture gradients exist near the fingers, lateral moisture movement is prevented by the mechanism described above. When water is applied again, beginning at 120 minutes, it moves preferentially down the previously formed finger pathways. This behaviour was observed in the Ouddorp experimental field as well (see Chapter 6).

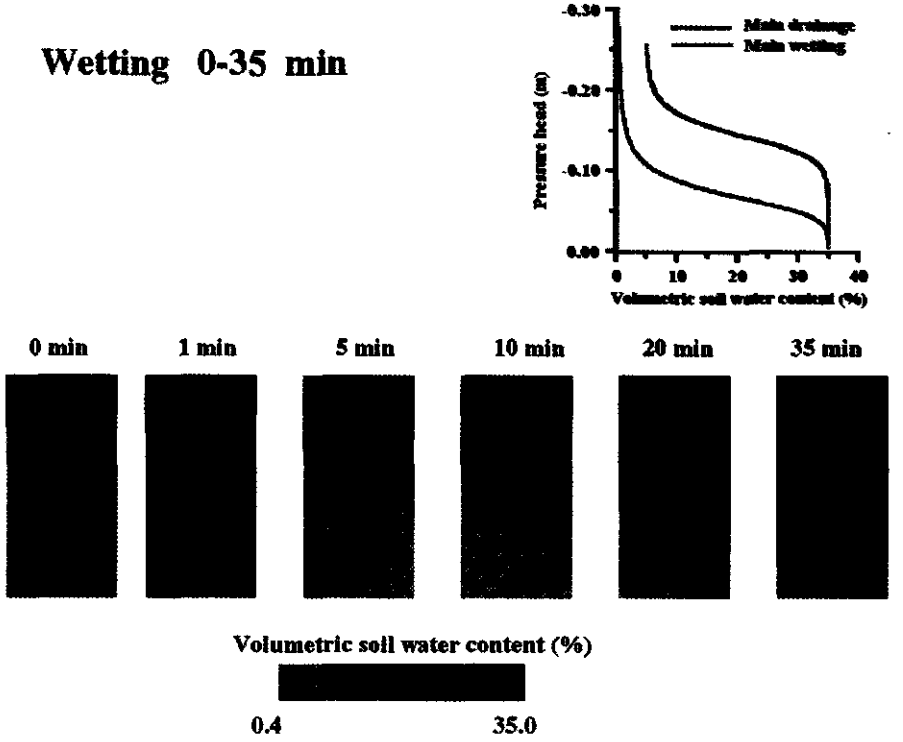

Fig. 8.3 *Illustration of diffuse flow in a soil during the first wetting cycle. The flow region and initial conditions are the same as in Fig. 8.2. The main wetting and main drainage branches of the water retention function for the soil are illustrated by the graphic inset.*

Now let us consider a soil for which fingered flow does not occur. The hysteretic water retention function is presented in Fig. 8.3, with images of water content distributions over a period of water application lasting 35 minutes. The initial condition and the boundary conditions are identical to those for the first case, except that we now consider only 35 minutes of continuous water application. For this porous medium, $h_{mwe} < h_{mae}$, and therefore water behind the wetting front will readily imbibe into the surrounding dry soil. The simulation results show that this imbibition does occur and the initially perturbed wetting front in this porous medium stabilizes after a very short period of time.

The simulation results depicted in Figs. 8.2 and 8.3 thus convincingly show that *the shape of the wetting branches determines whether a finger or a stable wetting front is formed.*

8.5.2 Hypothesis for the formation of heterogeneity-driven fingers

As was described above, the fingered flow pathways persist once they have formed. Repeated wetting and drying of these pathways over a protracted period of time will probably lead to the leaching of hydrophobic substances from the pores within the fingered flow pathways. This leaching will change the water retention functions of the porous medium lying within these pathways and make it more wettable than the surrounding water repellent medium. Thus, as time progresses, it is more likely that these pathways will develop into permanent preferential flow pathways, due to heterogeneous wettability. To test this hypothesis, the spatial distributions of soil water content and water repellency obtained from the soil block sampled on September 1, 1992 (see Chapter 5) were analyzed for correlative patterns.

The iso-surface volumetric soil water content of 8.5% has been visualized in Fig. 8.4, together with intersecting horizontal and vertical planes. The development is similar to that shown in Fig. 6.5, in that the fingers start at the layer interface at a depth of around 10 cm. Volumetric soil water content in the humous layer ranged from 12% to 40%, while the underlying dune sand had values of 12% and more within the fingers, and values as low as 1% to 5% in the surrounding soil. Just as in Fig. 6.5, soil water content differences between the fingers and the surrounding dry soil decrease with depth (Fig. 8.4). This can be attributed to the fact that water repellency decreases with depth (Fig. 8.5). It can be seen from the upper horizontal and vertical cutting planes in Fig. 8.5 that water repellency

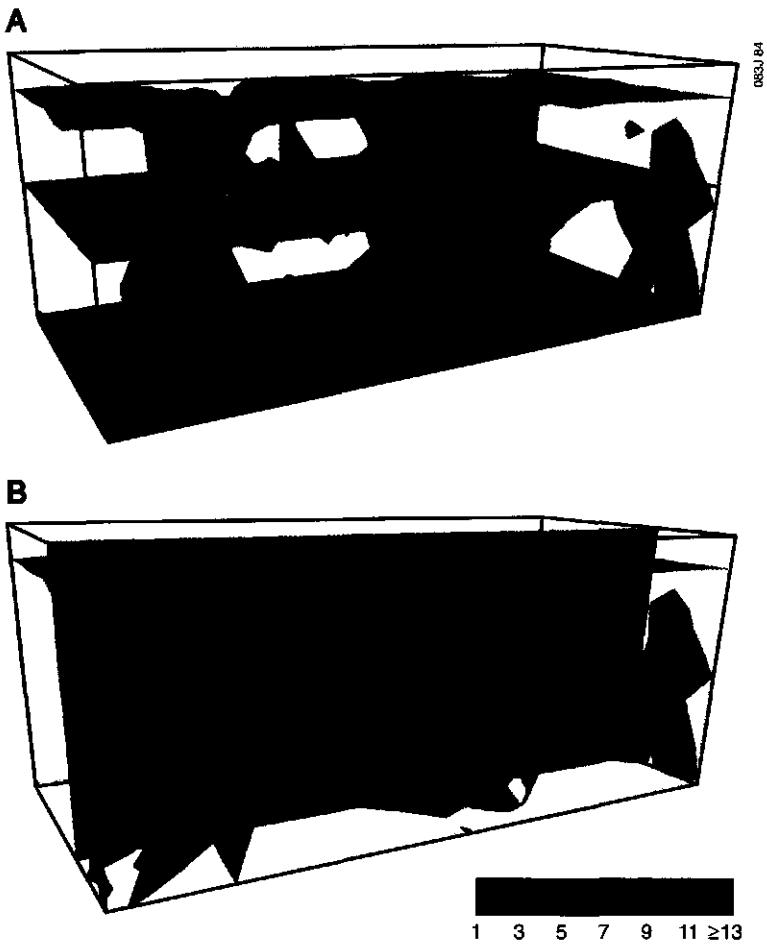

Fig. 8.4 *Spatial distribution of volumetric soil water content in the 60 cm wide, 120 cm long and 52 cm deep sand block sampled in Ouddorp on September 1, 1992. The 8.5% volumetric soil water content iso-surface and the intersecting horizontal (Fig. 8.4A) and vertical (Fig. 8.4B) planes indicate that the vertical fingers started at a depth of around 10 cm. Volumetric soil water content in the humous layer ranged from 12% to 40%, while lower water contents were found in the sandy subsoil (color legend indicates volumetric soil water content scale of the soil).*

is confined to a layer reaching to a depth of 40 cm, being most extreme at depths of 7 to 12 cm. Above and below this zone, water repellency is less severe. The origin of the finger at the center of Fig. 8.4 appears to be associated with a 'weak' area with a relatively low degree of water repellency compared to that found elsewhere at depths of 7 to 12 cm (Fig. 8.5).

Several studies have indicated that infiltrating water may be able to leach organic substances from the topsoil (Schnitzer and Desjardins, 1969; Goh et al., 1976). It has been hypothesized that the finger at the center of Fig. 8.4 is in the process of becoming a heterogeneity-driven finger. The transport of water repellent substances through the finger causes a decrease in the degree of water repellency around the top of the finger, i.e., at depths of 7 to 12 cm, and an increase at the bottom end of the finger, deeper in the profile. This will of course result in different soil water retention curves along the fingered flow pathway and thereby affect the characteristics of unsaturated water flow.

Leaching of water repellent substances through the finger is clearly illustrated by the water repellency distribution shown in the vertical cutting plane in Fig. 8.5, which intersects the entire finger at the center of Fig. 8.4. Relatively low degrees of water repellency were found around the top of the finger and relatively high degrees at the bottom end. A similar trend in the degree of water repellency was observed along the finger on the left, although the vertical cutting plane intersecting this finger is not shown in Fig. 8.5.

The relatively low degree of water repellency around the tops of the fingers promotes the occurrence of converging flow into the fingers, while deeper in the profile the relatively low degrees of water repellency in the soil surrounding the bottoms of the fingers cause diverging flow there. The occurrence of converging and diverging flow in the Ouddorp soil has been confirmed by a detailed tracer experiment (Chapters 2 and 3). The leaching of water repellent substances from the humous layer through the fingers is self-perpetuating, as decreasing water repellency around the top of the finger results in increasing infiltration and vice versa, causing the finger position to become increasingly fixed. This ultimately leads to increasing soil heterogeneity. *The findings thus indicate that, in the long term, originally instability-driven fingers might become heterogeneity-driven fingers.*

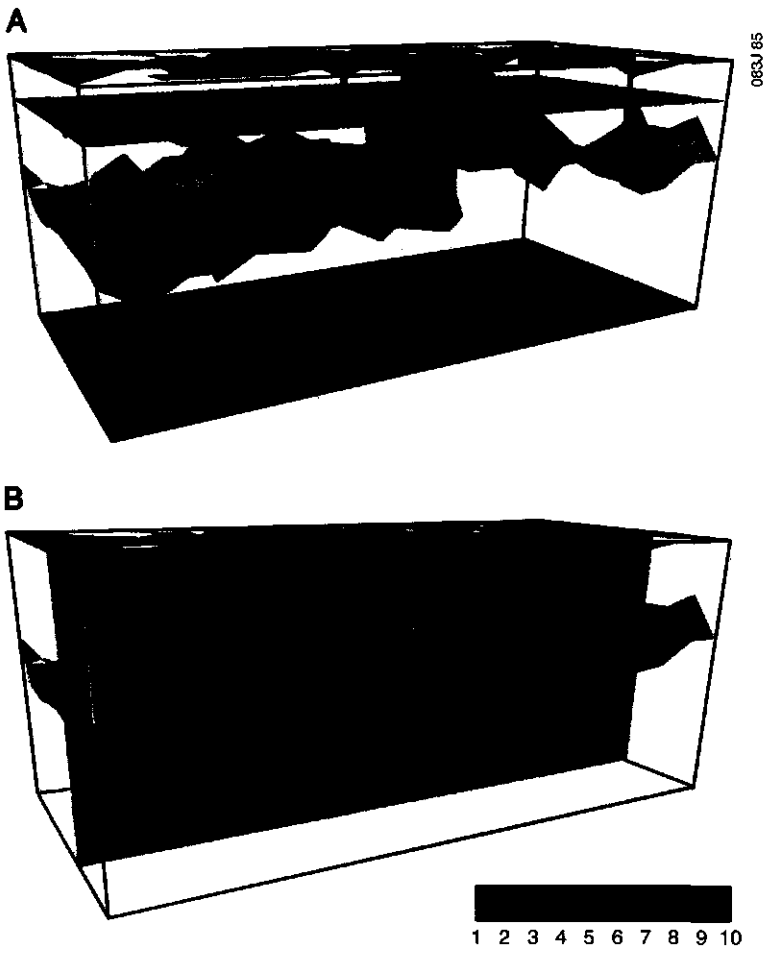

Fig. 8.5 *Spatial distribution of potential water repellency classes in the 60 cm wide, 120 cm long, and 52 cm deep sand block sampled in Ouddorp, showing a water repellent iso-surface and intersecting horizontal (Fig. 8.5A) and vertical (Fig. 8.5B) cutting planes. Degrees of potential water repellency are indicated by class values (1, wettable; 10, extremely repellent) in the color legend. Due to leaching of water repellent substances through the finger, the degree of water repellency was relatively low around the top of the finger, shown at the center of Fig. 8.4A and 8.4B, and relatively high at its bottom end.*

8.6 DISCUSSION

The development of water repellency in soils is a function of time, and generally increases in severity with the age of the vegetation (DeBano, 1969). This is why the degree of water repellency is often lower in arable land than in soils with a permanent vegetation cover (Dekker and Ritsema, 1996c). As a consequence, finger positions are probably only fixed in space over long periods of time in those soils with a permanent plant cover. In arable land, where vegetation types are rotated relatively quickly, and where topsoils are often removed and displaced by tillage practices, finger positions are unlikely to be fixed in space over longer periods of time than the growing season. Therefore, the effects of recurring fingers on the process of pedogenesis are expected to be most pronounced in areas with a permanent plant cover.

Mathematical solutions to Richard's equation are inherently stable (in a physical sense) (Milly, 1988), but when hysteresis in the water retention function is incorporated, the mathematical solutions may yield unstable flow as a natural outcome (Nieber, 1996). *This means that not incorporating hysteresis in a model for water repellent or coarse textured soils may result in seriously misleading outcomes, especially for solute transport prediction.* Most simulation models are based on some form of Richard's equation and fail to directly address the possible occurrence of unstable flow (Van Genuchten and Jury, 1987). Most field studies, even in sandy soils (Steenhuis et al., 1996), have shown that preferential flow is the rule rather than the exception, and may partly account for inaccuracies in the prediction of water and solute movement. Since water repellency is plant-induced, and often occurs in field soils (Wallis et al., 1991; Wallis and Horne, 1992), fingered flow may be more common than is presently thought. In our opinion, these models need to be adapted to account for the unstable flow phenomenon if they are to be employed to full benefit.

CHAPTER 9

EFFECT OF INITIAL SOIL WATER CONTENT ON THE EVOLUTION OF INFILTRATING WETTING FRONTS

Adapted version of 'Stable or unstable wetting fronts in water repellent soils - effect of antecedent soil moisture content' by C.J. Ritsema, J.L. Nieber, L.W. Dekker and T.S. Steenhuis, published in Soil and Tillage Research 47:111-123, 1998.

9 EFFECT OF INITIAL SOIL WATER CONTENT ON THE EVOLUTION OF INFILTRATING WETTING FRONTS

Abstract

Dry, water repellent soils are known to inhibit water infiltration, ultimately forcing water to flow via preferential paths through the vadose zone. A numerical study was performed to investigate the effect of antecedent soil water content on the evolution of infiltrating wetting fronts in water repellent soils. Results indicated that at relatively high soil water contents, i.e., above the critical water content level, infiltrating wetting fronts become stable. In this case, the water-entry pressure head of the boundary wetting branch is lower than the air-entry pressure head of the main drainage branch, causing dissipation of wetting front perturbations. In the opposite situation, with infiltration into initially dry soil, perturbations at the wetting front grow into fingers. In this case, the water-entry pressure head of the boundary wetting branch is higher than the air-entry pressure head of the main drainage branch, promoting finger formation from perturbations. The results presented illustrate the effect of antecedent moisture conditions on the formation of stable and unstable wetting fronts, and indicate the importance of the critical water content of the soil.

9.1 INTRODUCTION

Simulation models are widely used for predicting water and solute transport through soils. Over the last decade it has become increasingly evident that many models are often not capable to simulate actual water flow and transport processes in sufficient detail (Gee et al., 1991; Jury and Flühler, 1992). The main reason is the occurrence of preferential flow, a phenomenon which can be found in a variety of soils. For instance, preferentially moving water is often encountered in clay and peat soils, due to the presence of shrinkage cracks and/or biopores (Bouma and Dekker, 1978; Beven and Germann, 1982). Furthermore, development of unstable wetting fronts in soils may cause water to move preferentially along vertical fingers toward the groundwater. Unstable wetting fronts may be induced if the hydraulic conductivity of the soil increases with depth, as is found in fine over coarse textured soils (Hillel and Baker, 1988; Baker and Hillel, 1990) and in dense

Two simulations were done, one with infiltration into initially dry and the other into initially field-moist Ouddorp soil. The flow domain was 50 cm wide and 50 cm deep, while the humous top layer, water repellent sandy layer and wettable subsoil thicknesses were arbitrarily set at 5, 15 and 30 cm, respectively. The interface between the humous top layer and the water repellent sand layer was assumed to be wavy. For both the initially field-moist and the initially dry cases, rainfall was set at a constant intensity of 1.0 $mm.d^{-1}$. The initial conditions were similar for both simulations, except for the initial water content of the water repellent sand layer. The pressure head for the entire, initially dry water repellent soil was set at -200 cm and wetting occurred according to the main wetting curve (Table 9.1). For the initially field-moist soil, initial pressure in the water repellent layer was set at -100 cm, and wetting followed the boundary wetting curve (Table 1). Pressure heads for the humous top layer and the wettable subsoil were set at -500 cm and -100 cm, respectively, for both the initially dry and initially field-moist cases.

To simulate solute transport, an instantaneous pulse of bromide was imposed at the top of the flow domain at the start of the rainfall. The solute was applied at a rate of 2.0 $g.m^{-2}$. In the simulations, local dispersivities were set at 0.001 m for the longitudinal and 0.0002 m for the transverse dispersivity. The bottom boundary condition used in the simulations was free drainage, i.e. unit hydraulic head gradient.

Figs. 9.1 to 9.5 show numerical results for the evolution of an infiltrating wetting front and an applied bromide pulse in an initially dry (water repellent) and an initially field-moist (wettable) Ouddorp soil. Simulated water distributions in the soil profile for the initially dry Ouddorp soil are shown in Fig. 9.1 for different times. At the start of the simulation period, the domain above the wavy boundary (humous top layer) is wet enough to be wettable, while below this boundary, but above the interface between the two sand layers, the soil is water repellent. Following the start of the rainfall, the upper part of the profile wets until it becomes saturated. The water does not readily enter into the underlying water repellent soil, and will not enter it until the pressure head reaches the water entry value of the water repellent soil. Once the water pressure head at the wavy boundary reaches the water entry value, the front progresses downward at the troughs of the boundary, forming fingers. The fingers continue to progress downward until they reach the wettable bottom layer, at which point they rapidly drain into that layer. Large quantities of water are stored in the fingers and in the upper part of the top layer prior to the fingers reaching the bottom layer, so once they reach that layer the movement is rapid.

Steady-state flow is achieved within a few days after the fingers have reached the wettable layer.

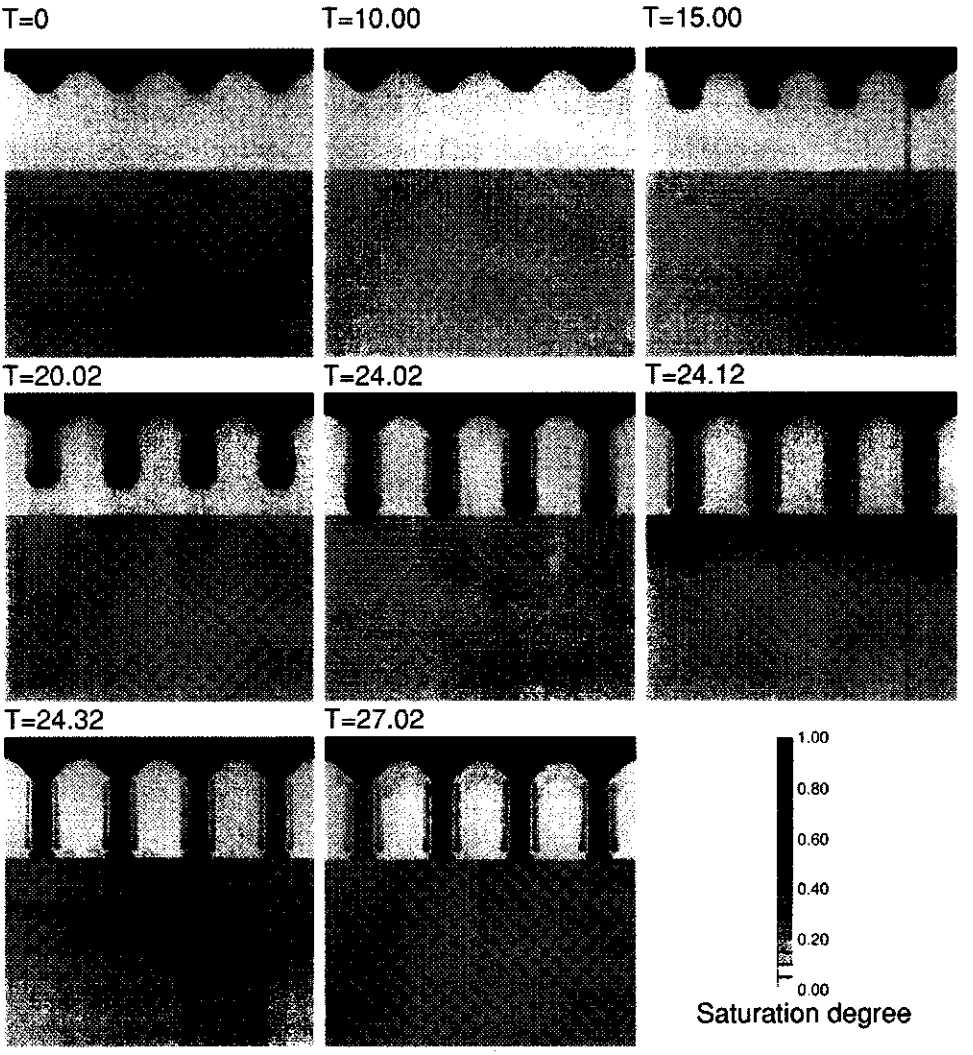

Fig. 9.1 *Numerical results showing the growth of fingered flow pathways during infiltration in an initially dry Ouddorp soil. Unit of time is day.*

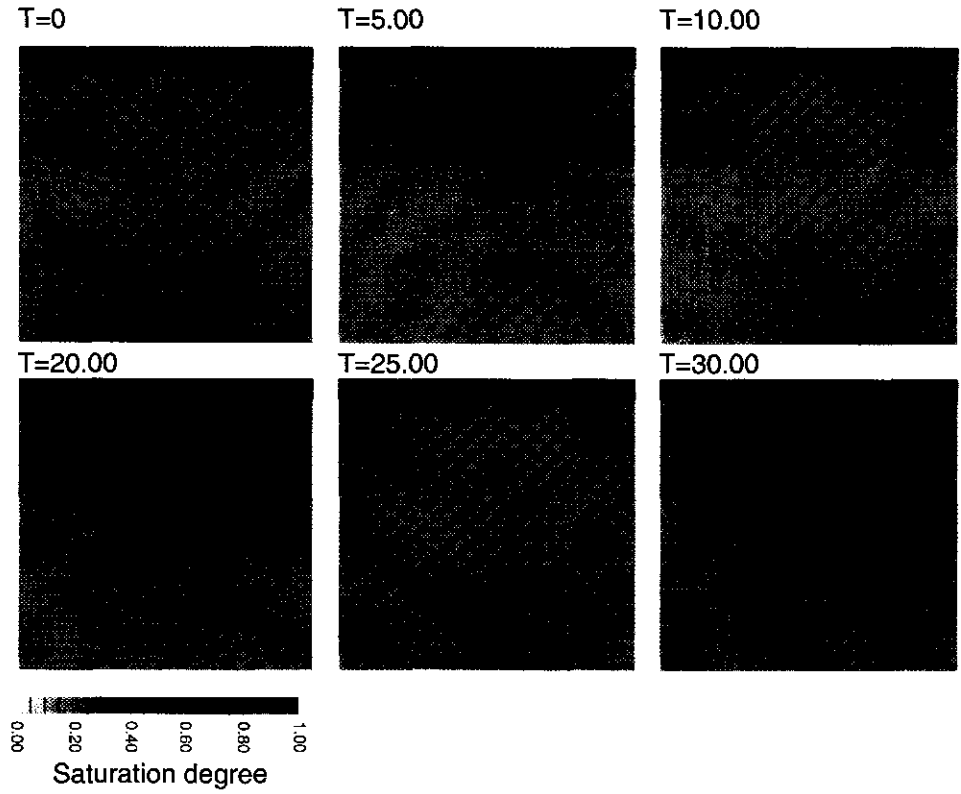

Fig. 9.4 *Numerical results showing the formation of a stable wetting front during infiltration in an initially field-moist Ouddorp soil.*

The bromide transport is shown in Fig. 9.5. The distribution of bromide in the direction of flow indicates a more gaussian-like spreading, as would be expected under stable flow conditions. Apparently, the distribution of bromide during infiltration into the field-moist soil was affected to some extent by the presence of the wavy interface (Fig. 9.5). The breakthrough curve for the solute at the bottom of the flow domain is illustrated in Fig. 9.3. The shape of this breakthrough curve indicates that the dispersion process produces a gaussian distribution of the solute. Bromide arrival at the bottom of the flow domain is much slower than computed for the initially dry situation (Fig. 9.3). *This means that when adsorbing compounds are surface-applied to an initially dry Ouddorp soil, these*

compounds will not only travel to the groundwater much faster than when they are applied to an initially field-moist soil, but the dose of these compounds entering the groundwater will be much higher as well, due to the fact that significant parts of the topsoil (i.e., buffering capacity!) will be bypassed by the fingered flow pathways.

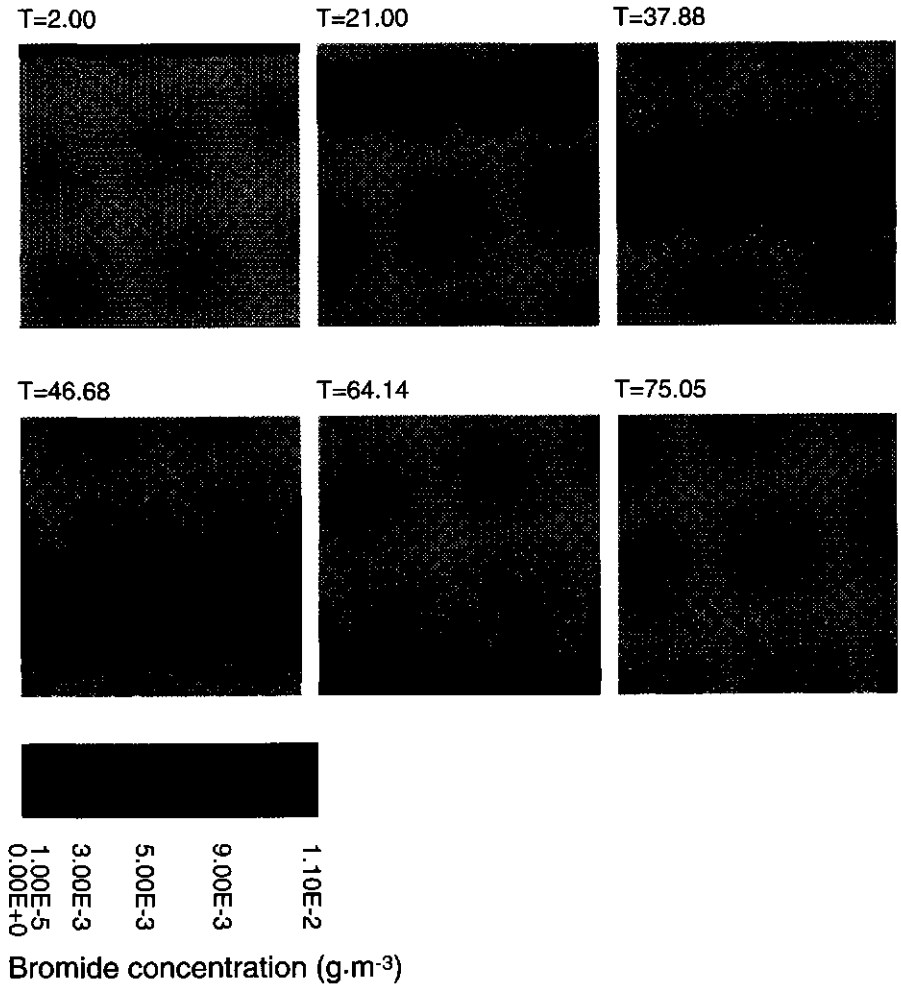

Fig. 9.5 *Numerical results showing the transport of bromide during infiltration in an initially field-moist Ouddorp soil.*

9.4 CONCLUSIONS

To conclude, the numerical results clearly indicate that the perturbations at an infiltrating wetting front can either propagate or dissipate, depending on the antecedent water content of the soil. Finger formation occurs in the Ouddorp soil during infiltration into the initially dry water repellent layer when the water-entry pressure head of the wetting branch is higher than the air-entry pressure head of the main drainage branch. No fingers are formed in the water repellent layer at higher initial water contents. The physical properties of the wettable subsoil preclude the formation of fingers under any circumstances.

During the bromide tracer experiments described in Chapters 2 and 7, water contents of (large parts of) the water repellent layer were often below the critical level, resulting in the formation of fingered flow pathways during infiltration events. However, if the water content of the water repellent sand layer exceeded the critical level (for instance due to very high rainfall or a drastic rise in the groundwater level), stable infiltrating wetting fronts would evolve.

This indicates that, at least from a soil protection and soil management point of view, it would be advisable to avoid extreme drying of water repellent soils, for instance by using sprinkler irrigation, in order to prevent the formation of fingers during subsequent rain events. In this way, accelerated downward transport of water and solutes through fingered flow pathways will be prevented.

CHAPTER 10

SUMMARY AND CONCLUSIONS

10 SUMMARY AND CONCLUSIONS

Recently, it has become clear that soil water repellency is much more wide-spread than was formerly thought. Water repellency has been reported in most continents of the world for varying land uses and climatic conditions.

At present, soil water repellency is receiving increasing attention from scientists and policy makers, due to the adverse and sometimes devastating effects of soil water repellency on environmental quality and agricultural crop production. This is illustrated, for instance, by the organization of two conferences on soil water repellency in Australia in 1990 and 1994 (Oades and Blackwell, 1990; Carter and Howes, 1994), and a forthcoming international workshop entitled 'Soil Water Repellency - Occurrence, Origins, Consequences, Modeling, and Amelioration' to be held in the Netherlands on September 2-4, 1998.

It is felt by many researchers that soil water repellency is one of the least understood phenomena in the vadose zone hydrology and soil science disciplines, and therefore, there is a strong need for intensified research efforts on this topic. This is all the important as many more areas inside and outside the Netherlands may become water repellent during the years and decades to come, due to changes in land use, changes in soil and water management, and changes in weather conditions.

10.1 RESEARCH SET-UP AND RESULTS

10.1.1 Research set-up

The present Doctoral thesis focused on investigating flow and transport mechanisms in an untilled, grass-covered, water repellent sandy soil in Ouddorp, the Netherlands. Research activities comprised detailed field experiments, sample collection, laboratory measurements, data analysis and interpretation, as well as model simulations.

Within the scope of this thesis, a total of 5 field experiments were executed over the last decade, viz.

- a field-scale bromide tracer experiment to investigate the general flow and transport mechanism (Chapters 2 and 3);

- sampling of 10 trenches to study the water content distributions of the soil in two dimensions over a one year cycle (Chapter 4);
- sampling of 10 soil blocks to study the three-dimensional water content distributions in relation with water repellency patterns (Chapter 5);
- a TDR study to obtain in situ soil water content data in a vertical trench over an 8 month period (Chapter 6);
- a plot-scale bromide tracer experiment to relate bromide distributions with soil water content and water repellency patterns (Chapter 7).

In all, around 23,500 soil samples were taken in the field, brought to the laboratory and used for the determination of water content, dry bulk density, degree of soil water repellency, tracer concentration and/or other properties. Besides the estimated 60,000 data derived from these samples, another 200,000 data of in situ soil water contents were collected during the 8-month TDR measurement campaign, of which only a small part was used in the present thesis. Sample and data collection in the field was done within a reasonable amount of time. Much more time, however, was needed in the laboratory to determine all necessary properties. Worse were the endless hours of feeding all the data into computer databases and checking them after completion in order to ensure that no errors had been made at this stage. An exciting phase was that of the data analysis, in which process mechanisms became unraveled and visualized. Almost all datasets were used as the basis for one of the Chapters in this thesis.

The final part of the thesis comprises modeling work aiming at physically understanding and simulating the process of fingered flow formation and recurrence (Chapter 8), and investigating the conditions under which fingered flow prevails (Chapter 9). This latter part was done in close cooperation with John L. Nieber and Hung V. Nguyen, both from the University of Minnesota, St.Paul, USA, and Tammo S. Steenhuis from Cornell University, Ithaca, USA.

10.1.2 Research results

The results of the field-scale bromide tracer experiment presented in Chapter 2 indicate a complex flow behavior in the water repellent sandy soil under investigation: distribution flow directs water and solutes laterally through the humous top layer towards the

vertically directed fingered flow pathways; fingered flow dominates in the water repellent sandy soil below the humous top layer, while diverging flow occurs in the wettable subsoil. Large parts of the extremely water repellent sandy soil layer are by-passed by water and bromide, as was amongst others indicated by the double-peaked bromide profiles.

The effect of distribution flow on the displacement of water and solutes in the humous top layer is discussed in more detail in Chapter 3. It was found that water flow and solute transport occur laterally through the distribution layer to locations with relatively low degrees of potential water repellency, enabling vertical infiltration and transport through preferential flow paths at these spots. In the Ouddorp experimental field, the distribution layer is very thin, of the order of a few centimeters.

Two-dimensional water content distributions of ten trenches are presented in Chapter 4, showing that fingered flow patterns can be found within the Ouddorp experimental field almost throughout the year. At the end of June, a relatively uniform dry situation was met, but rainfall in July caused fingers to develop relatively quickly, with finger diameters of 10 to 15 cm, increasing to a maximum of 25 cm in October. At the end of the winter, the profile showed a more or less uniformly wet pattern. Short-term variations in the number and size of fingers were related to the succession of weather conditions during the experimental period. The fingers were wet in the topsoil and became drier with depth. The presence of the fingers itself induces a system anisotropy in the actual hydraulic conductivity. Hysteresis tends to magnify this phenomenon, as it is one of the major causes of the long term persistence of fingers. The data presented suggest that finger merging is an irrelevant process in the experimental field. The percentages of actually water repellent soil indicated that volumes of soil can be excluded from water flow and solute transport for several hours or more. Spatial differences in bulk density seem not to be important to the differences found in soil water content.

In Chapter 5, three-dimensional soil water content distributions are presented for ten soil blocks sampled in the Ouddorp experimental field. Interpretation of the three-dimensional soil water content distributions indicates that the fingered flow patterns became less clear during periods of excessive rain (forced wetting due to upward movement of the

groundwater level) or during prolonged droughts. The position of the fingers seemed to be determined by slight variations in the degree of potential water repellency of the top layer. Fingers started in the top layer in places with relatively low degrees of water repellency.

During several rain events, dynamic formation and recurrence of fingers in a vertical trench in the Ouddorp experimental field were measured with an automated TDR device, as described in Chapter 6. The water content distributions thus obtained show that finger formation depends on the wetting history of the soil and the rainfall characteristics. Fingers developed rapidly during severe rain storms, causing significant portions of the infiltrating water to flow preferentially through the fingers to the deeper subsoil. Fingers recurred at the same sites during all rain events.

A plot-scale bromide tracer experiment was executed at the same site after the conclusion of the TDR measurements (Chapter 7). After 52 mm of rainfall, 32.5% of the applied bromide had leached to a depth below 79 cm. Indications were found that the distribution layer, i.e. the humous top layer, acted as a bromide reservoir, releasing bromide in limited amounts during rain events. Bromide could not be detected, or at very low concentrations only, in the dry spots between the fingers. The spots with the highest degree of actual water repellency were encountered in places with the highest degree of potential water repellency. In the actually wettable zone, diverging flow from the fingers towards the surrounding areas below dry, actually water repellent soil zones resulted in double-peaked bromide profiles. Despite the process of diverging flow, the highest bromide concentrations within the actually wettable zone were found in places below fingers. Long term application of manure increased pH values in the humous top layer and in the underlying fingers. The dry, actually water repellent soil regions between the fingers were not affected by the manure applications. The observed pH distribution could only be explained by the long term recurrence of the fingered flow pathways during successive rain events.

In Chapter 8, model simulations indicate that fingered flow results from hysteresis in the water retention function, and that the nature of the formation depends on the shape of the main wetting and main drainage branches of that function. Once fingers are established,

hysteresis causes fingers to recur along the same pathways during subsequent rainfall events. Three-dimensional water repellency distributions obtained from one of the sampled soil blocks indicated that leaching of water repellent substances from the fingered flow pathways caused the soil within the pathways to become more wettable than the surrounding soil. Thus, in the long term, instability-driven fingers may become heterogeneity-driven fingers.

Chapter 9 highlights the effect of initial soil water content on the evolution of infiltrating wetting fronts on basis of numerical results. Results indicate that in initially field-moist or wet conditions, infiltrating wetting fronts move through the soil in a stable, uniform way. When the initial water content of the soil drops below the critical soil water content level, infiltrating wetting fronts become unstable and fingered flow pathways emerge. The results convincingly show that preferential flow can be expected in water repellent soils when initial soil water contents are lower than the critical soil water content level (i.e. the level below which the soil becomes water repellent). This indicates that, at least from a soil management point of view, critical soil water content levels of water repellent soils should be determined in much more detail than has been done so far. Gathering of such information will make it easier to define appropriate guidelines for sustainable management of water repellent soils, with the aim of preventing these soils from becoming water repellent, and hence preventing the adverse consequences of preferential water flow and solute transport.

To conclude, the **major research findings** of this thesis are the following

- Water flow and transport in water repellent sandy soils show a typical behavior with distribution flow in the humous top layer, fingered flow in the water repellent sand layer, and diverging flow in the wettable subsoil.
- Fingers form during infiltration in dry soil when initial water contents are below the critical soil water content level.
- Fingers may expand or shrink in diameter depending on the sequence of weather conditions.
- Fingers recur at the same sites during successive rain events.
- In the long term, instability-driven fingers may become heterogeneity-driven

fingers.

- Finger formation results from hysteresis in the water retention function, and the nature of formation depends on the shape of the wetting and drainage branches of that function.

10.2 RECOMMENDATIONS FOR FUTURE RESEARCH

It is hoped that the results of the present study will contribute to a better understanding of flow and transport processes in water repellent soils. However, it is the author's view that much more research needs to be done to improve our understanding of the occurrence and functioning of water repellent soils both in agricultural and natural environments.

Practical experience has often shown that water repellency of soils leads to adverse effects for agricultural and natural environments, such as

- severe erosion and runoff;
- rapid leaching of surface-applied agrichemicals;
- significant loss of water and nutrient availability for crops;
- low crop and pasture production.

Before appropriate guidelines can be derived to prevent or combat these negative effects and to manage water repellent soil systems in an environmentally friendly and sustainable way, several aspects need to be investigated in detail. In the author's opinion, questions which urgently need solving include the following

- Where do water repellent soils occur, and what range of severity of water repellency can be expected under different conditions of climate and land use?
- How can information on water repellency be incorporated in soil maps?
- What are the causes of soil water repellency, and how is water repellency related to different vegetation types?
- What range of critical water contents exists for water repellent soils around the world?
- What is the effect of water repellency on hysteresis in the water retention function in fine and coarse textured soils?

- Which finger lengths and diameters can be expected in water repellent soils under different conditions of groundwater level and thickness of the wettable subsoil?
- How fast can instability-driven fingers in water repellent soils change into heterogeneity-driven fingers?
- How can we develop simple tools for predicting water flow and solute transport in soils with homogeneous/heterogeneous distributions of water repellency?
- Which amelioration techniques can be applied to reduce environmental degradation and production losses on agricultural water repellent soils?
- Which amelioration techniques are most promising from the environmental, crop production, and farming points of view?

I would like to conclude by expressing my sincere hope that the results of the present Doctoral thesis, and those by Louis W. Dekker and Hung V. Nguyen, will act as a stimulus for initiating new research projects on a broad range of topics related to water repellent soils. If this can be achieved, I trust that answers will be found, yielding a better understanding of the origins, occurrence, hydrological responses and agricultural functioning of water repellent soil systems world-wide.

CHAPTER 11

SAMENVATTING EN CONCLUSIES

11 SAMENVATTING EN CONCLUSIES

Het is de laatste tijd duidelijk geworden dat waterafstotende gronden veel meer voorkomen dan vroeger werd gedacht. Waterafstotende gronden zijn inmiddels op de meeste continenten geconstateerd, onder uiteenlopende omstandigheden van bodemgebruik en klimaat.

Momenteel neemt bij wetenschappers en beleidsmakers de belangstelling voor het verschijnsel van waterafstotende gronden toe, vooral als gevolg van de ongunstige, en soms schadelijke gevolgen van waterafstotendheid voor de kwaliteit van het milieu en de agrarische productie. Dit blijkt bijvoorbeeld uit het feit dat er in de afgelopen tien jaar in Australië twee conferenties aan het onderwerp zijn gewijd (Oades & Blackwell, 1990; Carter & Howes, 1994). Dit jaar wordt in Nederland een internationale workshop gehouden van 2-4 september onder de titel 'Soil Water Repellency - Occurrence, Origins, Consequences, Modeling and Amelioration'.

Volgens vele onderzoekers is waterafstotendheid van gronden een van de slechtst begrepen verschijnselen in de bodemkunde en de hydrologie van de onverzadigde zone. Er is dan ook grote behoefte aan intensief onderzoek op dit gebied. Dit is des te belangrijker omdat in de komende tientallen jaren bodems in allerlei nieuwe gebieden binnen en buiten Nederland waterafstotend kunnen worden als gevolg van veranderingen in het landgebruik, bodem- en waterbeheer en weersomstandigheden.

11.1 ONDERZOEKSOPZET EN -RESULTATEN

11.1.1 Onderzoeksopzet

Dit proefschrift gaat over onderzoek naar stromings- en transportmechanismen in een met gras begroeide, waterafstotende zandgrond in Ouddorp. Het onderzoek omvatte gedetailleerde veldexperimenten, monsternames, laboratoriumbepalingen, analyse en interpretatie van de gegevens, en computersimulaties.

In het kader van het onderzoek zijn in de loop van de afgelopen tien jaar in totaal vijf veldexperimenten gedaan, te weten

- een tracerexperiment op veldschaal met bromide als tracer om het algehele

stromings- en transportmechanisme te onderzoeken (Hoofdstukken 2 en 3);
- bemonstering van tien 5 m lange en 0,5 m diepe sleuven ter bestudering van tweedimensionale watergehalteverdelingen in de grond (Hoofdstuk 4);
- bemonstering van tien blokken ter bestudering van driedimensionale watergehalteverdelingen in de grond in relatie tot de mate van waterafstotendheid (Hoofdstuk 5);
- TDR-metingen van watergehaltes in een verticaal profiel gedurende acht maanden (Hoofdstuk 6);
- een bromidetracerexperiment op kleine plotschaal waarbij de bromideverdeling werd gerelateerd aan patronen van bodemwatergehalte en waterafstotendheid (Hoofdstuk 7).

In totaal zijn er in het veld zo'n 23.500 bodemmonsters genomen. In het laboratorium zijn daarvan het watergehalte, de dichtheid van de grond, de mate van waterafstotendheid, de concentratie van de tracer en/of andere eigenschappen bepaald. Naast de ca. 60.000 gegevens die aan deze monsters werden ontleend, zijn nog eens 200.000 in situ watergehaltes verzameld door middel van de TDR-metingen in een acht maanden durende meetcampagne. Slechts een klein deel van deze gegevens is gebruikt in dit proefschrift. Het verzamelen van monsters en gegevens in het veld kon binnen een redelijke termijn worden gerealiseerd, maar het bepalen van alle vereiste gegevens in het laboratorium nam veel meer tijd in beslag. Nog veel tijdrovender was het invoeren van alle gegevens in de computer en het controleren ervan om ervoor te zorgen dat er in dit stadium geen fouten werden gemaakt. Een interessante fase was die van de gegevensanalyse, waarbij geleidelijk aan de procesmechanismen duidelijk en zichtbaar werden. Vrijwel alle verzamelde gegevensbestanden werden gebruikt als basis voor een van de hoofdstukken in dit proefschrift.

De laatste fase van het onderzoek richtte zich op het fysisch verklaren en simuleren van vingervormige stromingspatronen (Hoofdstukken 8 en 9). Dit laatste deel van het onderzoek werd uitgevoerd in nauwe samenwerking met John L. Nieber en Hung V. Nguyen, beide verbonden aan de University of Minnesota in St. Paul (VS), en met Tammo S. Steenhuis van de Cornell University in Ithaca (VS).

11.1.2 Resultaten van het onderzoek

De in Hoofdstuk 2 gepresenteerde resultaten van het bromidetracerexperiment op veldschaal duiden op een complex stromingsgedrag in de onderzochte waterafstotende zandgrond: water en daarin opgeloste stoffen stromen in laterale richting door de humeuze toplaag naar verticaal georiënteerde vingervormige stroombanen; in de waterafstotende zandlaag verloopt het transport vooral via deze vingervormige banen, terwijl in de niet-waterafstotende ondergrond de stroming een divergerend karakter vertoont. Grote delen van de waterafstotende zandlaag komen zodoende in het geheel niet in aanraking met het water en de daarin opgeloste bromide. Dit werd onder meer duidelijk uit de gemeten bromideprofielen, die soms twee pieken vertoonden.

Het effect van de laterale verplaatsing van water en opgeloste stoffen in de humeuze toplaag wordt gedetailleerd besproken in Hoofdstuk 3. Het water en de daarin opgeloste stoffen bleken via de distributielaag in zijdelingse richtingen te worden getransporteerd naar plaatsen met een relatief geringe potentiële waterafstotendheid. Vanuit dergelijke plaatsen bleek het verder neergaande transport van water en opgeloste stoffen via vingervormige stroombanen te verlopen. Uit de metingen blijkt dat de distributielaag in het proefveld in Ouddorp erg dun is, in de orde van grootte van enkele centimeters.

In Hoofdstuk 4 worden de gegevens gepresenteerd over de tweedimensionale verdeling van het watergehalte in tien gegraven sleuven. Hieruit blijkt dat in het proefveld in Ouddorp bijna het gehele jaar door vingervormige stromingspatronen optreden. Eind juni werd een vrij uniforme droge situatie aangetroffen, maar na regenval in juli ontstonden al tamelijk snel vingers, met een diameter van 10 tot 15 cm, oplopend tot 25 cm in oktober. Aan het eind van de winter vertoonde het profiel een min of meer uniform vochtig patroon. Kortetermijnvariaties in de aantallen en afmetingen van de vingers konden worden gerelateerd aan de opeenvolgende weersomstandigheden gedurende de proefperiode. Het vochtgehalte in de vingers was het hoogst in de toplaag en nam met de diepte geleidelijk af. De aanwezigheid van de vingers leidt tot grote lokale verschillen in actuele doorlatendheid. Hysterese is de voornaamste factor in het langdurig blijven bestaan van de vingers. De gepresenteerde gegevens doen vermoeden dat in het proefveld vingervormige stroombanen niet of nauwelijks samenvloeiden. Uit de percentages actueel

waterafstotende grond blijkt dat delen van de bodem gedurende verscheidene uren, of nog langer, buiten het transport van water en opgeloste stoffen kunnen blijven. Ruimtelijke verschillen in dichtheid van de grond lijken geen invloed te hebben op de gevonden verschillen in watergehalte van de bodem.

In Hoofdstuk 5 wordt van tien bemonsterde bodemblokken in het proefveld te Ouddorp de driedimensionale verdeling van het watergehalte beschreven. Uit de interpretatie van deze driedimensionale watergehalteverdelingen blijkt dat de vingervormige stromingspatronen minder duidelijk werden tijdens perioden van overvloedige regenval (waarbij geforceerde bevochtiging door stijging van het grondwaterpeil op kan treden) en tijdens langdurige droogte. De positie van de vingers leek te worden bepaald door kleine variaties in de mate van potentiële waterafstotendheid in de toplaag. De vingers ontstonden op die plaatsen in de toplaag waar de mate van waterafstotendheid relatief laag was.

Tijdens een aantal regenperioden zijn de dynamische vorming en terugkeer van de vingerpatronen in een verticale sleuf in het proefveld te Ouddorp bestudeerd met behulp van een geautomatiseerd TDR-systeem. De resultaten zijn beschreven in Hoofdstuk 6. De hierbij gevonden watergehalteverdelingen laten zien dat de vorming van vingerpatronen afhankelijk is van de bevochtingsgeschiedenis van de bodem en van de regenvalkarakteristieken. Tijdens zware regenbuien ontstonden de vingers snel, waardoor aanzienlijke delen van het infiltrerende water via deze vingers naar de diepere ondergrond stroomden. In iedere regenperiode verschenen de vingers weer op dezelfde plek.

Na afloop van de TDR-metingen werd op dezelfde locatie een tracerexperiment met bromide uitgevoerd (hoofdstuk 7). Na een regenval van 52 mm bleek 32,5% van de toegediende bromide uitgespoeld te zijn naar een diepte van meer dan 79 cm. Er waren aanwijzingen dat de distributielaag als bromidereservoir fungeerde, waarbij bromide tijdens regen in beperkte hoeveelheden werd afgestaan. In de droge bodemdelen tussen de vingers werd weinig of geen bromide aangetroffen. Plaatsen met de sterkste actuele waterafstotendheid werden aangetroffen op plekken met de sterkste potentiële waterafstotendheid. Als gevolg van de divergerende stroming in de niet-waterafstotende ondergrond, die vanuit de vingers naar de omringende bodemdelen onder de droge,

actueel waterafstotende bodemzones was gericht, ontstonden bromideprofielen met twee pieken. Ondanks dit proces van divergerende stroming werden de hoogste bromideconcentraties in deze goed bevochtigbare zone toch gevonden onder de vingers. Langdurige bemesting leidde tot verhoogde pH-waarden in de humeuze toplaag en de daaronder gelegen vingervormige stroombanen. De droge, actueel waterafstotende bodemdelen tussen de vingers werden niet beïnvloed door de bemesting. De gevonden pH-verdeling kon alleen worden verklaard door het over langere termijn steeds weer terugkeren van de vingervormige stroombanen tijdens opeenvolgende regenperiodes.

De computersimulaties in Hoofdstuk 8 laten zien dat de vingervormige stromingspatronen het resultaat zijn van hysterese in de waterretentiefunctie, en dat de aard van de patronen afhangt van de vorm van de bevochtigings- en drainagetak van die functie. Als de vingers zich eenmaal gevormd hebben, zorgt hysterese ervoor dat bij volgende regenperiodes transport van water en opgeloste stoffen weer via dezelfde banen verloopt. Uit de driedimensionale waterafstotendheidsverdeling die werd afgeleid uit een van de bemonsterde bodemblokken bleek dat door het uitspoelen van waterafstotende verbindingen uit de vingervormige stroombanen de bodem binnen deze vingers gemakkelijker bevochtigbaar werd dan het omringende bodemmateriaal. Daardoor ontwikkelen vingers die in eerste instantie ontstaan op basis van instabiliteiten in het vochtfront zich op den duur tot vingers die het gevolg zijn van heterogeniteit in de bodem.

In hoofdstuk 9 worden op basis van numerieke resultaten de gevolgen beschreven van het initiële watergehalte van de bodem op de ontwikkeling van infiltrerende vochtfronten. Uit die resultaten blijkt dat in een aanvankelijk veldvochtige of natte bodem het infiltrerende vochtfront zich op stabiele, gelijkmatige wijze door de bodem omlaag beweegt. Bij een initieel droge situatie met bodemwatergehalten beneden de kritische waarde wordt het vochtfront echter onstabiel en ontstaan er vingervormige stroombanen. De resultaten tonen overtuigend aan dat in een waterafstotende bodem preferente stroming kan worden verwacht als het oorspronkelijke watergehalte van die bodem lager is dan het kritische bodemwatergehalte (d.w.z. het watergehalte waarbeneden de bodem waterafstotend wordt). Dat betekent vanuit het oogpunt van bodem- en milieubeheer dat de kritische bodemwatergehaltes van waterafstotende gronden waardevolle informatie kunnen opleveren over wanneer wel of wanneer geen preferente stroming verwacht mag worden.

Het zou daarom goed zijn dergelijke informatie van veel meer gronden te verzamelen dan tot nu toe is gebeurd. Met behulp van die gegevens wordt het gemakkelijker de juiste richtlijnen op te stellen voor een duurzaam beheer van potentieel waterafstotende gronden, met als doel te voorkomen dat deze bodems actueel waterafstotend worden en zodoende te vermijden dat preferente stroming van water en opgeloste stoffen zal optreden.

De **voornaamste onderzoeksresultaten** uit dit proefschrift laten zich als volgt samenvatten

- Stroming van water en transport van opgeloste stoffen in waterafstotende zandgronden vertonen een typisch gedrag, waarbij in de humeuze toplaag distributiestroming optreedt, in de waterafstotende zandlaag stroming door vingervormige banen, en in de bevochtigbare ondergrond divergerende stroming.
- De vingers ontstaan tijdens infiltratie van regenwater in initieel droge bodems als het watergehalte van die bodem beneden het kritische niveau ligt.
- De diameter van de vingers kan enigszins toe- of afnemen, afhankelijk van de opeenvolgende weersomstandigheden.
- Tijdens nieuwe regenperiodes keren de vingers op dezelfde plaatsen terug.
- Op den duur kunnen vingers die oorspronkelijk ontstaan zijn uit instabiele vochtfronten, veranderen in vingers die het gevolg zijn van heterogeniteit in bodemeigenschappen.
- De vorming van de vingers vloeit voort uit hysterese in de waterretentiefunctie, en de aard van de vingervorming hangt af van de vorm van de bevochtigings- en drainagetak van die functie.

11.2 SUGGESTIES VOOR TOEKOMSTIG ONDERZOEK

Het is mijn hoop dat de resultaten van dit onderzoek zullen bijdragen tot een beter inzicht in de stromings- en transportprocessen in waterafstotende gronden. De auteur is echter van mening dat er nog veel meer onderzoek nodig zal zijn om onze kennis van het vóórkomen en functioneren van waterafstotende gronden onder verschillend landgebruik te vergroten.

Uit ervaring is gebleken dat waterafstotendheid van bodems negatieve gevolgen kan hebben voor agrarische en natuurlijke terreinen, zoals

- ernstige bodemerosie en afspoeling;
- snelle uitspoeling van milieugevoelige stoffen;
- geringere beschikbaarheid van water en voedingsstoffen voor landbouwkundige gewassen;
- slechtere oogsten op akkerland en minder grasproductie op weiland.

Voordat geschikte richtlijnen kunnen worden opgesteld voor het op milieuvriendelijke en duurzame wijze beheren van waterafstotende gronden, moeten er nog vele aspecten nauwkeuriger onderzocht worden. Naar de mening van de auteur wachten de volgende vragen dringend op beantwoording

- Waar komen waterafstotende gronden voor, en welke mate van waterafstotendheid is te verwachten onder uiteenlopende omstandigheden van klimaat en landgebruik?
- Hoe kan informatie over waterafstotendheid verwerkt worden in bodemkaarten?
- Wat zijn de oorzaken van waterafstotendheid en hoe hangt dit verschijnsel samen met de verschillende vegetatietypen?
- Welke waarden van het kritische bodemwatergehalte kunnen we in waterafstotende gronden over de hele wereld aantreffen?
- Wat voor gevolgen heeft waterafstotendheid voor de hysterese in de waterretentiefunctie van gronden met fijne en grove textuur?
- Welke lengte en diameter kunnen de vingers in waterafstotende gronden aannemen bij uiteenlopende omstandigheden van grondwaterspiegel en dikte van de bevochtigbare ondergrond?
- Hoe snel kunnen in een waterafstotende bodem vingers die ontstaan zijn op basis van instabiliteit, veranderen in vingers die het gevolg zijn van heterogeniteit?
- Hoe kunnen er eenvoudige hulpmiddelen ontwikkeld worden om de waterstroming en het transport van opgeloste stoffen in gronden met homogene/heterogene verdelingen van waterafstotendheid te simuleren?
- Welke maatregelen kunnen er worden ontwikkeld om de milieutechnische achteruitgang en de productieverliezen op waterafstotende gronden die in gebruik zijn voor de landbouw te beperken?
- Van welke maatregelen kunnen de beste resultaten verwacht worden voor het milieu, de oogst en het agrarische bedrijf?

Tenslotte hoop ik dat de resultaten van dit promotieonderzoek en die van Louis W. Dekker en Hung V. Nguyen een stimulans zullen vormen voor het starten van nieuwe onderzoeksprojecten op het gebied van waterafstotende gronden. De resultaten van dergelijke projecten zullen meer inzicht bieden in het ontstaan, het vóórkomen, de hydrologische gevolgen en het agrarisch functioneren van waterafstotende bodemsystemen over de gehele wereld.

REFERENCES

Abbott, L.K. and A.D. Robson. 1981. Infectivity and effectiveness of five endomycorrhizal fungi: competition with indigenous fungi in field soils. Austr. J. Agric. Res. 32: 621-630, 1981.

Abulaban, K., J.L. Nieber and D. Misra. 1998. Modeling plume behavior for nonlinearly sorbing solutes in saturated homogeneous porous media. Adv. Water Resour., in press.

Adams, S., B.R. Strain and M.S. Adams. 1969. Water repellent soils and annual plant cover in a desert scrub community of southeastern California. In: Proc. Symp. 'Water Repellent Soils', May 1968, Riverside, California, pp. 289-296.

Adams, S., B.R. Strain and M.S. Adams. 1970. Water repellent soils, fire, and annual plant cover in a desert scrub community of southeastern California. Ecology 51:696-700.

Agus, F. and D.K. Cassel. 1992. Field-scale bromide transport as affected by tillage. Soil Sci. Soc. Am. J. 56:254-260.

Ahuja, L.R. and J.D. Ross. 1982. Interflow of water through a sloping soil with seepage face. Soil Sci. Soc. Am. J. 46:245-250.

Baker, J.M. and R.R. Allmaras. 1990. System for automating and multiplexing soil moisture measurements by time-domain reflectometry. Soil Sci. Soc. Am. J. 54:1-6.

Baker, R.S. and D. Hillel. 1990. Laboratory tests of a theory of fingering during infiltration into layered soils. Soil Sci. Soc. Am. J. 54:20-30.

Bathke, G.R. and D.K. Cassel. 1991. Anisotropic variation of profile characteristics and saturated hydraulic conductivity in an Ultisol landscape. Soil Sci. Soc. Am. J. 55:333-339.

Bathke, G.R., D.K. Cassel and P.A. McDaniel. 1992. Bromide movement at selected sites in a dissected piedmont landscape. J. Env. Qual. 21:469-475.

Bear, J. and Y. Bachmat. 1990. Introduction to modeling of transport phenomena in porous media, Kluwer Academic Publushers, Dordrecht, The Netherlands. 553 pp.

Beven, K. and P. Germann. 1982. Macropores and water flow in soils. Water Resour. Res. 18:1311-1325.

Beven, K.J. 1989. Interflow. In: *Unsaturated flow in hydrologic modeling*, edited by Morel-Seytoux, pp. 191-219., Kluwer Acad. Publ., Dordrecht.

Beven, K.J. 1991a. Infiltration, soil moisture, and unsaturated flow. In *Recent advances in the modeling of hydrologic systems*, edited by D.S. Bowles and P. E. O'Connell, pp. 137-166, Kluwer Acad. Publ., Dordrecht.

Beven, K.J. 1991b. Spatially distributed modeling: conceptual approach to runoff prediction. In *Recent advances in the modeling of hydrologic systems*, edited by D.S. Bowles and P. E. O'Connell, pp. 373-387, Kluwer Acad. Publ., Dordrecht.

Bisdom, E.B.A., L.W. Dekker and J.F.T. Schoute. 1993. Water repellency of sieve fractions from sandy soils and relationships with organic material and soil structure. Geoderma 56:105-118.

Bishay, B.G. and H.K. Bakhati. 1976. Water repellency of soils under citrus trees in Egypt and means of improvement. Agric. Resour. Rev. (Cairo) 54:63-74.

Blackwell, P. 1993. Improving sustainable production from water repellent sands. W.A. Journal of Agriculture 34:158-167.

Boels, D., J.B.M.H. van Gils, G.J. Veerman and K.E. Wit. 1978. Theory and systems of automatic determination of soil moisture characteristics and unsaturated hydraulic conductivities. Soil Sci. 126:191-199.

Bond, R.D. 1964. The influence of the microflora on the physical properties of soils. II. Field studies on water repellent sands. Austr. J. Soil Res. 2:123-131.

Bond, R.D. 1969. Factors responsible for water repellence of soils. In: Proc. Symp. 'Water Repellent Soils', May 1968, Riverside, California, pp. 259-264.

Bouma, J. and L.W. Dekker. 1978. A case study on infiltration into dry clay soil I. Micromorphological observations. Geoderma 20:27-40.

Bronswijk, J.J.B. 1991. Magnitude, modeling and significance of swelling and shrinkage processes in clay soils, Doctoral Thesis, Agricultural University Wageningen, The Netherlands.

Bronswijk, J.J.B., W. Hamminga and K. Oostindie. 1995. Field-scale solute transport in a heavy clay soil. Water Resour. Res. 31:517-526.

Bruneau, P. and C. Gascuel-Odoux. 1990. A morphological assessment of soil microtopography using a digital elevation model on one square metre plots. Catena 17:315-325.

Burch, G.J., I.D. Moore and J. Burns. 1989. Soil hydrophobic effects on infiltration and catchment runoff. Hydr. Processes 3:211-222.

Burke, W., D. Gabriels and J. Bouma. 1986. Soil structure assessment. In: A.A. Balkema, Rotterdam/Boston. 92 pp.

Cameron, D.R. 1978. Variability of profile distribution patterns of bulk density in clay, loamy and sandy soils. Commun. Soil Sci. Pl. Anal. 9:375-387.

Cameron, D.R., C.G. Kowalenko and C.A. Campbell. 1979. Factors affecting nitrate nitrogen and chloride leaching variability in a field plot. Soil Sci. Soc. Am. J. 43:455-460.

Capriel, P., T. Beck, H. Borchert, J. Gronholz and G. Zachmann. 1995. Hydrophobicity of the organic matter in arable soils. Soil Biol. Biochem. 27:1453-1458.

Carter, D.J. and K.M.W. Howes. 1994. Proc. of the 2nd. Nat. Water Repellency Workshop, Aug. 1-5, 1994, Perth, Western Australia, pp. 215.

Celia, M.A. and P. Binning. 1992. A mass conservative numerical solution for two-phase flow in porous media with application to unsaturated flow. Water Resour. Res. 28:2819-2828.

Crabtree, R.W. and S.T. Trudgill. 1985. Hillslope hydrochemistry and stream response on a wood, permeable bedrock: the role of stemflow. J. Hydr. 80:161-178.

Crockford, S., S. Topalidis and D.P. Richardson. 1991. Water repellency in a dry sclerophyll forest - measurements and processes. Hydr. Processes 5:405-420.

Dalen, V. 1976. Immiscible flow by finite elements. In: First Int. Conf. on Finite Elements in Water Resources, 3.69-3.90.

Danneberger, K. and S. White. 1988. Treating localised dry spots. Golf Course Mgt. Feb.:6-8.

Das, D.K. and B. Das. 1972. Characterization of water repellency in Indian soils. Indian J. Agric. Sci. 42:1099-1102.

De Bakker, H. 1979. Major soils and soil regions of The Netherlands, Junk, Den Haag and Pudoc, Wageningen, 203 pp.

DeBano, L.F. 1969. Water repellent soils: a worldwide concern in management of soil and vegetation. Agric. Sci. Rev. 7:11-18.

DeBano, L.F. 1981. Water repellent soils: a state of the art, Gen. Tech. Rep. PSW-46, Pacific Southwest Forest and Range Experiment Station, 21 pp.

DeBano, L.F. 1971. The effect of hydrophobic substances on water movement in soil

during infiltration. Soil Sci. Soc. Am. Proc. 35:340-343.

DeBano, L.F. 1979. Effects of fire on soil properties. In: California forest soils, Un. Calif., Div. Agric. Sci. 4094, Berkeley, California, pp. 109-118.

DeBano, L.F. and J.S. Krammes. 1966. Water repellent soils and their relation to wildfire temperatures. Bull. Int. Assoc. Sci. Hydrol. 11:14-19.

DeBano, L.F. and J. Letey. 1969. Water repellent soil. In: Proc. Symp. 'Water Repellent Soils', May 1968, Riverside, California, pp. 354.

DeBano, L.F., S.M. Savage and D.A. Hamilton. 1976. The transfer of heat and hydrophobic substances during burning. Soil Sci. Soc. Am. J. 40:779-782.

DeBano, L.F., J.F. Osborn, S. Krammes and J. Letey. 1967. Soil wettability and wetting agents ... our current knowledge of the problem. U.S. Forest Serv. Res. Pap. PSW-43. Pacific S.W. Forest & Range Exp. Sta., Berkely, California, pp. 13.

Dekker, L.W. 1998. Moisture variability resulting from water repellency in Dutch soils. Doctoral Thesis, Wageningen Agricultural University, Netherlands, pp. 240.

Dekker, L.W. and P.D. Jungerius. 1990. Water repellency in the dunes with special reference to the Netherlands. Catena Suppl. 18:173-183.

Dekker, L.W. and C.J. Ritsema. 1994. How water moves in a water repellent sandy soil. I. Potential and actual water repellency. Water Resour. Res. 30:2507-2517.

Dekker, L.W. and C.J. Ritsema. 1995. Fingerlike wetting patterns in two water repellent loam soils. J. Env. Qual. 24:324-333.

Dekker, L.W. and C.J. Ritsema. 1996a. Variation in water content and wetting patterns in Dutch water repellent peaty clay and clayey peat soils. Catena 28:89-105.

Dekker, L.W. and C.J. Ritsema. 1996b. Preferential flow paths in a water repellent clay soil with grass cover. Water Resour. Res. 32:1239-1249.

Dekker, L.W. and C.J. Ritsema. 1996c. Uneven moisture patterns in water repellent soils. Geoderma 70:87-99.

De Rooij, G.H. 1995. A three-region analytical model of solute leaching in a soil with a water repellent top layer. Water Resour. Res. 31:2701-2707.

Diment, G.A. and K.K. Watson. 1983. Stability analysis of water movement in unsaturated porous materials. 2. Numerical studies. Water Resour. Res. 19:1002-1010.

Diment, G.A., K.K. Watson and P.J. Blennerhassett. 1982. Stability analysis of water

movement in unsaturated porous materials. 1. Theoretical considerations. Water Resour. Res. 18:1248-1254.

Doerr, S.H., R.A. Shakesby and R.P.D. Walsh. 1996. Soil hydrophobicity variations with depth and particle size fraction in burned and unburnt *Eucalyptus globulus* and *Pinus pinaster* forest terrain in the Águeda basin, Portugal. Catena 27:25-47.

Dormaar, J.F. and L.E. Lutwick. 1975. Pyrogenic evidence in Paleosols along the North Saskatchewan River in the Rocky Mountains of Alberta. Can. J. Earth Sci. 12:1238-1244.

Dunne, T., Weihua Zhang and B.F. Aubry. 1991. Effects of rainfall, vegetation and microtopography on infiltration and runoff. Water Resour. Res. 27:2271-2285.

Emerson, W.W. and R.D. Bond. 1963. The rate of water entry into dry sand and calculation of the advancing contact angle. Austr. J. Soil Res. 1:9-16.

Freeze, R.A. 1971. Three-dimensional, transient, saturated-unsaturated flow in a groundwater basin. Water Resour. Res. 7:347-365.

Gee, G.W., T. Kincaid, R.J. Lenhard and C.S. Simmons. 1991. Recent studies of flow and transport in the vadose zone, Twentieth General Assembly of the International Union of Geodesy and Geophysics, Vienna, Austria, Aug. 11-24, U.S. National Report 1987-1990, Contributions in Hydrology, 227-239.

Gilmour, D.A. 1968. Water repellence of soils related to surface dryness. Austr. For. 32:143-148.

Giovannini, G. and S. Lucchesi. 1984. Differential thermal analysis and infrared investigations on soil hydrophobic substances. Soil Sci. 137:457-463.

Giovannini G., S. Lucchesi and S. Cervelli. 1983. Water repellent substances and aggregate stability in hydrophobic soil. Soil Sci. 135:110-113.

Giovannini, G., S. Lucchesi and S. Cervelly. 1987. The natural evolution of a burnt soil: a three year investigation. Soil Sci. 143:220-226.

Glass, R.J., T.S. Steenhuis, G.H. Oosting and J.Y. Parlange. 1988. Uncertainty in model calibration and validation for the convection-dispersion process in the layered vadose zone, in: Wieringa, P.J. and D. Bachelet, Validation of flow and transport models for the unsaturated zone: Conference Proceedings; May 23-26, Ruidoso, New Mexico, Research Report 88-SS-04 Dept. of Agronomy and Horticulture, New Mexico State University, Las Cruses, 545 pp.

Glass, R.J., J.Y. Parlange and T.S. Steenhuis. 1989a. Wetting front instability: 1. Theoretical discussion and dimensional analysis. Water Resour. Res. 25:1187-1194.

Glass, R.J., T.S. Steenhuis and J.Y. Parlange. 1989b. Wetting front instability: 2. Experimental determination of relationships between system parameters and two-dimensional unstable flow field behavior in initially dry porous media. Water Resour. Res. 25:1195-1207.

Glass, R.J., T.S. Steenhuis and J.Y. Parlange. 1989c. Mechanism for finger persistence in homogeneous, unsaturated, porous media: theory and verification. Soil Sci. 148:60-70.

Glass, R.J., S. Cann, J. King, N. Baily, J.Y. Parlange and T.S. Steenhuis. 1990. Wetting front instability in unsaturated porous media: A three-dimensional study in initially dry sand. Transport in Porous Media 5:247-268.

Glover, J., and M.D. Gwynne. 1962. Light rainfall and plant survival in East Africa. I. Maize. J. Ecol. 50:111-118.

Goh, K.M., T.A. Rafter, J.D. Stout and T.W. Walker. 1976. The accumulation of soil organic matter and its carbon isotope content in a chronosequence of soils developed on aeolian sand in New Zealand. N.Z. J. Soil Sci. 27:89-100.

Grelewicz, A. and W. Plichta. 1985. The effect of the physical state of the surface of organic soil material on its wettability. Forest Ecology and Management 11:245-256.

Gwynne, M.D. and J. Glover. 1961. Light rainfall and plant survival: measurement of stemflow run-off. Nature 191:1321-1322.

Hammond, L.C. and T.L. Yuan. 1969. Methods of measuring water repellency of soils. In: Proc. Symp. 'Water Repellent Soils', May 1968, Riverside, California, pp. 49-60.

Heimovaara, T.J. and W. Bouten. 1990. A computer controlled 36-channel Time Domain Reflectometry system for monitoring soil water contents. Water Resour. Res. 26:2311-2316.

Hendrickx, J.M.H. and L.W. Dekker. 1991. Experimental evidence of unstable wetting fronts in homogeneous non-layered soils, Contribution for The National Symposium on Preferential Flow, Dec. 16-17, Chicago, Illinois, U.S.A.

Hendrickx, J.M.H., C.J. Ritsema, O.H. Boersma, L.W. Dekker, W. Hamminga and

J.W.H. van der Kolk. 1991. A motor-driven, portable soil core sampler for volumetric sampling. Soil Sci. Soc. Am. J. 55:1792-1795.

Hendrickx, J.M.H., L.W. Dekker and O.H. Boersma. 1993. Unstable wetting fronts in water repellent field soils. J. Env. Qual. 22:109-118.

Heijs, A.W.J., C.J. Ritsema and L.W. Dekker. 1996. Three-dimensional visualization of preferential flow patterns in two soils. Geoderma 70:101-116.

Hill, E.D. and J.-Y. Parlange. 1972. Wetting front instability in layered soils. Soil Sci. Soc. Am. Proc. 36:697-702.

Hillel, D. and R.S. Baker. 1988. A descriptive theory of fingering during infiltration into layered soils. Soil Sci. 146:51-56.

Hills, R.C. and S.G. Reynolds. 1969. Illustrations of soil moisture variability in selected areas and plots of different sizes. J. Hydr. 8:27-47.

Holzhey, C.S. 1969. Water repellent soils in Southern California. In: Proc. Symp. 'Water Repellent Soils', May 1968, Riverside, California, pp. 31-41.

Huyakorn, P.S. and G.F. Pinder. 1978. A new finite element technique for the solution of two-phase flow through porous media. Adv. Water Resour. 1:285-298.

Hurley, D.G. and G. Pantelis. 1985. Unsaturated and saturated flow through a thin porous layer on a hillslope. Water Resour. Res. 21:821-824.

Imeson, A.C., J.M. Verstraten, E.J. van Mulligen and J. Sevink. 1992. The effects of fire and water repellency on infiltration and runoff under Mediterranean type forest. Catena 19:345-361.

Jackson, C.R. 1992. Hillslope infiltration and lateral downslope unsaturated flow. Water Resour. Res. 28:2533-2539.

Jamison, V.C. 1942. The slow reversible drying of sandy surface soils beneath citrus trees in central Florida. Soil Sci. Soc. Am. Proc. 7:36-41.

Jamison, V.C. 1945. The penetration of irrigation and rainwater into sandy soils of Central Florida. Soil Sci. Soc. Am. Proc. 10:25-29.

Jamison, V.C. 1946. Resistance to wetting in the surface of sandy soils under citrus trees in central Florida and its effect upon penetration and the efficiency of irrigation. Soil Sci. Soc. Am. Proc. 11:103-109.

Jamison, V.C. 1969. Wetting resistance under citrus trees in Florida. In: Water Repellent Soils: Proceedings of a Symposium, edited by L.F. DeBano and J. Letey, University of California, Riverside.

Jaramillo, D.F. and F.E. Herrón. 1991. Evaluacion de la repelencia al agua de algunos andisols de antioquia bajo cobertura de Pinus patula. Acta Agronomica 41:79-85.

Jungerius, P.D. and L.W. Dekker. 1990. Water erosion in the dunes. In: Dunes of the European Coasts, Catena Suppl. 18:185-193.

Jungerius, P.D. and M.J. ten Harkel. 1994. The effect of rainfall intensity on surface runoff and sediment yield in the grey dunes along the Dutch coast under conditions of limited rainfall acceptance. Catena 23:269-279.

Jury, W.A. and K. Roth. 1990. Evaluating the role of preferential flow on solute transport through unsaturated field soils. In: *Field-scale water and solute flux in soils*, edited by K. Roth et al., pp. 23-28, Birkhäuser Verlag, Basel.

Jury, W.A. and H. Flühler. 1992. Transport of chemicals through soil: mechanisms, models, and field applications. Adv. Agron. 47:141-201.

Kaluarachchi, J.J. and J.C. Parker. 1989. An efficient finite element method for modeling multiphase flow. Water Resour. Res. 25:43-54.

King, P.M. 1981. Comparison of methods for measuring severity of water repellence of sandy soils and assessment of some factors that effect its measurement. Austr. J. Soil Res. 19:275-285.

Klute, A., 1986. Methods of soil analysis. 1. Physical and mineralogical methods. Second Edition, Agronomy 9, Part 1. ASA, SSSA. Madison, Wisconsin, USA.

Knight, J.H., I. White and S.J. Zegelin. 1994. Sampling volume of TDR probes used for water content monitoring. Proceedings of the symposium and workshop on Time Domain Reflectometry in Environmental, Infrastructure, and Mining Applications. United States Department of Interior Bureau of Mines, Special Publication SP 19-94.

Krammes, J.S. 1960. Erosion from mountainside slopes after fire in southern California. U.S. Forest Serv. Res. Note 171. Pacific S.W. Forest & Range Exp. Sta., Berkeley, California, pp. 8.

Krammes, J.S. and L.F. DeBano. 1965. Soil wettability: a neglected factor in watershed management. Water Resour. Res. 1:283-286.

Krammes, J.S. and J. Osborn. 1969. Water repellent soils and wetting agents as factors influencing erosion. in: Proc. Symp. 'Water Repellent Soils', May 1968, Riverside, California, pp. 177-187.

Kung, K.J.S. 1990a. Preferential flow in a sandy vadose zone: 1. Field observations. Geoderma 46:51-58.

Kung, K.J.S. 1990b. Preferential flow in a sandy vadose zone: 2. Mechanisms and implications. Geoderma 46:59-71.

Letey, J. 1969. Measurement of contact angle, water drop penetration time, and critical surface tension. In: Proc. Symp. 'Water Repellent Soils', May 1968, Riverside, California, pp. 43-47.

Letey, J., J.F. Osborn and R.E. Pelishek. 1962. Measurement of liquid-solid contact angles in soil and sand. Soil Sci. 93:149-153.

Letey, J., J.F. Osborn and N. Valoras. 1975. Soil water repellency and the use of nonionic surfactants. California Water Resources Center, Contribition No. 154, Un. of California, Davis, USA.

Liu, Y., B.R. Bierck, J.S. Selker, T.S. Steenhuis and J.-Y. Parlange. 1993. High-intensity x-ray and tensiometer measurements in rapidly changing preferential flow fields. Soil Sci. Soc. Am. J. 57:1188-1192.

Liu, Y., T.S. Steenhuis and J.-Y. Parlarge. 1994a. Closed form solution for finger width in sandy soils at different water contents. Water Resour. Res. 30:949-952.

Liu, Y., T.S. Steenhuis and J.-Y. Parlange. 1994b. Formation and persistence of fingered flow in coarse grained soils under different moisture contents. J. Hydr. 159:187-195.

Loague, K. 1992. Soil water content at R-5. 1. Spatial and temporal variability. J. Hydr. 138:119-129.

Lu, T.X., J.W. Biggar and D.R. Nielsen. 1994. Water movement in glass bead porous media. 1. Experiments of capillary rise and hysteresis. Water Resour. Res. 30:3275-3281.

Ma'shum, M. and V.C. Farmer. 1985. Origin and assessment of water repellency of a sandy South Australian soil. Austr. J. Soil Res. 23:623-626.

Ma'shum, M., M.E. Tate, G.P. Jones and J.M. Oades. 1988. Extraction and characterization of water repellent materials from Australian soils. J. Soil Sci. 39:99-109.

Ma'shum M., J.M. Oades and M.E. Tate. 1989. The use of dispersible clays to reduce water repellency of sandy soils. Austr. J. Soil Res. 27:797-806.

McCord, J.T. and D.B. Stephens. 1987. Lateral flow beneath a sandy hillslope without

an apparent impeding layer. Hydr. Processes 1:225-238.

McCord, J.T., D.B. Stephens and J.L. Wilson. 1991. Hysteresis and state-dependent anisotropy in modeling unsaturated hillslope hydrologic processes. Water Resour. Res. 27:1501-1518.

McGhie, D.A. 1980. The contribution of the Mallet Hill surface to runoff and erosion in the Narrogin region of Western Australia. Austr. J. Soil Res. 18:299-307.

McGhie. D.A. 1987. Non-wetting soils in western Australia. N.Z. Turf Manage. J. 2:13-16.

McGhie, D.A. and A.M. Posner. 1980. Water repellence of a heavy textured Western Australian soil. Austr. J. Soil Res. 18:309-323.

McGhie, D.A. and A.M. Posner. 1981. The effect of plant top material on the water repellence of fired sands and water repellent soils. Austr. J. Agr. Res. 32:609-620.

Miles, J.C., H.R. Thomas and J. Abrishami. 1988. The effect of small density changes on the movement of water through an unsaturated sand. J. Hydr. 104:93-110.

Miller, D.E. 1963. Lateral moisture flow as a source of error in moisture retention studies. Soil Sci. Soc. Am. Proc. 27:716-717.

Milly, P.C.P. 1988. Advances in modeling of water in the unsaturated zone. In: E. Custodio et al. (Eds), Groundwater Flow and Quality Modelling, R. Reidel Publishing Co., pp 489-514.

Miyamoto, S. 1985. Effects of wetting agents on water infiltration into poorly wettable sand, dry sod and wettable soils. Irr. Sci. 125:184-187.

Mosley, M.P. 1982. Subsurface flow velocities through selected forest soils, South Island, New Zealand. J. Hydr. 55:65-92.

Mualem, Y. 1974. A conceptual model of hysteresis. Water Resour. Res. 10:514-520.

Mustafa, M.A. and J. Letey. 1971. The effect of two nonionic surfactants on aggregate stability of soils. Soil Sci. 107:343-347.

Nakaya, N. 1982. Water repellency of soils. Japan Agr. Res. Quart. 16:24-28.

Návar, J. and R. Bryan. 1990. Interception loss and rainfall redistribution by three semi-arid growing shrubs in northeastern Mexico. J. Hydr. 115:51-63.

Nguyen, H.V., J.L. Nieber, P. Odura, C.J. Ritsema, L.W. Dekker and T.S. Steenhuis. 1998a. Modeling solute transport in a water repellent soil. J. Hydr., in press.

Nguyen, H.V., J.L. Nieber, C.J. Ritsema, L.W. Dekker and T.S. Steenhuis. 1998b.

Modeling gravity-driven unstable flow in a water repellent soil. J. Hydr., in press.

Nieber, J.L. 1996. Modeling finger development and persistence in initially dry porous media. Geoderma 70:207-230.

Nielsen, D.R., J.W. Biggar and K.T. Erh. 1973. Spatial variability of field-measured soil-water properties. Hilgardia 42:215-260.

Nimmo, J.R. and K.C. Akstin. 1988. Hydraulic conductivity of a sandy soil at low water content after compaction by various methods. Soil Sci. Soc. Am. J. 52:303-310.

Oades, J.M. and P. Blackwell. 1990. Proc. of the Nat. Workshop on Water Repellency in Soils, Waite Institute, Adelaide.

Osborn, J.F. 1969. The effect of wetting agents and water repellency on the germination and establishment of grass. In: Proc. Symp. 'Water Repellent Soils', May 1968, Riverside, California, pp. 297-314.

Osborn, J.F., J. Letey, L.F. DeBano and E. Terry. 1967. Seed germination establishment as affected by non-wettable soils and wetting agents. Ecology 48:494-497.

Osborn, J.F., R.E. Pelishek, J.S. Krammes and J. Letey. 1964. Soil wettability as a factor in erodibility. Soil Sci. Soc. Am. Proc. 28:294-295.

Parkin, T.B. and E.E. Codling. 1990. Rainfall distribution under a corn canopy: Implications for managing agrochemicals. Agron. J. 82:1166-1169.

Parlange, J.-Y. and D.E. Hill. 1976. Theoretical analysis of wetting front instability in soils. Soil Sci. 122:236-239.

Parlange, M.B., T.S. Steenhuis, D.J. Timlin, F. Stagnitti and R.B. Bryant. 1989. Subsurface flow above a fragipan horizon. Soil Sci. 148:77-86.

Pelishek, R.E., J.F. Osborn and J. Letey. 1962. The effect of wetting agents on infiltration. Soil Sci. Soc. Am. Proc. 26:595-598.

Pini, G. and G. Gambolati. 1990. Is simple diagonal scaling the best preconditioner for conjugate gradients on supercomputers? Adv. Water Resour. 13:147-153.

Philip, J.R. 1975a. Stability analysis of infiltration. Soil Sci. Soc. Am. Proc. 39:1042-1049.

Philip, J.R. 1975b. The growth of disturbances in unstable infiltration flows. Soil Sci. Soc. Am. Proc. 39:1049-1053.

Philip, J.R. 1991. Soils, natural science, and models. Soil Sci. 151:91-98.

Raats, P.A.C. 1973. Unstable wetting fronts in uniform and nonuniform soils. Soil

Sci. Soc. Am. Proc. 37:681-685.

Raats, P.A.C. 1984. Tracing parcels of water and solutes in unsaturated zones. In: Pollutants in Porous Media: The Unsaturated Zone between Soil Surface and Groundwater, editors Yaron, B., Dagan, G., and Goldshid, J., Springer-Verlag, Berlin, Germany, 4-16.

Reynolds, S.G. 1970. The gravimetric method of soil moisture determination. Part III. An examination of factors influencing soil moisture variability. J. Hydr. 11:288-300.

Rietveld, J. 1978. Soil non-wettability and its relevance as a contributing factor to surface runoff on sandy soils in Mali. Landbouw Hogeschool Wageningen, Netherlands.

Ritsema, C.J. and L.W. Dekker. 1994a. Soil moisture and dry bulk density patterns in bare dune sands. J. Hydr. 154:107-131.

Ritsema, C.J. and L.W. Dekker. 1994b. How water moves in a water repellent sandy soil. 2. Dynamics of fingered flow. Water Resour. Res. 30:2519-2531.

Ritsema, C.J. and L.W. Dekker. 1995. Distribution flow: A general process in the top layer of water repellent soils. Water Resour. Res. 31:1187-1200.

Ritsema, C.J. and L.W. Dekker. 1996a. Influence of sampling strategy on detecting preferential flow paths in water repellent sand. J. Hydr. 177:33-45.

Ritsema, C.J. and L.W. Dekker. 1996b. Water repellency and its role in forming preferred flow paths in soils. Austr. J. Soil Res. 34:475-487.

Ritsema, C.J. and L.W. Dekker. 1998. Three-dimensional patterns of moisture, water repellency, bromide and pH in a sandy soil. J. of Cont. Hydr. 31:85-103.

Ritsema, C.J., L.W. Dekker, E.G.M. van den Elsen, K. Oostindie, J.L. Nieber and T.S. Steenhuis. 1997b. Recurring fingered flow pathways in a water repellent sandy field soil. Hydrology and Earth System Sciences 4:777-786.

Ritsema, C.J., L.W. Dekker, J.M.H. Hendrickx and W. Hamminga. 1993. Preferential flow mechanism in a water repellent sandy soil. Water Resour. Res. 29:2183-2193.

Ritsema, C.J., L.W. Dekker and A.W.J. Heijs. 1997a. Three-dimensional fingered flow patterns in a water repellent sandy field soil. Soil Sci. 162:79-90.

Ritsema, C.J., L.W. Dekker, J.L. Nieber and T.S. Steenhuis. 1998a. Modeling and field evidence of finger formation and finger recurrence in a water repellent sandy

soil. Water Resour. Res. 34:555-567.

Ritsema, C.J., J.L. Nieber, L.W. Dekker and T.S. Steenhuis. 1998b. Stable or unstable wetting fronts in water repellent soils - effect of antecedent soil moisture content. Soil and Tillage Res. 47:111-123.

Ritsema, C.J., T.S. Steenhuis, J.-Y. Parlange and L.W. Dekker. 1996. Predicted and observed finger diameters in field soils. Geoderma 70:185-196.

Roberts, F.J. 1966. The effects of sand type and fine particle amendments on the mergence and growth of subterannean clover (*Trifolium subterraneum* L.) with particular reference to water relations. Austr. J. Agr. Res. 17:657-672.

Roberts, F.J. and B.A. Carbon. 1971. Water repellency in sandy soils of southwestern Australia. I. Some studies related to field occurrence. Fld. Stn. Rec. Div. Pl. Ind. CSIRO (Austr.) 10:13-20.

Roberts, F.J. and B.A. Carbon. 1972. Water repellence in sandy soils of southwestern Australia. II. Some chemical characteristics of hydrophobic skins. Austr. J. Soil Res. 10:35-42.

Saffigna, P.G., C.B. Tanner and D.R. Keeney. 1976. Non-uniform infiltration under potato canopies caused by interception, stemflow, and hilling. Agron. J. 68:337-342.

Saffman, P.G. and G.I. Taylor. 1958. The penetration of a fluid into a porous medium or Hele-Shaw cell containing a more viscous liquid. Proc. R. Soc. Lond. Ser. A245:312-331.

Sanchez, C.A., A.M. Blackmer, R. Horton and D.R. Timmons. 1987. Assessment of errors associated with plot size and lateral movement of nitrogen-15 when studying fertilizer recovery under field conditions. Soil Sci. 144:344-351.

Savage, S.M. 1974. Mechanism of fire-induced water repellency in soil. Soil Sci. Soc. Am. Proc. 38:652-657.

Savage, S.M, J.P. Martin and J. Letey. 1969a. Contribution of humic acid and a polysaccharide to water repellency in sand and soil. Soil Sci. Soc. Am. Proc. 33:149-151.

Savage, S.M., J.P. Martin and J. Letey. 1969b. Contribution of some soil fungi to natural and heat-induced water repellency in sand. Soil Sci. Soc. Am. Proc. 33:405-409.

Savage, S.M., J. Osborn, J. Letey and C. Heaton. 1972. Substances contributing to

fire-induced water repellency in soils. Soil Sci. Soc. Am. Proc. 36:674-678.

Scholl, D.G. 1971. Soil wettability in Utah juniper stands. Soil Sci. Soc. Am. Proc. 35:344-350.

Schnitzer, M., and J.G. Desjardins. 1969. Chemical characteristics of a natural soil leachate from a humic podzol. Can. J. Soil Sci. 49:151-158.

Schreiner, O. and E.C. Shorey. 1910. Chemical nature of soil organic matter. U.S. Dep. Agr., Bur. Soils, Bull. 74, pp. 17.

Scott, D.F. and D.B. van Wyk. 1990. The effects of wildfire on soil wettability and hydrological behaviour of an afforested catchment. J. Hydr. 121:239-256.

Scott, D.F. and D.B. van Wyk. 1992. The effects of fire on soil water repellency, catchment sediment yields and streamflow. In: Fire in South African Mountain Fynbos, Ecological Series 193:216-239.

Selim, H.M. 1987. Water seepage through multilayered anisotropic hillside. Soil Sci. Soc. Am. J. 51:9-16.

Selker, J.S., T.S. Steenhuis and J.Y. Parlange. 1989. Preferential flow in homogeneous sandy soils without layering, Paper No. 89-2543, American Society of Agricultural Engineers, St. Joseph MI, 22 pp.

Selker, J.S., T.S. Steenhuis and J.-Y. Parlange. 1991. Estimation of loading via fingered flow. In: Irrigation and Drainage: Conference Proceedings; July 22-26, Honolulu, Hawaii, USA, edited by W.F. Ritter, pp. 81-87.

Selker, J.S., T.S. Steenhuis and J.-Y. Parlange. 1992a. Wetting front instability in homogeneous sandy soils under continuous infiltration. Soil Sci. Soc. Am. J. 56:1346-1350.

Selker, J.S., J.-Y. Parlange and T.S. Steenhuis. 1992b. Fingered flow in two dimensions 2. Predicting finger moisture profile. Water Resour. Res. 28:2523-2528.

Sinaï, G., D. Zaslavsky and P. Golany. 1981. The effect of soil surface curvature on moisture and yield - Beer Sheba observation. Soil Sci. 132:367-375.

Specht, R.L. 1957. Dark Island Heath. IV. Soil moisture patterns produced by rainfall interception and stemflow. Austr. J. Bot. 5:137-150.

Steenhuis, T.S., C.J. Ritsema and L.W. Dekker. 1996. Introduction. Geoderma 70:83-85.

Steenhuis, T.S., J.S. Selker, J. Bell, K.J.S. Kung and J.-Y. Parlange. 1991. Effects of soil layering on infiltration. In *Irrigation and drainage: Proc. of the 1991 Nat.*

Conf., edited by W.F. Ritter, pp. 74-80, American Society of Civil Engineers, Honolulu, Hawaï.

Stolte, J., G.J. Veerman and M.C.S. Wopereis, 1992. Manual soil physical measurements, version 2.0. Wageningen, The Netherlands. DLO Winand Staring Centre. Technical Document 2.

Tamai, N., A. Takashi and G.J. Jeevaraj. 1987. Fingering in two-dimensional, homogeneous, unsaturated porous media. Soil Sci. 144:107-112.

Topp, G.C., J.L. Davis and A.P. Annan. 1980. Electromagnetical determination of soil water content: Measurement in coaxial transmission lines. Water Resour. Res. 16:579-582.

Van Dam, J.C., J.M.H. Hendrickx, H.C. van Ommen, M.H. Bannink, M.Th. van Genuchten and L.W. Dekker. 1990. Water and solute movement in a coarse textured water repellent field soil. J. Hydr. 120:359-379.

Van den Elsen, H.G.M., J. Kokot, W. Skierucha and J.M. Halbertsma. 1995. An automatic Time Domain Reflectometry device to measure and store soil moisture contents for stand-alone field use. Agrophysics 9:235-241.

Van Genuchten, M.Th. 1980. A closed-form equation for predicting the hydraulic conductivity of unsaturated soils. Soil Sci. Soc. Am. J. 44:892-898.

Van Genuchten, M.Th. and W.A. Jury. 1987. Progress in unsaturated flow and transport modeling. Rev. Geophys. 25:135.

Van Genuchten, M.Th. 1991. Recent progress in modeling water flow and chemical transport in the unsaturated zone. In *Hydrological interactions between atmosphere, soil and vegetation: Proceedings of the Vienna Symposium*, Aug. '91, IAHS Publ. No. 204:169-183.

Van 't Woudt, B.D. 1959. Particle coatings affecting the wettability of soils. J. Geophys. Res. 64:263-267.

Van Wesenbeeck, I.J. and R.G. Kachanoski. 1988a. Spatial and temporal distribution of soil water in the tilled layer under a corn crop. Soil Sci. Soc. Am. J. 52:363-368.

Van Wesenbeeck, I.J., R.G. Kachanoski and D.E. Rolston. 1988b. Temporal persistence of spatial patterns of soil water content in the tilled layer under a corn crop. Soil Sci. Soc. Am. J. 52:934-941.

Wallach, R. and D. Zaslavsky. 1991. Lateral flow in a layered profile of an infinite

uniform slope. Water Resour. Res. 27:1809-1818.

Wallis, M.G. and D.J. Horne. 1992. Soil water repellency. Adv. Soil Sci. 20:91-146.

Wallis, M.G., D.J. Horne and K.W. McAuliffe. 1989. A survey of dry patch and its management in New Zealand golf greens. 2. Soil core results and irrigation interaction. N.Z. Turf Mgt. J. 3:15-17.

Wallis, M.G., D.J. Horne and K.W. McAuliffe. 1990. A study of water repellency and its amelioration in a yellow brown sand. 2. The use of wetting agents and their interaction with some aspects of irrigation. N.Z.J. Agr. Res. 33:145-150.

Wallis, M.G., D.R. Scotter and D.J. Horne. 1991. An evaluation of the intrinsic sorptivity water repellency index on a range of New Zealand soils. Austr. J. Soil Res. 29:353-362.

Wander, I.W. 1949. An interpolation of the cause of water repellent sandy soils found in citrus groves of central Florida. Science 110:299-300.

Wang, Z., J. Feyen and C.J. Ritsema, 1998. Susceptibility and predictability of conditions for preferential flow. Water Resour. Res., in press.

Watson, C.L. and J. Letey. 1970. Indices for characterizing soil water repellency based upon contact angel - surface tension relationships. Soil Sci. Soc. Am. Proc. 34:841-844.

Way, B. 1990. Irrigation system performance. N.Z. Turf Mgt. J. 4:22-23.

Whalley, W.R. 1993. Considerations on the use of time-domain reflectometry (TDR) for measuring soil water content. J. Soil Sci. 44:1-9.

White, I., P.M. Colombera and J.R. Philip. 1976. Experimental study of wetting front instability induced by sudden change of pressure gradient. Soil Sci. Soc. Am. J. 40:824-829.

White, I., P.M. Colombera and J.R. Philip. 1977. Experimental study of wetting front instability induced by gradual change of pressure gradient and by heterogeneous porous media. Soil Sci. Soc. Am. Proc. 41:483-489.

White, R.E. 1985. The influence of macropores on the transport of dissolved and suspended matter through soil. Adv. Soil Sci. 3:95.

Wierenga, P.J. and M.Th. van Genuchten. 1989. Solute transport through small and large unsaturated soil columns. Ground Water 27:35-42.

Wilson, G.V., P.M. Jardine, R.J. Luxmoore, L.W. Zelazny, D.A. Lietzke and D.E. Todd. 1991. Hydrogeochemical processes controlling subsurface transport

from an upper subcatchment of Walker Branch Watershed during storm events. 1. Hydrologic transport processes. J. Hydr. 123:297-316.

Witter, J.V., P.D. Jungerius and M.J. ten Harkel. 1991. Modeling water erosion and the impact of water repellency. Catena 18:115-124.

Zaslavsky, D. and G. Sinaï. 1981a. Surface hydrology: I. Explanation of phenomena. J. Hydraul. Div. 107:1-16.

Zaslavsky, D. and G. Sinaï. 1981b. Surface hydrology: III. Causes of lateral flow. J. Hydraul. Div. 107:37-52.

Zaslavsky, D. and G. Sinaï. 1981c. Surface hydrology: IV. Flow in sloping, layered soil. J. Hydraul. Div. 107:53-64.

CURRICULUM VITAE

Coenraad Johan Ritsema was born on February 6, 1958 in Jakarta, Indonesia. After completing secondary school (Atheneum-B, Rijksscholengemeenschap Schoonoord, Zeist, Netherlands), he started studying physical geography at the University of Utrecht in 1977. He graduated in 1985, having specialized in soil erosion (University of Utrecht), soil physics (Wageningen Agricultural University) and fluid mechanics (Technical University Delft).

In 1985, he started working at the Department of Groundwater Quality of the Institute of Land and Water Management Research (ICW), Wageningen, by way of alternative national service. After its completion in 1987, he became employed at the same Institute to study physical and chemical processes in acid sulphate soils in the humid tropics. With the merging of ICW in the DLO Winand Staring Centre in 1990, he became a senior researcher at the Department of Soil Physical Transport Phenomena, and in 1994 he was appointed Head of Department. In recent years, his research interests have been preferential flow, flow and transport in water repellent soils, and soil erosion processes.

The results of his work have been disseminated via 40 refereed papers in international scientific journals like Water Resources Research (8), Journal of Hydrology (7), Hydrological Processes (4), Geoderma (4) Soil Science Society of America Journal (2), Journal of Environmental Quality (2), Soil and Tillage Research (2), Soil Science (2), Plant and Soil (2), Journal of Contaminant Hydrology (1), Australian Journal of Soil Research (1), Journal of Soil Science (1), Agricultural Water Management (1), Hydrology and Earth System Sciences (1), Earth Surface Processes and Landforms (1), and Catena (1). Furthermore, he (co)authored 10 book chapters, 6 refereed papers in national research journals, 32 non-refereed publications, and another 80+ congress and symposia contributions. He is a regular reviewer of manuscripts submitted for publication in most of the above-mentioned Journals. In 1994, he received the Editors' Citation for Excellence in Refereeing for Water Resources Research. He was guest editor of special issues of Geoderma and the Journal of Hydrology, and was organizer of 2 international symposia.

During the last years, he obtained and directed over 10 million guilders of research funds as coordinator of several large international research projects. Collaborations are on-going with Universities and Research Institutes in, e.g. Europe, USA, Australia, and China.